UNIVERSITY *of the*
WESTERN CAPE

An assessment of the spatial distribution of neglected and underutilized crop species (NUS) (Taro and Sweet potatoes) using very high-resolution UAV remotely sensed data in small-holder farms of Swayimane, South Africa.

By

Mishkah Abrahams
3852812

A thesis submitted in the fulfilment of the requirements for a master's degree in Geography and Environmental Studies in the Department of Geography, Environmental Studies and Tourism, University of the Western Cape.

Supervisor: Doctor Mbulisi Sibanda
Co-supervisor: Professor Timothy Dube and Professor Tafadzwanashe Mabhaudhi

January 2024

ABSTRACT

This work explores the potential of neglected and underutilized crop species (NUS) in addressing agricultural, food, and nutrition security challenges exacerbated by climate change, particularly in Southern Africa. Mainstream crops like maize are adversely affected by climate variability, leading to increased insecurities. Despite the importance of NUS, limited research attention and market preference hinder their development. Additionally, there is a lack of criteria for determining their spatial extent in smallholder croplands, complicated by field fragmentation and intercropping. To overcome these challenges, this study employs unmanned aerial vehicles (UAVs) and high-throughput phenotyping technologies for accurate mapping of NUS, specifically sweet potato and taro, in smallholder farms in the Kwazulu-Natal Province, South Africa. Three specific objectives guide the study. These were (1) to conduct a systematic review of literature on the mapping the spatial distribution and health of NUS crops in sub-Saharan Africa, (2) to evaluate the performance of three robust classifiers in mapping the spatial distribution of NUS crops based on multispectral UAV data and, (3) to assess the performance of object based image analysis (OBIA) and pixel based analysis (PBIA) techniques combined with GTB classifier in mapping and delineating the spatial distribution of NUS crops. Review of literature revealed a lack of studies in the Global South, highlighting the potential of machine learning algorithms with optimal near-infrared and red-edge vegetation indices in mapping NUS. Despite slow progress due to high costs and regulations, the review findings suggested that integrating machine learning techniques with UAV-acquired data is crucial for efficient monitoring of NUS crops in small-scale agricultural areas. This will provide essential information for enhancing the efficiency of food production in small-scale agricultural areas located in the Global South. In addressing the second objective results showed that the tree-based classifiers, i.e., Random Forest (RF) and Gradient Tree Boost (GTB), demonstrated superior performance compared to Support Vector Machine (SVM), achieving an accuracy rate of over 90% in effectively distinguishing NUS crops. SVM produced lower accuracy rates ranging from (42%-74%) and kappa values (0.32 -0.70) across all its models. The dataset composed of bands combined with the vegetation indices optimally performed when compared to spectral bands dataset. The most optimal classification spectral variables selected by the GTB algorithm, which yielded superior performance compared to SVM and RF, were primarily derived from the visible bands (Red, Red edge) and the near-infrared (NIR) band. In comparatively assessing the performance of OBIA and PBIA techniques based on GTB for mapping NUS crops, results showed that the PBIA-GTB model exhibited a slightly better performance compared to OBIA, with accuracies consistently ranging between 1% and 7% higher. The findings of this study suggest that multispectral remotely sensed data acquired using unmanned aerial vehicles (UAVs) could optimally map the spatial patterns and distributions of NUS amongst other crops in complex and fragmented smallholder croplands. The ability to precisely delineate the spatial distribution of NUS crops is crucial and required for various purposes which include biodiversity conservation, climate resilience, ensuring food security, and promoting sustainable agriculture. The findings derived from this study represents a significant step forward in providing local communities and smallholder farmers with invaluable knowledge that can contribute to the cultivation and utilisation of these crop species, to achieve sustainable development practices.

I

Keywords: Drone, Random Forest, Remote sensing, Smallholder farms, Support Vector Machine, Sweet-potato, Taro.

PREFACE

The research work reported in this thesis was conducted in the Faculty of Arts and Humanities, University of the Western Cape, Cape Town, South Africa from January 2021 to December 2023. This work was part of a Water Research Commission funded project No C2022/2023-00930 titled '*Unmanned aerial vehicle high-throughput phenotyping of neglected and underutilized crops species (NUS) for improved water use and productivity in smallholder farms*'. Doctor Mbulisi Sibanda, Professor Tafadzwanashe Mabhaudhi and Professor Timothy Dube supervised the research project.

I declare that the research work presented in this thesis has never been submitted or examined by any other academic institution. This thesis represents my original work except where other authors have been cited or properly acknowledged.

Mishkah Abrahams: Signed_____   Date:17/01/2024

DECLARATION

I, **Mishkah Abrahams,** state that:

1. The research reported in this thesis, except where referenced, is my work.
2. This thesis has not been submitted to any institution for any degree or qualification.
3. This thesis does not contain other person's data, pictures, graphs or other information, unless specifically acknowledged as being sourced from other persons.
4. All authored work in this thesis has been sourced as intext references, and a full reference list has been provided. In instances where other sources have been quoted:
    i. Their ideas have been properly paraphrased and referenced.
    ii. Proper quotation marks and referencing have been made where direct quotes are used.
5. This thesis does not contain text, graphics or tables copied and pasted from the Internet unless specifically acknowledged, and the source is detailed in the thesis and the reference list.

Singed _____**Date**: 17/01/2024

LIST OF PUBLISHED PAPERS

1) Abrahams, Mishkah, Mbulisi Sibanda, Timothy Dube, Vimbayi GP Chimonyo, and Tafadzwanashe Mabhaudhi. "A systematic review of UAV applications for mapping neglected and underutilised crop species' spatial distribution and health." Remote Sensing 15, no. 19 (2023): 4672.

DEDICATION

I would like to dedicate my dissertation to my beloved family and friends. In particular, I want to express a profound sense of gratitude to my loving parents, whose words of encouragement and support has had a lasting impact on me. Their consistent faith in my abilities, along with their encouragement to keep trying, has served as a source of motivation throughout my academic journey.

ACKNOWLEDGMENTS

TABLE OF CONTENTS

IX

LIST OF FIGURES

LIST OF TABLES

UNIVERSITY *of the*

WESTERN CAPE

ABBREVIATIONS

3D-CNN	3-Dimensional Convolutional Neural Network
AGB	Above Ground Biomass
AGDW	Above Ground Dry Weight
AGL	Above Ground Level
AHP	Analytical Hierarchical Process
ANN	Artificial Neural Network
ARVI	Atmospherically Resistant Vegetation Index
AVHRR	Advanced Very-High Resolution Radiometer
BPNN	Back Propagation Neural Network
CAA	Civil Aviation Authorities
CIgreen	Green Chlorophyll Index
CO2	Carbon Dioxide
CRP	Calibrated Reflectance Panel
DEM	Digital elevation Model
DSM	Digital Surface Model
DT	Decision Tree
EGI	Excess Green index
ELM	Empirical Line Method
EM	Electromagnetic
EXG	Excess Green
GEE	Google Earth Engine
GIS	Geographic Information Systems
GLM	Generalised Linear Model
GNDVI	Green Normalised Difference Vegetation Index
GNSS	Global Navigation Satellite System receiver
GPS	Global Positioning System
GTB	Gradient Tree Boost
JM	Jeffries-Matusita
KNN	K-Nearest Neighbour
LAI	Leaf Area Index
LDA	Linear Discriminant Analysis
LR	Linear Regression
M300	Matrice 300 Series
ML	Machine Learning
MODIS	Moderate Resolution Imaging Spectroradiometer
MSI	Multispectral Sensor Instrument
NB	Naïve Bayes
OA	Overall Accuracy
OBIA	Object Based Image Analysis
PBIA	Pixel Based Image Analysis
PCA	Principle Components Analysis
PLSR	Partial Least Squares Regression
PRISMA	Preferred Reporting Items for Systematic Reviews and Meta-Analyses
NDVI	Normalised Difference Vegetation Index
NDRE	Red-edge Normalised Difference Vegetation Index
NDGRI	Normalised Difference Green/Red Index
NIR	Near-Infrared
NUS	Neglected and Under-utilised Crop Species
QTL	Quantitative Trait Loci

RBF	Radial Basis Function
RE	Red-Edge
RF	Random Forest
RFR	Random Forest Regression
RGB	Red-green-blue
RMSE	Root Mean Square Error
RS	Remote Sensing
SAVI	Soil Adjusted Vegetation Index
SNIC	Simple Non-Iterative Clustering
SNP	Single-nucleotide Polymorphism
SR	Simple Ratio
SSA	Sub-Saharan Africa
SVM	Support Vector Machine
SVR	Support Vector Regression
UAV	Unmanned Aerial Vehicle
UV	Ultra-Violet
VIs	Vegetation indices
VTOL	Vertical take-off and Landing
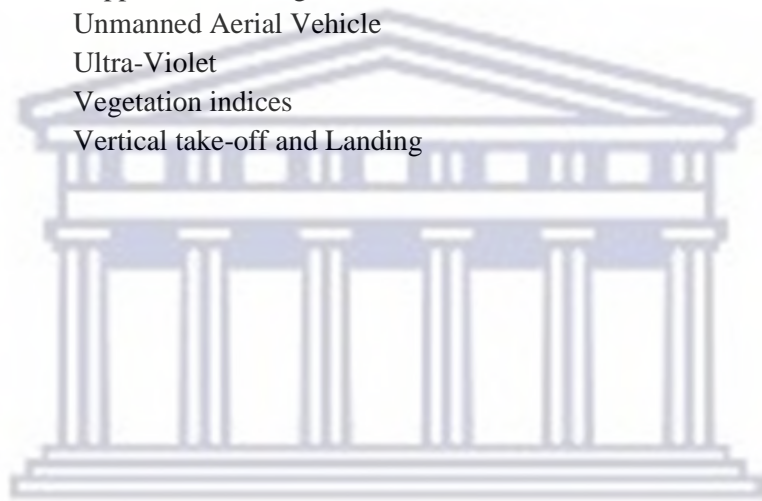
CHAPTER 1

BACKGROUND AND INTRODUCTION

1.1. Introduction

The issue of ensuring sufficient and reliable access to nutritious food, also known as food security, is becoming a growing concern in developing regions like sub-Saharan Africa (Hlophe-Ginindza and Mpandeli, 2021). The rising issue of food insecurity could lead to unpredictable challenges. Food demands are estimated to increase twofold by 2050 due to rapid population growth and fast economic progress in developing countries (Keating et al., 2014). Meanwhile, arable land is adversely affected by land degradation and the impacts of global warming, posing a significant threat to food and nutritional security. In light of this, numerous developing countries face the formidable task of eradicating hunger, malnutrition, and poverty (Sustainable Development Goals 1 & 2). However, small-scale farmers face significant pressures to achieve optimal agricultural productivity despite the constant changes in land and environmental circumstances. These include loss of farm income (85% and 80%), increased livestock mortalities (72% and 65%), and pest and disease incidences (65% and 56%) (Majaha, 2023). Moreover, the increased incidence of droughts has extensively exacerbated this predicament. For instance, the drought of 2015-16 resulted in a decline of 8.4% in agricultural production in South Africa (Majaha, 2023). Despite the significant contributions made by smallholder farmers, they do not receive adequate support from governmental or financial institutions. Furthermore, compared to their large-scale counterparts, they encounter marginalisation in both markets and policy initiatives (IFAD, 2013). Therefore, it is essential to breed stress-tolerant crops that are resource-use efficient and suitable for marginal environments to achieve sustainable food and nutrition security within disadvantage smallholder communities,

Neglected and underutilised crop species (NUS) are alternative crops that have demonstrated an ability to grow and produce yields in adverse conditions such as water-scarce areas and marginal land (Mabhaudhi et al., 2017). NUS crops (e.g., taro and sweet potato) provide higher nutritional value due to their nutrient composition and fibre content. Hence, promoting their wider cultivation has the potential to help solve several issues concerning food security faced by marginal farming systems (Mabhaudhi et al., 2017). However, lack of market preference has slowed their introduction into commercial and subsistence food systems. Additionally, there is limited research on NUS crop health, nutritional characteristics, and ability to grow and repair degraded farmland (Mabhaudhi et al., 2017). While the commercial, environmental, and socio-economic roles of NUS have been recorded, a limited understanding of emerging NUS remains.

Furthermore, despite their significant role, the spatial distribution and arrangement of smallholder crop fields remain largely unknown. This lack of clarity in delineating NUS crop parcels is due to the limited accessibility to data and skills among smallholder farmers, which are often associated with high costs (Persello et al., 2019). Therefore, precise, and accurate information based on NUS crop spatial extent and yield estimates must be gathered to improve crop productivity within smallholder farms while addressing food and nutrition insecurities and poverty.

Acquiring an understanding of the spatial distribution of NUS holds great importance in facilitating informed decision-making based on area suitability, spatial organisation, and health and vegetation trends, which will maximise productivity and food security (Mugiyo et al., 2021) . Since smallholder farming systems often implement crop rotation practices; frequent delineation of crops spatial arrangement can provide significant advantages in monitoring changes in crop rotation patterns and cultivated areas (Xing et al., 2022). Additionally, this will aid in undetstanding the extent of natural resource utilisation by smallholder farming systems, such as water and land resources. Traditionally,

1

conventional techniques for gathering data, such as conducting field surveys, have been employed to document cultivated crops' spatial distribution and aerial coverage. However, field surveys often lack spatial reference associated with crop fields, resulting in limited accuracy and precision. These surveys are also known for being time-consuming, labour-intensive, and costly (Ren et al., 2022). As a result, there is a requirement for alternative approaches that are cost-effective and can provide timely and dependable statistics on crop distribution.

This necessitates introducing sophisticated methods to track NUS spatial distribution and characteristics at various scales. Remote sensing (RS) technology and GIS techniques have been advocated for quantifying the spatial extent, land suitability and spatially explicit crop health monitoring for improved agricultural management. Near real-time monitoring of crop spatial distribution and area coverage has been extensively researched using medium to high-resolution remotely sensed data (Jindo et al., 2021, Ahmad et al., 2021, de Lima et al., 2021). In a study conducted by Mazarire et al. (2020), it was found that Sentinel-2 multispectral instrument (MSI) data, coupled with machine learning algorithms, effectively distinguished various crop types, achieving remarkable overall accuracies of 95%. Contrastingly, due to coarser spatial resolution, moderate resolution sensors (i.e., Landsat series) may have difficulties producing accurate results based on crop spatial distribution. According to Hall et al. (2018), a major source of error can arise when diverse crops with similar phenologies are intercropped. This could be reified by utilising higher spatial and temporal resolution datasets.

Adopting high to ultra-high-resolution datasets from unmanned aerial vehicles (UAVs) is recommended to enhance crop analysis in smallholder farms. These datasets can capture minute variations in crop attributes within agricultural fields smaller than a hectare (Avneri et al., 2023, Chimonyo et al., 2020, Mazarire, 2020). The significance of deploying UAVs for high throughput phenotyping in smallholder croplands is that they bridge a gap between field observations and conventional air and space-borne remote sensing through the provision of proximal near-real-time monitoring over various areas in an affordable way (Manfreda et al., 2018). Unlike moderate to high-resolution sensors such as Worldview 3 and Sentinel 2 MSI, UAVs offer the advantage of being deployable at user-defined ground ranges and return intervals (Brewer et al., 2022) . However, Worldview is associated with exorbitant acquisition expenses, while Sentinel-2 MSI could mask out some information depending on the size of the field. This makes UAV-based datasets particularly suitable for mapping NUS crops like taro and sweet potatoes, frequently cultivated in small fields.

Recognising the significance of high-throughput UAV data characterised by enhanced spatial and temporal resolutions, it is imperative to thoroughly evaluate the synergistic effectiveness of high-resolution data in conjunction with resilient machine learning methodologies and spectral enhancement techniques to precisely quantify the spatial distribution of NUS crops. Machine learning algorithms have been demonstrated to accurately map the distribution of commercially important crops (Ndlovu et al., 2021). Common machine-learning techniques in crop classification include random forests, artificial neural networks, and support vector machines. For example, using UAV data, Liu et al. (2018) classified mainstream crops like rice, soybean, wheat, and corn. The combination of RGB data from UAVs and the SVM algorithm resulted in accuracy rates exceeding 73 percent and a Kappa statistic of 70. Including optimal vegetation indices and digital surface model elevation data further elevated the accuracies to more than 90 percent. Hence, this observation highlights the crucial role of machine learning algorithms, specifically those incorporating spectral and image enhancement techniques, in effectively classifying various types of crops. Therefore, this study sought to evaluate the application of UAV-based proximal remote sensing in mapping the spatial distribution of NUS, specifically sweet potato and taro, among other crops in a smallholder cropland area.

2

1.2. Rationale

NUS (Taro and sweet potatoes) are important for food security and nutrition yet they remain under-utilised and under-researched. As climate-resilient and viable crops for smallholder farms, promoting their production could help address hunger and dietary deficiencies. However, key information about their distribution and extent is currently unknown, limiting efforts to optimise their cultivation. Remotely sensed data from technologies such as unmanned aerial vehicles (UAVs) offers a potential solution. UAVs can collect high-resolution, near-real-time imagery at field scale in smallholder croplands, which is almost impossible with readily available satellite remotely sensed data. The combination of machine learning and image analysis techniques, with UAV data has the potential to enhance the mapping of spatial patterns of taro and sweet potato crops within smallholder farming systems. The assessment of the efficacy of UAV data in monitoring NUS holds immense importance and could provide valuable insights into their actual areal coverage and distribution at the farm scale. This information could help support efforts to promote and improve the production of these climate-resilient, nutrient-dense crops to enhance food security and nutrition among smallholder communities.

1.3. Aim and Specific objectives.

The main objective of this study is to evaluate the utility of UAV high-throughput phenotyping remotely sensed data in mapping and delineating the spatial distribution of NUS crop species (taro and sweet potato crops) in smallholder farms.

To achieve this overarching objective, this study specifically sought
1. To conduct a systematic review of literature on the utility of UAVs in mapping the spatial distribution and health of NUS.
2. To evaluate the performance of Random Forest algorithm (RF), Support Vector Machine (SVM) and Gradient Tree Boost (GTB) algorithms in mapping the spatial distribution of NUS in smaller holder fields.
3. To compare PBIA-GTB and OBIA methods in mapping and delineating the spatial distribution of NUS crops at farm scale.

1.4. Chapter Overview

In addressing the overarching objective, a total of 5 chapters were generated, and some of them were presented as standalone chapters. Specifically, chapters 2 to 4 are presented as standalone manuscripts. Considering that all these chapters address the same over aching aim within the same study area and data sets, inevitable overlaps between some chapters were anticipated. Despite these overlaps, each chapter presents specific aspects of mapping NUS in a cropland area characterised by multicopying in typical smallholder cropland in Southern Africa. The chapter outline of this study is as follows:

*   Chapter 1: This chapter will outline an overview and introduction of the study. The background, aim, objectives and the main concept of the study will be discussed.
*   Chapter 2: This chapter presents a systematic review of the utility of UAVs in mapping the spatial distribution and health of NUS and will discuss the body of knowledge and different views on the subject matter. This paper has since been published in Remote Sensing (MDPI) (Abrahams, M.; Sibanda, M.; Dube, T.; Chimonyo, V.G.P.; Mabhaudhi, T. A Systematic Review of UAV Applications for Mapping Neglected and Underutilised Crop Species' Spatial Distribution and Health. Remote Sens. 2023, 15, 4672. https://doi.org/10.3390/rs15194672).
*   Chapter 3: This chapter compares RF, GTB and SVM in mapping the spatial distribution of NUS crops using various datasets.

- Chapter 4: This chapter assesses the efficacy of Gradient tree boost on pixel and object-based image analysis platforms to map NUS crops within smallholder fields.
- Chapter 5: This chapter serves as a synthesis, offering an overview of all essential research findings related to the study's objectives. It presents a comprehensive summary of the key research outcomes and their implications. Additionally, this chapter includes conclusions drawn from the findings and provides recommendations for future research directions.

-

References

Ahmad, U., Alvino, A., & Marino, S. (2021). A Review of Crop Water Stress Assessment Using Remote Sensing. *Remote Sensing*, *13*(20), 4155.

Avneri, A., Aharon, S., Brook, A., Atsmon, G., Smirnov, E., Sadeh, R., Abbo, S., Peleg, Z., Herrmann, I., & Bonfil, D. J. (2023). UAS-based imaging for prediction of chickpea crop biophysical parameters and yield. *Computers and Electronics in Agriculture*, *205*, 107581.

Brewer, K., Clulow, A., Sibanda, M., Gokool, S., Naiken, V., & Mabhaudhi, T. (2022). Predicting the Chlorophyll Content of Maize over Phenotyping as a Proxy for Crop Health in Smallholder Farming Systems. *Remote Sensing*, *14*(3), 518. https://www.mdpi.com/2072-4292/14/3/518

Chimonyo, V. G. P., Wimalasiri, E. M., Kunz, R., Modi, A. T., & Mabhaudhi, T. (2020). Optimizing traditional cropping systems under climate change: a case of maize landraces and Bambara groundnut. *Frontiers in Sustainable Food Systems*, *4*, 562568.

De Lima, I. P., Jorge, R. G. & De Lima, J. L. P. 2021. Remote sensing monitoring of rice fields: Towards assessing water saving irrigation management practices. *Frontiers in Remote Sensing,* 2**,** 762093.

Hall, O., Dahlin, S., Marstorp, H., Archila Bustos, M. F., Öborn, I., & Jirström, M. (2018). Classification of maize in complex smallholder farming systems using UAV imagery. *Drones*, *2*(3), 22.

Hlophe-Ginindza, S. N., & Mpandeli, N. (2021). The Role of Small-Scale Farmers in Ensuring Food Security in Africa. *Food Secur. Afr.*

IFAD, U. 2013. Smallholders, food security and the environment. *Rome: International Fund for Agricultural Development,* 29.

Jindo, K., Kozan, O., Iseki, K., Maestrini, B., van Evert, F. K., Wubengeda, Y., Arai, E., Shimabukuro, Y. E., Sawada, Y., & Kempenaar, C. (2021). Potential utilization of satellite remote sensing for field-based agricultural studies. *Chemical and Biological Technologies in Agriculture*, *8*(1), 1-16.

Keating, B. A., Herrero, M., Carberry, P. S., Gardner, J., & Cole, M. B. (2014). Food wedges: framing the global food demand and supply challenge towards 2050. *Global Food Security*, *3*(3-4), 125-132.

Liu, B., Shi, Y., Duan, Y., & Wu, W. (2018). UAV-based Crops Classification with joint features from Orthoimage and DSM data. *International Archives of the Photogrammetry, Remote Sensing & Spatial Information Sciences*, *42*(3).

Mabhaudhi, T., Chimonyo, V. G., Chibarabada, T. P., & Modi, A. T. (2017). Developing a roadmap for improving neglected and underutilized crops: A case study of South Africa. *FRONTIERS IN PLANT SCIENCE*, *8*, 2143.

Majaha, J. (2023). The impact of drought in the South African agricultural sector and the skills implications.

Manfreda, S., McCabe, M. F., Miller, P. E., Lucas, R., Pajuelo Madrigal, V., Mallinis, G., Ben Dor, E., Helman, D., Estes, L., & Ciraolo, G. (2018). On the use of unmanned aerial systems for environmental monitoring. *Remote Sensing*, *10*(4), 641.

Mazarire, T., Ratshiedana, P., Nyamugama, A., Adam, E., & Chirima, G. (2020). Exploring machine learning algorithms for mapping crop types in a heterogeneous agriculture landscape using Sentinel-2 data. A case study of Free State Province, South Africa. *S. Afr. J. Geomat*, *9*, 333-347.

Mugiyo, H., Chimonyo, V. G., Sibanda, M., Kunz, R., Nhamo, L., Masemola, C. R., Dalin, C., Modi, A. T., & Mabhaudhi, T. (2021). Correction: Multi-criteria suitability analysis for neglected and underutilised crop species in South Africa. *Plos one*, *16*(10), e0259427.

Ndlovu, H. S., Odindi, J., Sibanda, M., Mutanga, O., Clulow, A., Chimonyo, V. G., & Mabhaudhi, T. (2021). A comparative estimation of maize leaf water content using machine learning techniques and unmanned aerial vehicle (UAV)-based proximal and remotely sensed data. *Remote Sensing*, *13*(20), 4091.

Persello, C., Tolpekin, V., Bergado, J. R., & De By, R. (2019). Delineation of agricultural fields in smallholder farms from satellite images using fully convolutional networks and combinatorial grouping. *REMOTE SENSING OF ENVIRONMENT*, *231*, 111253.

Ren, T., Xu, H., Cai, X., Yu, S., & Qi, J. (2022). Smallholder crop type mapping and rotation monitoring in mountainous areas with Sentinel-1/2 imagery. *Remote Sensing*, *14*(3), 566.

Xing, H., Chen, B., & Lu, M. (2022). A sub-seasonal crop information identification framework for crop rotation mapping in smallholder farming areas with time series sentinel-2 imagery. *Remote Sensing*, *14*(24), 6280.

CHAPTER 2

A SYSTEMATIC REVIEW OF UAV APPLICATIONS FOR MAPPING NEGLECTED AND UNDERUTILISED CROP SPECIES' SPATIAL DISTRIBUTION AND HEALTH

Abstract: Timely, accurate spatial information on the health of neglected and underutilised crop species (NUS) is critical for optimising their production and to ensure food and nutrition security in developing countries. Unmanned aerial vehicles (UAVs) equipped with multispectral sensors have significantly advanced remote sensing, enabling the provision of near-real-time data for crop analysis at the plot level in small, fragmented croplands where NUS are often grown. The objective of this study was to systematically review the literature on the remote sensing (RS) of the spatial distribution and health of NUS, evaluating the progress, opportunities, challenges, and associated research gaps. This study systematically reviewed 171 peer-reviewed articles from Google Scholar, Scopus, and Web of Science using the PRISMA approach. The findings of this study showed that the United States (n = 18) and China (n = 17) were the primary study locations, with some contributions from the Global South, including southern Africa. The observed NUS crop attributes included crop yield, growth, leaf area index (LAI), above-ground biomass (AGB), and chlorophyll content. Only 29% of studies explored stomatal conductance and the spatial distribution of NUS. Twenty-one studies employed satellite-borne sensors, while only eighteen utilised UAV-borne sensors in conjunction with machine learning (ML), multivariate, and generic GIS classification techniques for mapping NUS' spatial extent and health. The use of UAVs in mapping NUS is progressing slowly, particularly in the Global South, due to exorbitant purchasing and operational costs of these UAV's and restrictive regulations governing their usage. Subsequently, research efforts must be directed toward combining ML techniques and UAV-acquired data to monitor NUS' spatial distribution and health to provide necessary information for optimising food production in smallholder croplands in the Global South.

Keywords: crop health; drones; food security; NUS; precision agriculture; spatial distribution; stomatal conductance; UAV

2.1. Introduction

Inherent water scarcity, which is exacerbated by factors such as climate change, population expansion, and changes in land use (Food and Organisation, 2021, Fan and Rue, 2020, Mabhaudhi et al., 2017), has intensified the pressure on the agricultural sector, particularly in ensuring long-term food supply for the expanding populations (Mugiyo et al., 2021, Joshi et al., 2020). Most of the agricultural production in developing regions is derived from rainfed farms, which occupy 97% of croplands (Li et al., 2021). However, 80% of these croplands are smallholder farms that contribute most of the food production in developing regions (Fan and Rue, 2020, Mabhaudhi et al., 2017). However, these croplands are marginal due to suppressing agronomic and climatological infrequencies. Therefore, climate variability and soil degradation have drastically reduced the production of staple cereal crops, such as maize, amplifying food and nutrition security issues in these regions. This has placed local food systems on the verge of catastrophe. Hence, establishing innovative methods to combat food and nutrition insecurity while optimising production is urgently needed. A paradigm shift from cultivating susceptible cereal crops towards diversifying climate-smart crops, such as underutilised crop species (NUS), is necessary (Muruganantham et al., 2022). NUS, referred to as alternative, traditional, orphaned, or neglected crops, are adapted to flourish in fragile production systems where land degradation and drought are topical . Examples include millet, quinoa, teff, Bambara ground nuts, sweet

7

potato, and taro (Mugiyo et al., 2021, Mabhaudhi et al., 2017, Joshi et al., 2020). These crops are stress-tolerant, require fewer inputs, and are highly adaptable to a broad spectrum of ecological niches (Butilă and Boboc, 2022). Including NUS in fragile production systems is one of many strategies for safeguarding the well-being of minority populations, meeting sustainable development goals (SDGs), leveraging indigenous knowledge systems, and facilitating traditional food and cultural heritages.

A major challenge to mainstreaming NUS is that basic information on genetic and phenotypic traits remains scanty and localised, and productivity is generally low. Generating spatially explicit information on NUS' biochemical and morphological characteristics to optimise their productivity could contribute to their development and promotion. In this regard, spatially explicit, high-throughput phenotyping technologies are required to augment the rapid advancements in phenotyping NUS. This will aid in maximising their productivity in fragmented smallholder croplands.

Generally, field surveys and other traditional methods have been widely used to measure the spatial extent, suitability, growth, and morphological attributes of NUS. However, such methods are time-consuming and expensive, making them unsuitable for continuous precision crop monitoring in areas with numerous crop varieties. Over the past few decades, satellite-based Earth-observation technologies, such as Landsat and MODIS, have effectively monitored plant growth and health changes (Duarte et al., 2022). Satellite-borne remote sensing technologies provide non-invasive, accurate, fast, and cost-effective data for estimating traits such as stomatal conductance and chlorophyll content as a proxy for crop productivity, hence their use (Ankrah et al., 2023). However, the resolution of these freely available satellite sensors provides limited information for high-throughput phenotyping, particularly in the context of highly fragmented and diverse smallholder croplands (Opole, 2012). In this regard, smallholder croplands require very high-spatial-resolution remote-sensing technologies that are affordable and highly efficient (Opole, 2012).

The advent of UAV-based phenotyping allows access to data with extremely high levels of detail and precision. This is ideal for the precise, consistent phenotyping of smallholder farms at the plot level (Opole, 2012). However, the capacity of UAV-mounted sensors to differentiate crop types based on their spectral responses as a mechanism for plausible high-throughput field phenotyping is yet to be determined (Everitt et al., 2007). RS and ML techniques have recently greatly aided high-throughput phenotyping technologies (Everitt et al., 2007). For example, Li et al. (2021) combined three ML techniques, which included random forest (RFR), support vector regression (SVR), and artificial neural network (ANN), in combination with optimal VI's to predict the red-clover dry matter yields in various phenological growth periods.

Despite the usefulness of UAVs, their application in agriculture, rural development, and, more importantly, resource management remains limited (Mabhaudhi et al., 2013). Although some studies have attempted to assess the literature on the application of drone-acquired data (Malinao and Hernandez, 2018, Mazarire et al., 2020), most of these studies did not systematically and quantitatively assess the literature on mapping the spatial distribution and health of NUS crops with a special interest in Global South trends. The objective of this study was to systematically review the literature on the application of UAV remotely sensed data for mapping the spatial distribution and health of NUS, with a particular focus on sweet potatoes and taro. The aim was to understand this field's progress, challenges, opportunities, and gaps. Gaining insights into mapping NUS' spatial extent, morphological features, and biochemical traits through remotely sensed data acquired by UAVs could pave the way for enhancing food production in South Africa's smallholder croplands.

2.2. Materials and Methods
2.2.1. Literature Search

This review followed the Preferred Reporting Items for Systematic Reviews and Meta-Analyses (PRISMA) checklist and guidelines for gathering and analysing the literature. In the initial literature search phase, keywords, terms, and phrases for searching the literature were generated from other literature reviews on NUS (Shao et al., 2020, Che'Ya et al., 2021, Grüner et al., 2021). The methodology followed in this study was adopted from the literature (Butilă and Boboc, 2022, Duarte et al., 2022, Ankrah et al., 2023, Azizan et al., 2021). The following keywords and their variants were used in this study to search for relevant literature: "neglected and underutilised crop species", "orphan crops", "traditional crops", "unmanned aerial vehicle(s)", "drone(s)", "remote sensing", "GIS", "crop health", "stomatal conductance" and "leaf area index", and "chlorophyll". Furthermore, the following PRISMA statement and its variants were used to search for research pertaining to taro and sweet potatoes: "Taro", "sweet potato", "unmanned aerial vehicle(s)", "drone(s)", "remote sensing", "GIS", "crop health", "stomatal conductance" and "leaf area index", and "chlorophyll".

The SCOPUS, Web of Science, and Google Scholar databases were utilised to collect literature using the established key search terms. The PRISMA statement served as the framework for the literature search procedure. This search was not restricted in terms of time. The Google Scholar, Scopus, and Web of Science literature searches yielded 109, 1036, and 90 articles, respectively ($n = 1235$). In preparation for screening, all obtained material was organised in EndNote. The screening procedure considered in this study followed the PRISMA procedure, reported as a flowchart (Figure 2-1). For an article to be considered in the meta-analysis, it had to meet the following criteria;

    (a)   The study focuses on NUS crops, traditional, or orphaned crops, and no other vegetation types (e.g., forests or shrubs) were included, since they denoted different ecosystems;

    (b)   The study focuses on NUS productivity (i.e., LAI, chlorophyll, or stomatal conductance) or spatial distribution;

    (c)   The study was based on UAV or drone remotely sensed data, GIS, or remote-sensing techniques in NUS crop productivity and health mapping;

    (d)   The article was published in an accredited journal;

    (e)   The article was written in English;

    (f)   The article was accessible.

After eliminating all duplicates ($n = 650$), 585 remained. In this case, literature not written in English was excluded from the analysis ($n = 20$). The next step was to assess whether the retrieved literature covered the context of mapping the spatial distribution or assessed productivity elements of neglected and underutilised crops based on remotely sensed data by examining the abstracts. After the title and abstract screening, 332 studies were excluded, and 253 remained. Of the remaining articles, 82 were not accessible as full texts and were excluded, with 171 articles remaining. The full-length articles of the selected abstracts were then sought and downloaded as PDF documents. After the screening procedure, 171 articles were retained (Figure 2-1). Then, the bibliographic information, including author names, year of publication, title, journal name, issue, volume number, keywords, and abstracts, was exported from Endnote as a text file to Microsoft Excel. The Excel database was then used to extract and store qualitative and quantitative data from each article, as indicated in the proceeding phase.
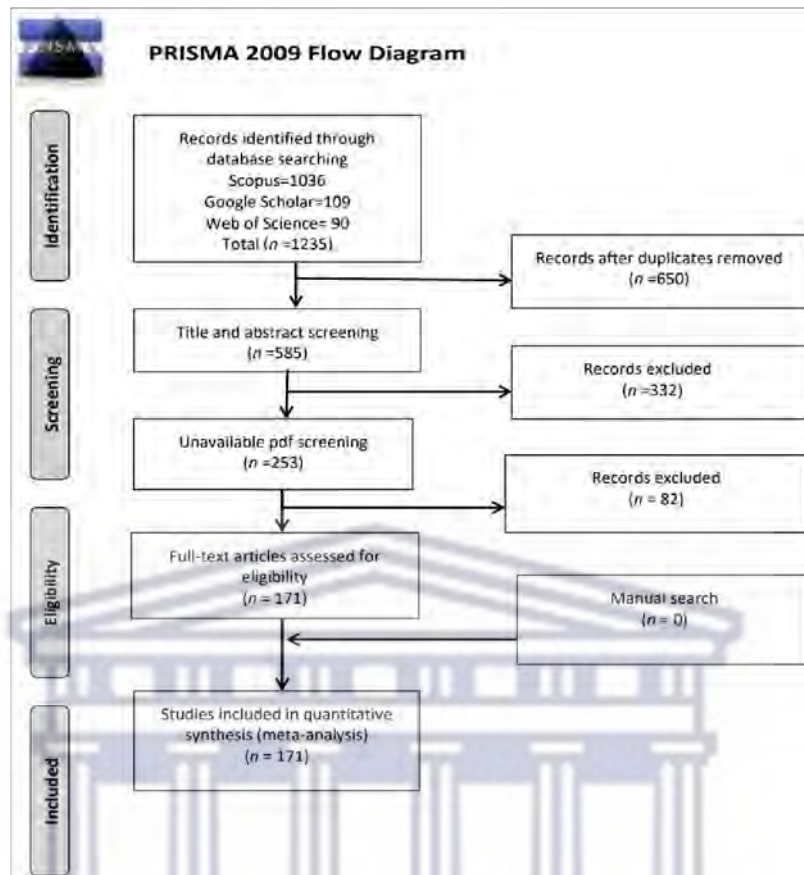
Figure 2-1: PRISMA flow diagram for selection of studies considered in the review.

2.2.2. Data Extraction

In the preceding phase, the extracted data in an Excel database were used to generate and extract information on progress, gaps, challenges, and opportunities of using UAV technologies to map the spatial distribution of different NUS and their health attributes. Specifically, information related to the study country, region, NUS type, the type of crop health attribute investigated, sensor type and platform type, vegetation indices, predictive or classification algorithms, and optimum spectral variables obtained were all retrieved from the literature and documented in the spreadsheet. Some categorical variables were converted into numeric values to facilitate analysing and evaluating trends in the retrieved literature. During this step, relevant bibliometric information was also collected. As mentioned above, the qualitative and quantitative information extracted from each article was added to the Excel spreadsheet with the author names, region, year of publication, article title, journal name, and abstract, among the other bibliometric data gathered.

2.2.3. Data Analysis

The retrieved literature and extracted data were subjected to quantitative and qualitative analyses during this phase. Basic statistical frequencies were calculated for quantitative analysis. In addition, exploratory trend analysis was carried out on the frequency of publications to assess the progress made in mapping NUS' spatial distribution and health attributes utilizing satellite and drone-borne sensors. A bibliometric analysis was also conducted to identify trends in co-occurring key terms from the retrieved literature. The trends were identified by quantitatively examining the occurrence and co-occurrence of key terms in the titles and abstracts using the VOS viewer software. Furthermore, the

10

VOS viewer software used the titles and abstracts of all the retrieved literature (171 articles) and only those based on UAV-derived datasets (18 articles). This assisted in evaluating how concepts and topics evolved in mapping NUS using satellite-based remotely sensed data to drone-acquired data. VOS viewer provides network visualisation of key terms in linked clusters. Creating a map in a VOS viewer includes four steps, which are:

(1)   Selecting a counting method (binary counting or full counting);

(2)   Selecting a minimum number of occurrences for a term (calculating similarity index);

(3)   Calculating the relevance score for the co-occurrence terms and displaying the most relevant items based on this score;

(4)   Displaying a map based on the selected terms.

Since only the occurrence, co-occurrence of key terms, and frequency distributions were computed, bias assessment was not conducted. As aforementioned, the PRISMA checklist (http://www.prisma-statement.org/, accessed on 1 July 2022) was used as a guideline to avoid biased reporting. In this regard, no further robust bias statistical assessments were conducted since only exploratory data analysis was conducted. The review was divided into two main sections to address the research objectives. The first section investigated recent advances in mapping NUS crops' spatial distribution and health using remotely sensed data. This section presented and discussed quantitative literature trends in analysing NUS's spatial distribution and health. Throughout this phase, the crop health attributes, Earth-observation sensors (cameras), sensor platforms, algorithms, and optimal spectral variables used by the community of practice in the retrieved literature were assessed and presented. The last phase discussed the challenges, gaps, and opportunities for knowledge generation in mapping NUS's spatial distribution and health using drone-derived remotely sensed data.

2.3. Results

Figure 2-2 shows the co-occurrence of topical concepts derived from titles and abstracts from (a) studies based on satellite-borne data and (b) drone-acquired data. Figure 2-2a illustrates seven topical clusters in dark blue, light blue, red, green, purple, yellow, and orange for mapping crop spatial extent and health status. The key terms from the "red" cluster were "agriculture", "spad value", "low cost", "remote sensing data", "hyperspectral data", "multispectral data", "VIS", "processing", "size", and "crop field", which directly imply the utility of "low-cost remote sensing" systems for mapping and monitoring NUS crop productivity (spad-value/chlorophyll) with remotely sensed data in smallholder crop fields (Figure 2-2a). The second-largest cluster linked to UAVs was in yellow and contained "growth", "variety", "trait", "detection", "plant-height", "UAVs", "drone", "dsm", "rgb", and "msi". This cluster articulates the use of drone remotely sensed ("UAVs") data in detecting and mapping relevant NUS phenotypical attributes ("growth", "variety", "trait", "detection", and "plant height"). The third cluster in dark blue included 'growth stage', "lai", "crop height", "agdw", "canopy nitrogen", "weight", "fusion", "plsr", and "rmse" as the key terms in order of importance (Figure 2-2). This cluster relates to the estimation of NUS crop productivity attributes ("lai", "crop height", "agdw", "canopy nitrogen", "weight", "lai", "crop height", "agdw", "canopy nitrogen", and "weight") using remotely sensed data and regression techniques. The fourth cluster in green contained "population", "climate change", "water stress", "food security", "African leafy vegetable", "suitable area", "moisture", "SSA" (Sub-Saharan Africa), and "validation", among others. This links to the food and nutrition security issues in SSA, which are highly impacted by climate variability, such that NUS crops ("African leafy vegetable") are the only suitable crops because of their drought tolerance. The fifth cluster, which is light blue, features co-occurring terms, such as "species", "reflectance", "density", "waveband", "nir", "classification", and "palmer amaranth". This cluster relates to the impact of species variability and plant or foliage density, which causes the spectral signatures of NUS crops to vary at different

11

wavebands of the EM spectrum, facilitating optimal classification accuracies. The sixth cluster is characterised by the co-occurrence of terms such as "plant", "amaranth", "phenological", and "growth stage", which relates to the assessment of NUS crops' phenological characteristics.
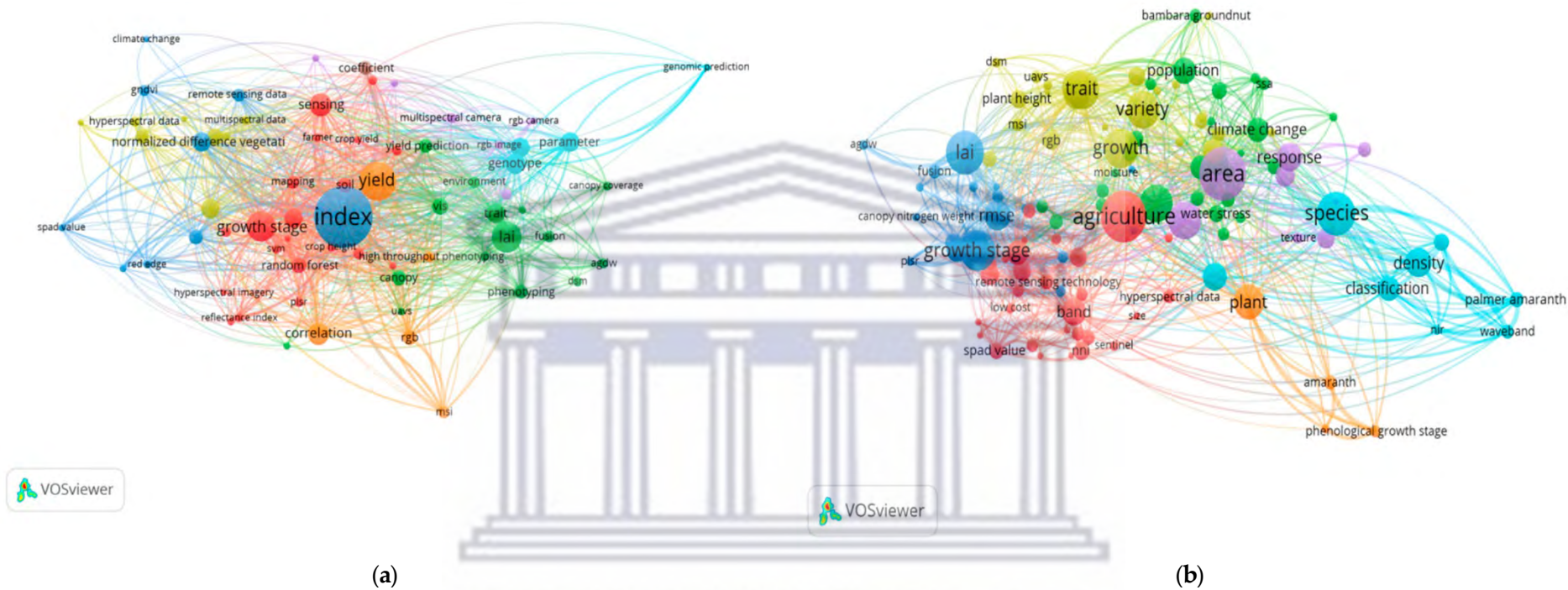
Figure 2-2: Topical concepts identified using a bibliometric analysis of titles and abstracts of articles that utilised (**a**) all remote sensing sensors and (**b**) only drone-acquired data in mapping the NUS. Various coloured lines establish connections between keywords that co-occurred within the same documents.

Figure 2-2b illustrates seven topical clusters in dark blue, light blue, red, green, purple, yellow, and orange, which were derived using abstracts and titles that utilised drone remotely sensed data in mapping NUS crop spatial extent and healthiness. The key terms from the red clusters were "mapping", "crop height", "growth stage", "yield" and, "crop yield", "reflectance index", "hyperspectral imagery", "random forest", and "svm". This cluster relates to using high-resolution remotely sensed data in mapping and monitoring NUS productivity elements, such as growth stage, using machine learning. The key terms in the green cluster are "phenotyping", "LAI", "canopy coverage", "trait", "agdw", "prediction", "uavs", "dsm", "fusion", "VIS", and "environment". This cluster relates to using UAV remotely sensed data that could be fused with other data for assessing the structural attributes of NUS crops (phenotyping). The third cluster in dark blue has the key terms of "remotely sensed data", "gndvi", "normalised difference vegetation", "rededge", "spad value", and "climate change". This cluster relates to the utility of the widely used spectral variables ("gndvi", "normalised difference vegetation", and "red-edge") in monitoring the health of NUS crops. The fourth cluster is orange and has co-occurrence terms, such as "high throughput phenotyping", "rgb", "msi", "yield", and "correlation". This cluster can be attributed to applying the high-throughput phenotyping of NUS through RGB and multispectral spectrums in estimating crop yield. The fifth cluster in light blue had "genotype", "parameter", and "genomic parameters". This cluster suggests examining the genetic composition of NUS crops by assessing optimal parameters to assess and infer their crop health. The sixth cluster has "multispectral camera", "rgb camera", "rgb image". This cluster relates to using general colour imagery (in red, green, and blue spectrums) acquired using drones for mapping NUS. The last cluster has "hyperspectral data" and "multispectral data". This cluster relates to the utility of multispectral and hyperspectral data in mapping and monitoring NUS crop spatial distributions and health.

2.3.1. *Progress in Mapping the Spatial Distribution and Health Status of Neglected and Underutilised Crop Species*

Significant progress has been attained in detecting, mapping, and monitoring NUS crops' spatial distribution and health status using remotely sensed data (Figure 2-3). However, it should be noted that this progress relates to the collective of NUS, but not each individual species. The period between 2003 and 2013 is marked by a low frequency of published literature based on all Earth-observation sensors (Figure 2-3). Between 2014 and 2022, there was a rapid increase in articles that mapped the health and spatial distribution of NUS using all Earth-observation sensors. Again, from 2014 to 2022, there was a rapid growth in the literature that utilised UAV-acquired remotely sensed data to characterise NUS attributes. Despite substantial progress, only a few studies have demonstrated the effectiveness of remote sensing technologies in NUS crop classification, characterising their suitability ranges or discriminating their varieties based on their phenotypic traits. Specifically, only 3% and 4% of the retrieved studies utilised drone and satellite-borne remotely sensed data in mapping the spatial distribution of NUS crops, respectively. However, most of the retrieved literature evaluated NUS phenological and phenotypic characteristics.

15
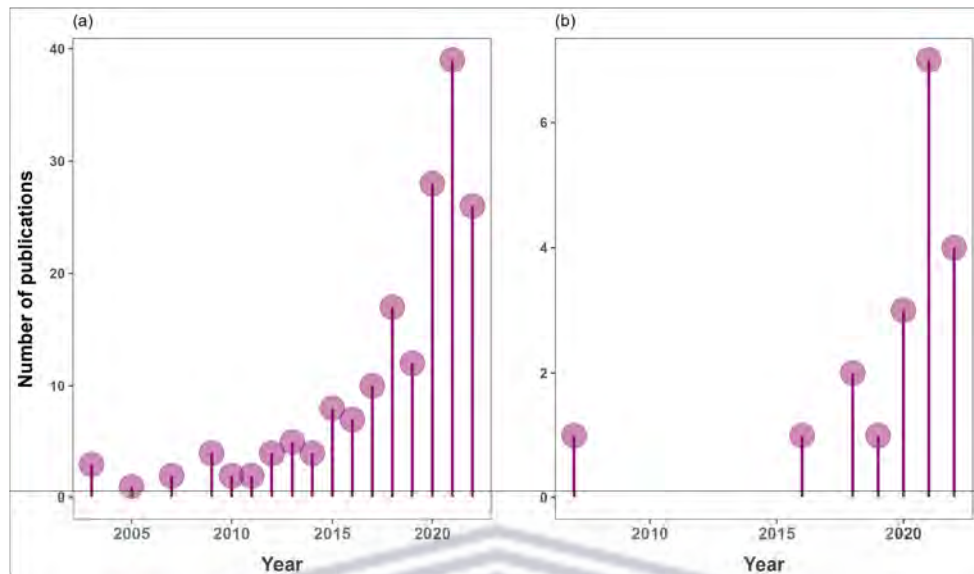
Figure 2-3: Frequency of published articles on remote sensing applications of NUS based on (**a**) all sensors and (**b**) drones.

Regarding geographic distribution, the studies included in the meta-analysis were conducted in 47 countries. Most of the retrieved literature was conducted in Asia, America, and Africa. On a national scale, most of the studies were conducted in the United States of America (n = 18) (Opole, 2012, Everitt et al., 2007), followed by South Africa (n = 18) (Mabhaudhi et al., 2013, Mazarire et al., 2020) and China (n = 17) (Malinao and Hernandez, 2018, Shao et al., 2020), (Figure 2-4). Interestingly, most of the African studies were conducted in southeast Africa.
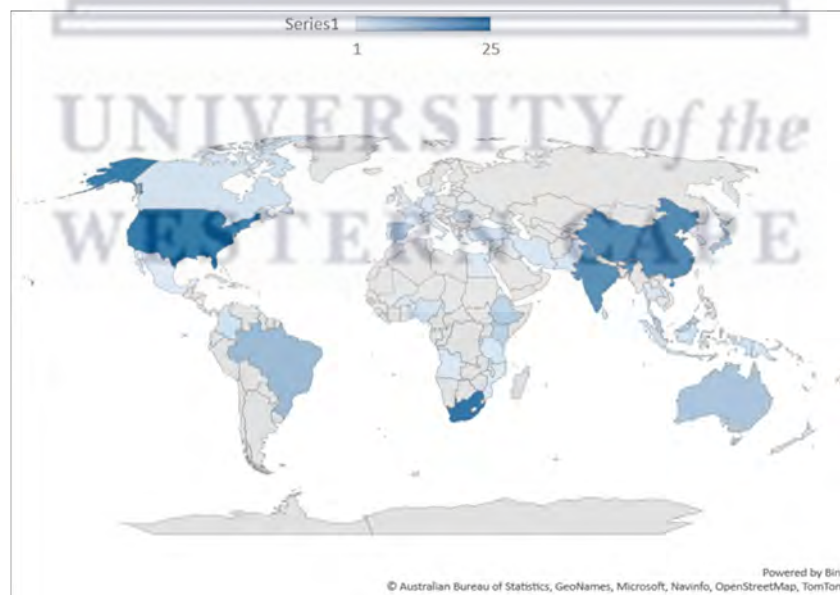
Figure 2-4: Spatial distribution of studies on remote sensing the attributes and spatial distribution of NUS.

The most prevalent NUS in the retrieved literature included sweet potato (Ipomoea *batatas*), sorghum (*Sorghum bicolor*), amaranth (*Amaranthus cruentus*), cassava (*Manihot esculenta*), cowpea (*Vigna unguiculata*), millet (i.e., pearl (*Pennisetum glaucum L.R. Br.*), finger *(Eleusine coracana)*, and proso

16

millet *(Panicum milliaceum)*) (Figure 2-5a). UAV-based remotely sensed data was utilised in mapping the attributes of amaranth (*n*= 6) (Che'Ya et al., 2021), Legume (*Fabaceae*) (*n* = 2)(Grüner et al., 2021), Sweet potato (*n* = 2) (Ramírez et al., 2021), sorghum (*n* = 2)(Shi et al., 2016), and bambara groundnut (*Vigna subterranea*) (*n* = 2) (Suhairi et al., 2020) (Figure 2-5b). Most of the retrieved literature remotely sensed various NUS using hyperspectral data, hence the decline in the frequency of NUS studies that utilised drone and satellite-acquired remotely sensed data (Figure 2-5).
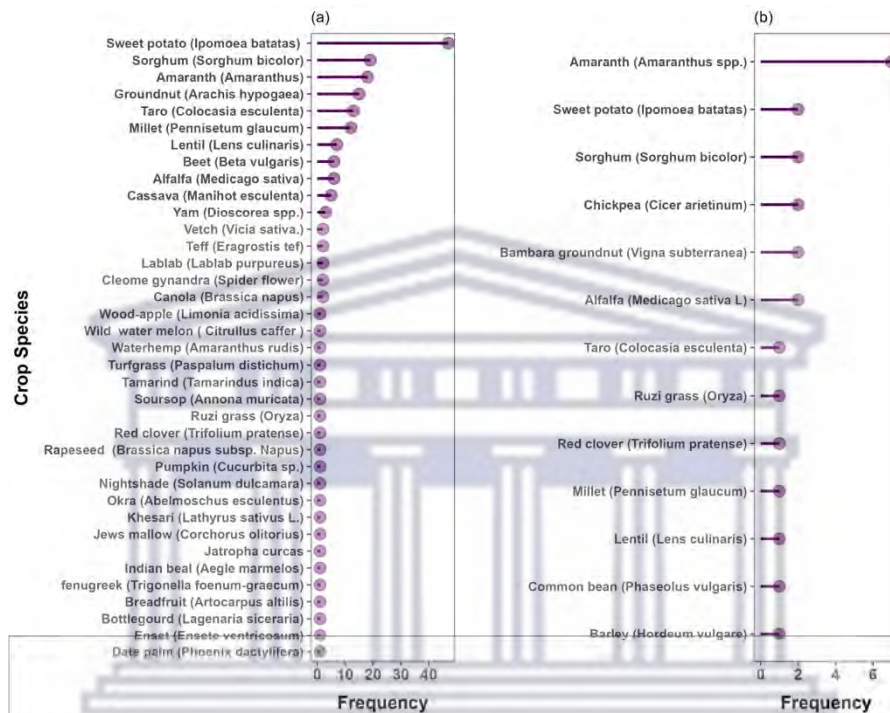
Figure 2-5: Frequency of NUS in the literature remotely sensed using (**a**) all various sensors and (**b**) exclusively drone-borne sensors.

Eight key broad research themes emerged from the reviewed literature on NUS. These include phenotyping, crop genetics, crop productivity, crop physiology, phenology, crop adaptation, classification, and land suitability (Figure 2-6). Most reviewed studies focused on quantifying NUS' physiological and phenological crop traits. A relatively small number of studies characterised crop classification and spatial extent. Five studies discriminated crops based on drone-acquired data, while six articles were based on satellite-borne remotely sensed data (Figure 2-6). The most extensively researched areas based on all satellite-borne sensors included phenology (*n* = 142), crop physiology (*n* = 110), and crop productivity (*n* = 104). When considering only the drone-borne sensors, 16 studies focused on NUS phenology. These studies mainly assessed external crop attributes, such as crop LAI, biomass, crop height, and crop yield periods across the growing season. For example, Jewan et al. (2022) monitored six distinct phenological stages of the Bambara groundnut, estimating its yield. Only nine studies assessed NUS crop productivity, while seven research studies examined NUS crop health and physiology. For instance, Avneri et al. (2023) assessed the utility of a UAV imaging platform coupled with an RGB sensor to monitor chickpea's physiological and morphological parameters, such as LAI, biomass, and yield, during irrigation periods.

Moreover, five studies focused on characterizing NUS crop spatial distribution using classification methods, and four concentrated on NUS's climatic suitability and adaptation. For example, Ramírez et al. (2021) utilised vegetation and temperature indices to characterise various sweet potato genotypes based on productivity and resilience under drought treatments. Only five studies utilised crop phenotyping and breeding techniques. In many instances, crop phenotyping and genotyping included

17

single-nucleotide polymorphism (SNP) markers. SNP markers provide a broad range of applications in various crops, including plant variety and cultivar characterization, quantitative trait loci (QTL) analysis, the production of a high-density genetic map, and genome-wide association analysis (Xia et al., 2019). And lastly, four studies focused on land suitability. Many of the retrieved studies mapped the productivity and water stress-related elements.
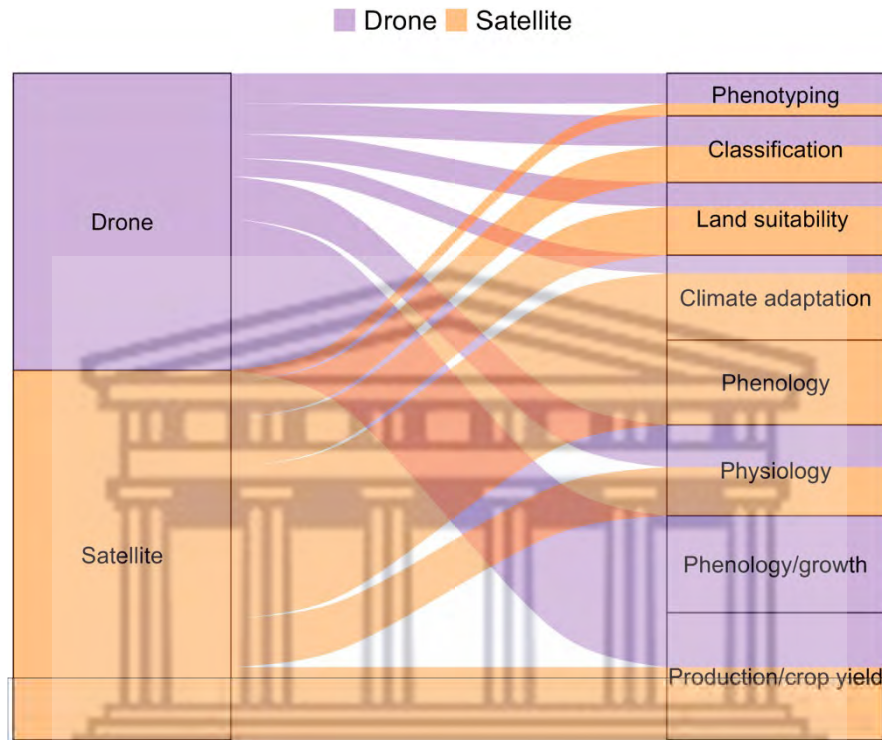
Figure 2-6: Frequency of articles that utilised remotely sensed data from drones and satellites to map NUS attributes. The thickness of the lines represents the frequency in the retrieved literature. (See Supplementary Materials spreadsheet 454 for frequency values).

Specifically, the most extensively researched NUS health attributes included crop yield, growth attributes, crop health, chlorophyll content, leaf water content, biomass, photosynthesis, LAI, stomatal conductance, canopy height, plant weight, leaf nitrogen, and canopy temperature (Figure 2-7a). The most researched NUS attributes in the context of UAV-based remote sensing were crop yield ($n = 15$), growth attributes ($n = 13$), biomass ($n = 11$), crop health ($n = 10$), chlorophyll content ($n = 9$), canopy cover ($n = 7$), plant/canopy height ($n = 7$), LAI ($n = 6$), leaf nitrogen ($n = 5$), leaf size attributes ($n = 5$), leaf water content ($n = 3$), and leaf temperature ($n = 3$). As aforementioned, there were very few studies that classified and characterised the spatial distribution of NUS (Figure 2-7b)(Mugiyo et al., 2021).
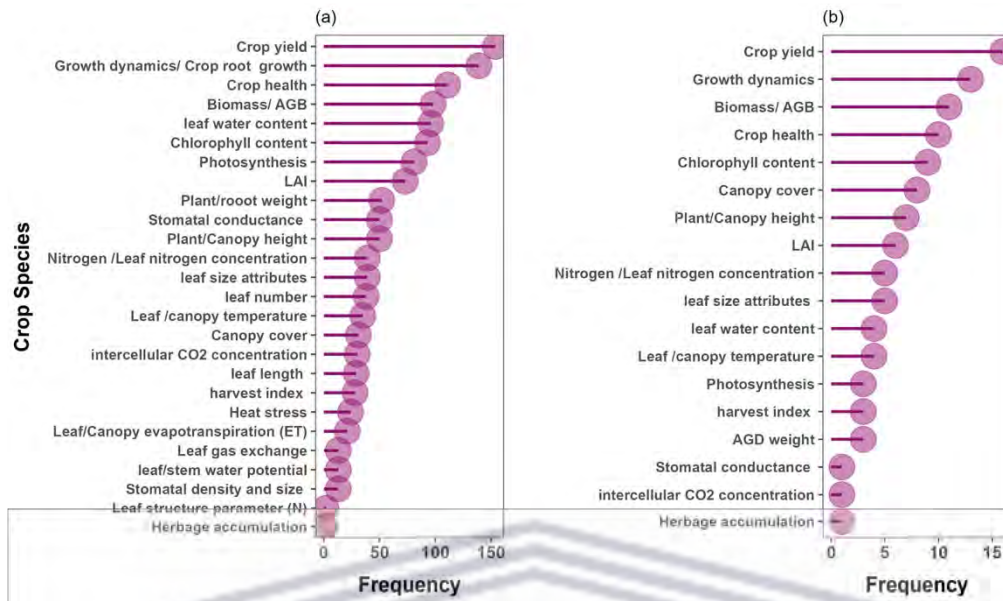
Figure 2-7: Frequency of studies that remotely sensed a specific crop attribute based on (**a**) all satellite and drone-borne sensors and (**b**) drone-borne sensors only.

2.3.2. Assessing Literature on Classification and Stomatal Conductance Estimation of Taro and Sweet Potato Crops

Based on the findings, 12 articles characterised the spatial distribution of various NUS (Figure 2-8). Sweet potato, lentil, and chickpea were the crops that received substantial attention in the literature (Figure 2-8). Overall, a limited number of studies have utilised UAV remotely sensed data to classify NUS. There is a gap in the research focusing on UAV classifications from 2008 to 2019. Furthermore, 2020 was the most predominant year for NUS classification studies. Nevertheless, research on the spatial distribution of NUS remains sparse and limited to developed regions. The increase in literature could point to an increase in the interest in NUS and the general application of UAV-acquired remotely sensed data.
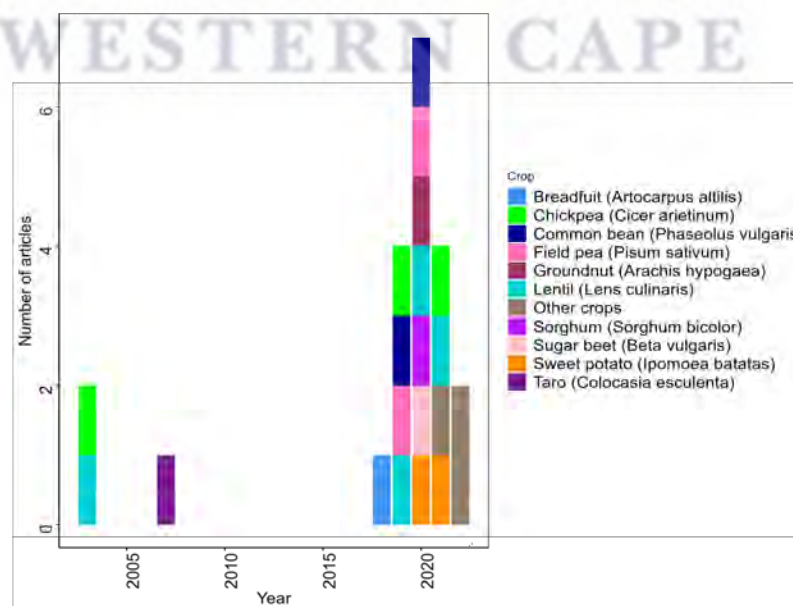
Figure 2-8: Frequency of published articles on NUS classifications

19

Fifty articles estimated the stomatal conductance of NUS based on satellite-borne remotely sensed data. Specifically, studies in the USA and China mapped these NUS mostly using sensors, such as Planet scope, analytical spectral devices, UAVs, MODIS, and Sentinel 2 MSI (Supplementary Figures S1 and S2). There was a modest amount of research on stomatal conductance between 2003 and 2011. However, the literature related to farmscale stomatal conductance increased from 2013 to 2022 (Figure 2-9). In remote sensing, the stomatal conductance of NUS, sweet potato received more research attention (17 studies), followed by taro (5 studies), cowpea (5 studies), sorghum (4 studies), and amaranth (4 studies) (Figure 2-9). Meanwhile, very few studies have been conducted concerning the stomatal conductance of crops such as cassava and millet. These crops were less frequent in the retrieved literature (Figure 2-9a,b) than previously stated. However, there were few studies on remote sensing applications for estimating the stomatal conductance of taro based on UAV-acquired remotely sensed data from the retrieved literature. The specific countries and sensors used in mapping these NUS are detailed in Supplementary Table S6.
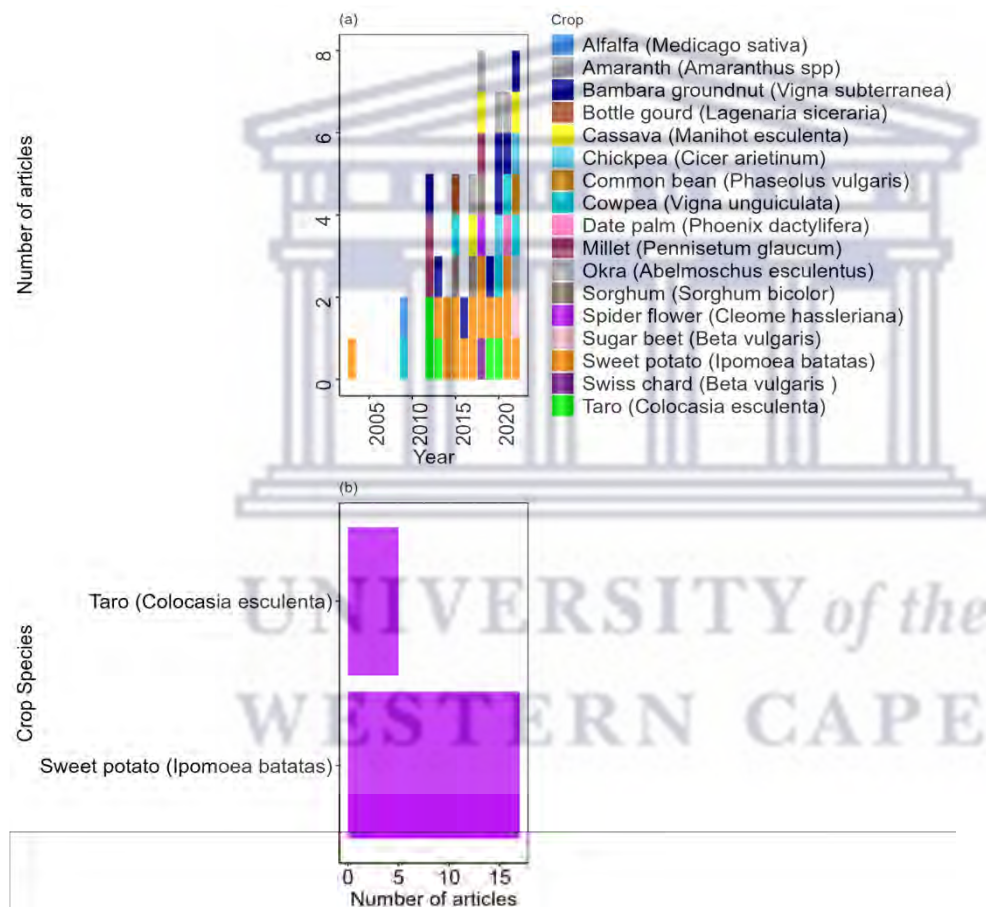
Figure 2-9: Frequency of published articles on mapping NUS stomatal conductance based on (**a**) all sensors for all NUS and (**b**) only on sweet potato and taro

2.3.3. Types of Sensors and Their Spectral Resolutions

The utilization of Earth-observation sensors in the remote sensing of NUS studies is significant. Thirteen different sensor types were noted in the reviewed literature (Figure 2-10). In terms of sensors, the findings of this review revealed that the spectrophotometer was the most widely used sensor for characterizing the health status of NUS, being used in 27 studies. Furthermore, research results indicate that various studies have used handheld hyperspectral devices to acquire in situ remotely sensed data to detect and map NUS biophysical and phenological attributes. The most predominant sensors in the

20

retrieved literature were spectrophotometers (27), UAV-borne sensors ($n = 18$), spectrometers ($n = 18$), radiometers ($n = 11$), Sentinel- 2 MSI ($n = 9$), MODIS ($n = 3$), and LiDAR ($n = 3$) (Figure 2-10a). Meanwhile, the most frequently used drone-borne sensors were RGB cameras (in 11 studies)(Parra et al., 2021), RedEdge-MX (in three studies) (Pereira et al., 2022), and Canon (in three studies)(Jewan et al., 2022). These were followed by thermal cameras (Sobejano-Paz et al., 2020), Parrot Sequoia, Micasense Altum (Ramírez et al., 2021), CMOS cameras (Liu et al., 2021), and MCA6 (Che'Ya et al., 2021) in order of frequency in the retrieved literature (Figure 2-10b).
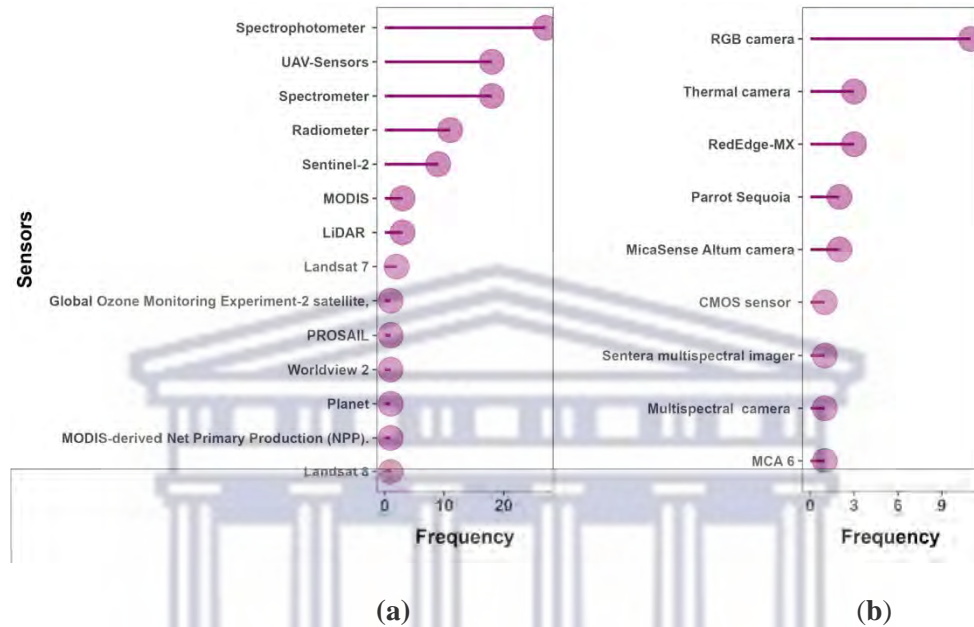
Figure 2-10: Frequency of (**a**) all sensor and (**b**) drone-borne sensors that have been used to map the spatial distribution of NUS and their attributes. (RGB represents red, green, and blue).

Across all platforms, the multispectral (broadbands) were highly utilised in the literature compared with hyperspectral (narrow) bands. The visible section of the electromagnetic spectrum, specifically the red, green, and blue (RGB) sections, are primarily the most utilised wavelengths in mapping the spatial distribution of NUS crops and their health attributes (Figure 2-11). Specifically, the RGB sections of the electromagnetic spectrum (EM) were utilised in 17, 18, and 49 studies based on drone, satellite-borne, and hyperspectral sensors, respectively (Figure 2-11). The second most widely used section of the electromagnetic spectrum in the literature was the NIR section, utilised in 12 studies with drone-acquired data, 18 studies with satellite-borne sensors, and 38 with spectroscopy. When considering only the drone-borne sensors, seven studies utilised the electromagnetic spectrum's red edge (RE) section. In comparison, 12 studies utilised the satellite remotely sensed RE section, while 44 studies utilised RE bands from spectroscopy. Few studies attempted to engage the thermal bands in characterising the spatial distribution of NUS and their health attributes. Four studies used drone-acquired thermal remotely sensed data and a similar number of studies used satellite-acquired thermal bands. Also, only five studies utilised the spectroscopy thermal section of the EM (Figure 2-11). When considering drone-borne sensors, only 2 studies utilised the ultra-violet (UV) and 38 studies used the spectroscopy UV section of the EM.

21
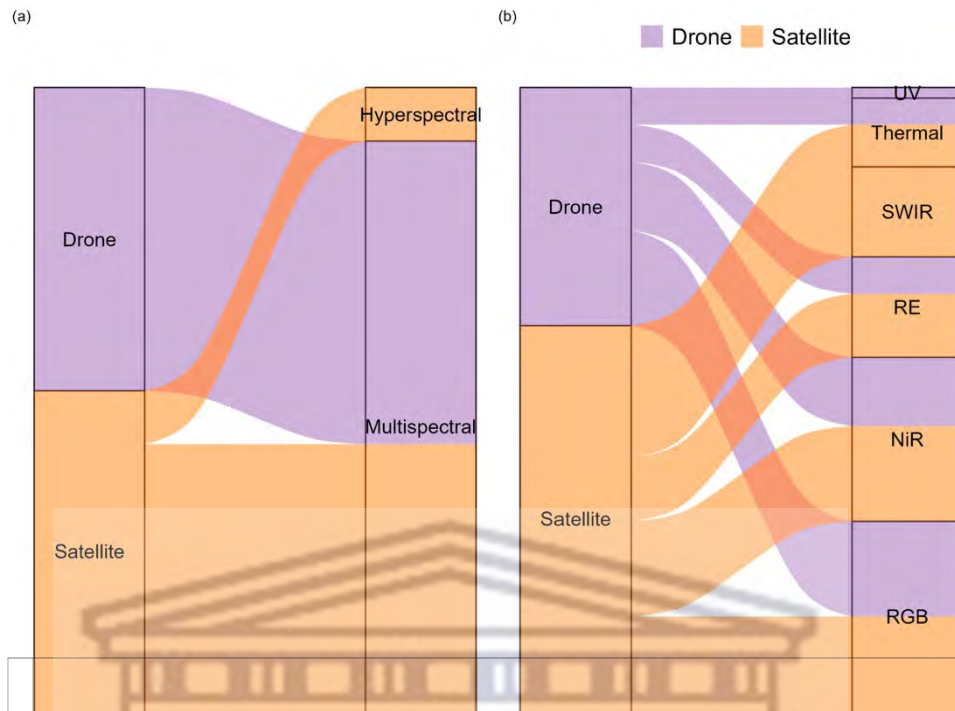
Figure 2-11: Visual distribution (frequency) of (**a**) Spectral characteristics of satellite and drone borne sensor, and (**b**) specific sections of the electromagnetic spectrum they covered in the literature (See Supplementary Table S2 for frequency values). UV is ultraviolet, SWIR is shortwave infrared, RE is red edge, NiR is near-infrared, and RGB is the red, green, and blue spectra. (See Supplementary Materials spreadsheet for frequency values.

2.3.4. UAV Platforms Utilised in the Literature

Regarding the drone platforms, the DJI fleet was utilised in a marginally higher number of studies in relation to all other platforms ($n = 12$). The Octocopter (Huang et al., 2018), mikrokopter (Che'Ya et al., 2021), and Sensfly eBee (Li et al., 2021) each featured in separate single studies (Figure 2-12b). When assessing the frequency of each specific sensor in the retrieved literature, it was observed that the DJI Phantom 4 Pro was the most frequently used platform across the board (appearing in six studies) (Jewan et al., 2022), followed by the Octocopter UAV, which was utilised in one study (Sankaran et al., 2018) (Figure 2-12a). Furthermore, quadcopters were the most widely used drone platform type, followed by fixed-wing drones (Figure 2-12b). Quadcopter drones were utilised in 16 studies, and fixed-wing drones were used in only 2 studies. Furthermore, the DJI UAVs were popular in mapping a wider range of crops and research domains when compared with other platforms (Supplementary Tables S3 and S4). This could indicate that these platforms are more popular and versatile.

22
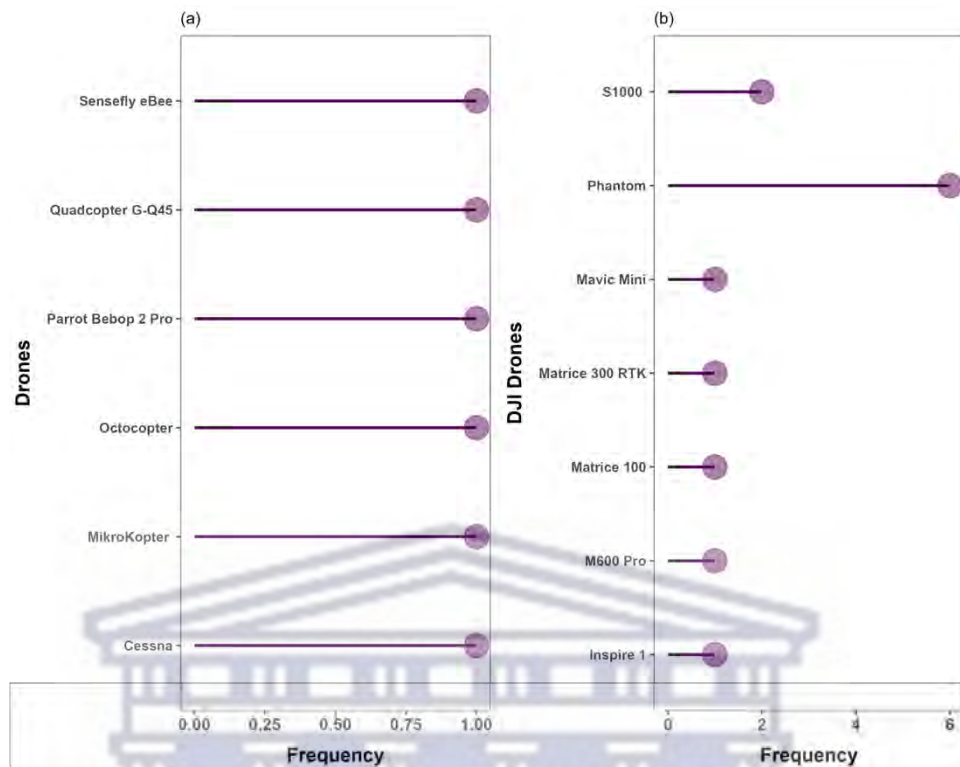
Figure 2-12: Frequency of (**a**) summarised drone platforms (**b**) and DJI drones utilised in the literature to map the spatial distribution of NUS and their health attributes.

2.3.5. Derived Vegetation Indices in Remote the Spatial Distribution and Health of NUS Crops

Algebraic combinations derived from multiple spectral bands, which are commonly known as vegetation indices (VIs), were used to estimate vegetation vigour and vegetative characteristics (canopy biomass, absorbed radiation, and chlorophyll content) in the retrieved literature (Candiago et al., 2015). Furthermore, the visible (green: 530–570 nm, red: 640–680 nm, and red edge: 730–740 nm), near-infrared (770–810 nm), and red edge (730–740 nm) sections of the electromagnetic spectrum were common in studies that assessed crop health. The reflectance values of these prominent wavelengths are generally used to calculate vegetation indices, such as the normalised difference vegetation index (NDVI), NDVI–red edge (NDRE) simple ratio (SR), green normalised difference vegetation index (GNDVI), green chlorophyll index (CIgreen), and soil-adjusted vegetation index (SAVI), which were frequently used in the retrieved literature (Figure 2-11). All VIs that were used in the literature are also listed in Supplementary Table S1. In this regard, there is still room to assess more image transformations in mapping the spatial distribution of NUS, such as sweet potato and taro, dominant in smallholder croplands.

2.3.6. Statistical and Machine Algorithms Were Utilised in Mapping the Spatial Distribution and Health of NUS Crops

This study's findings show that several basic statistical procedures, simple regression techniques, and machine learning techniques were used in mapping the spatial distribution and health of NUS crops. These algorithms can be further subdivided into three categories, which are (i) generic GIS classifications, (ii) machine learning and regression techniques, and (iii) multivariate techniques. Based on Figure 2-13, the main machine learning algorithms utilised in conjunction with drone-acquired data were linear regression (39%), random forest (28%), support vector machine (SVM) (22%), and artificial neural network (ANN) (17%), in order of frequency in the literature. Linear regression techniques were

23

the most frequent regression algorithms in assessing NUS crop health (Figure 2-12) (Suhairi et al., 2020, Huang et al., 2018). The frequency of linear regression and machine learning-based algorithms was also detected during the bibliometric analysis, as illustrated in Figure 2-2b (red cluster). The RF was the second most widely used machine learning ensemble, followed by SVM, PLS, linear discriminant analysis, and artificial neural network (ANN), in order of frequency in the retrieved literature.

Figure 2-13: Frequency of machine learning and general regression techniques used in remote sensing NUS attributes based on all sensors and drone-borne sensors. (GLM is generalised linear model, RF/DRF is random forest, LR is linear regression, SVM is support vector machine, OLS is ordinary least squares regression, ANN is artificial neural network, BPNN is back propagation neural network, GAM is generative adversarial networks, LDA is linear discriminant analysis, and PLS is partial least squares regression. (See Supplementary Materials spreadsheet for frequency values).

In terms of generic statistics and classification techniques, Pearson correlation, ANOVA, maximum likelihood (ML), OBIA, and the empirical line method (ELM) were the most frequently utilised algorithms based on satellite and drone-borne remotely sensed data (Figure 2-14). The Mahalanobis distance, parallelepiped, k-means, and canny edge filtering were some of the popular generic classification algorithms used to map NUS based on satellite and drone-acquired remotely sensed data. Studies that were based on generic classification were relatively few for each algorithm (<5) when compared with all other algorithms utilised in the retrieved literature (Figure 2-14a). Generic classification procedures, such as the analytical hierarchical process (AHP), cluster analysis, fuzzy logic, and multilayer perceptron, have not yet been utilised in conjunction with drone-acquired remotely sensed data for crop mapping (Figure 2-14b).
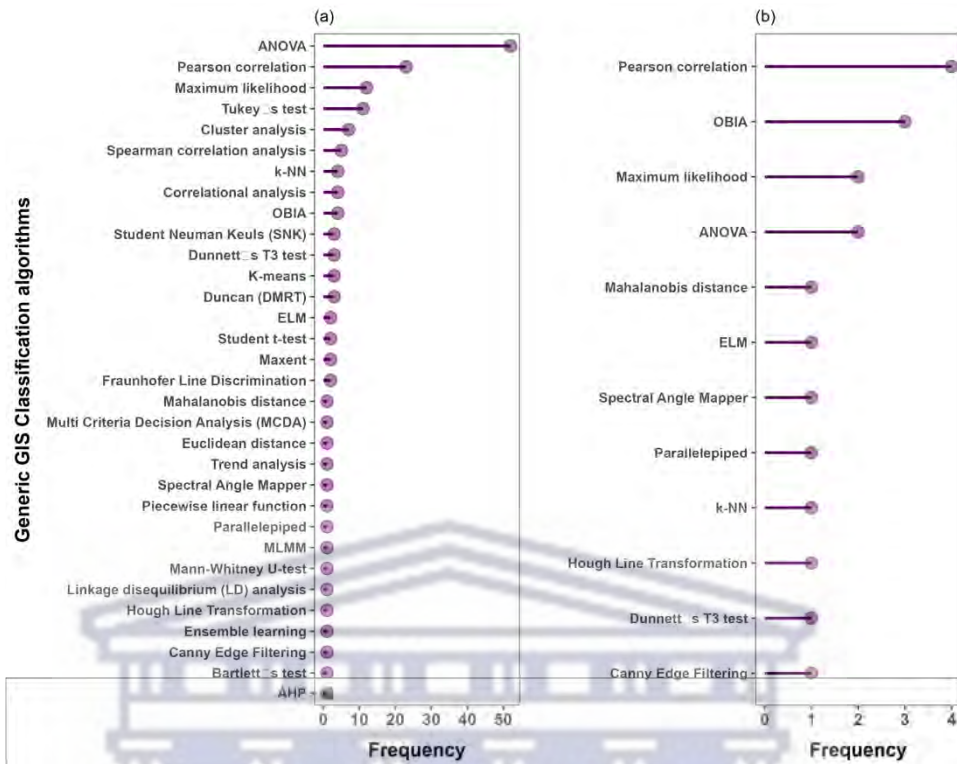
Figure 2-14: Frequency of generic GIS classification techniques used in remote sensing NUS attributes based on (**a**) all sensors and (**b**) drone-borne sensors.

Regarding multivariate techniques, PCA followed by cluster analysis and multiple regression were the most frequently used algorithms based on satellite and drone-acquired data combined (Figure 2-15). Studies based on linear mixed model and machine learning algorithm classifications were relatively few (<5) compared with PCA and cluster analysis. There seemed to be scanty literature (<5) that utilised multivariate techniques in conjunction with drone-acquired data for mapping the spatial distribution of NUS and their health attributes.

Figure 2-15: Frequency of multivariate techniques used in remote sensing NUS attributes based on all sensors and drone-borne sensors. (See Supplementary Materials spreadsheet for frequency values).

25

2.4. Discussion

2.4.1. Evolution of Drone Technology Applications in Remote Sensing

There have been numerous shifts in the key terms of the literature on the remote sensing of the distribution and health status of NUS crops. Specifically, there was a shift in the topical terms from mere correlations based on RGB remotely sensed data in mapping NUS attributes between 2018 and 2019 to using hyperspectral data in predicting and mapping NUS crop health attributes, such as yield and AGB, in 2020. Currently, research efforts are being exerted towards the fusion of drone-acquired data with satellite remotely sensed datasets in conjunction with robust machine learning algorithms, such as PLSR and SVM, in characterising yield genotype canopy coverages, amongst others. Progress is discussed in detail in the following sub-sections.

2.4.1.1. Frequency of Publication and Their Geographic Distribution

This study's findings revealed that the articles that utilised drone-based remotely sensed data in mapping the spatial distribution, health, and productivity elements of NUS crops increased gradually from 2009 to 2014 (Figure 2-3). This trend was similar to that of published studies that utilised satellite remotely sensed data (Figure 2-3b). The rapid changes, improvements, and increased accessibility of Earth-observation sensors and platforms could explain this. That period was characterised by limited access to high spatial-resolution remotely sensed data for crop monitoring. These findings are echoed by numerous reviews, which include Mutanga et al. (2017) and Sibanda et al. (2021b). In the context of satellite-borne sensors, the research period from 2009 to 2014 was mainly dominated by the utility of Landsat and MODIS (Funk and Budde, 2009). These sensors were incapable of capturing the land fragmentation and heterogeneity associated with NUS. Moreover, the only accessible fine-spatial-resolution images were those procured from commercial sensors, such as WorldView and QuickBird. These sensors are often associated with exorbitant costs that restrict research activities, especially in under-developed countries. The potential of NUS was still being researched during that period, and research investments were not channelled to the use of satellite-borne sensors. However, the period between 2015 and 2022 was marked by a rapid increase in drone platforms and associated sensors, hence the rapid increase. This would suggest an increase in the interest in NUS and the improved capabilities of drone and satellite sensors. Interestingly, most of these drone-related studies were conducted by universities and agricultural institutions in China, America, South America, Europe, and Australia (Supplementary Table S6). This could be attributed to the fact that the earliest drone technologies emerged in these regions between 1849 and 1916 (Sibanda et al., 2021b). Also, some of the mentioned countries are pioneers in the research and preservation of NUS. Since then, technology has been spreading and advancing. As a result, there is an increasing need to improve the application of UAV technologies for precision agriculture in accordance with NUS spatial extent and health assessments. Furthermore, it was noted that most of the studies were conducted on experimental plots, in some instances with irrigation facilities at university experimental plots. Generally, commercial farmers who are endowed with resources are the most dominant users of these technologies in under-developed regions, such as southern Africa. No studies were conducted in rainfed smallholder croplands in the retrieved literature on remote sensing NUS. The findings of this study imply that these technologies are slowly being embraced and incorporated from developed countries to the Global South.

2.4.1.2. NUS Crop Attributes That Have Been Remotely Sensed Using Drone-Acquired Data

The limited number of studies focusing on NUS suggests that the utility of UAVs is still in its infancy in practice. In the retrieved literature, there were no studies that indicated whether there are any spectral

26

libraries that have been generated for NUS. This could imply that, despite the significant efforts in advancing the remote sensing of NUS, more efforts are still required to match with other crops, such as maize. Although the results revealed that, from the year 2020 going onwards, there has been an increase in the number of studies, (Merkert and Bushell, 2020) noted that there are still few research efforts directed towards NUS (Figure 2-8). In developing countries where NUS are beginning to gain recognition, the limited number of studies could be attributed to the expenses associated with drones and their accessories. Furthermore, the requirements to license and operate a drone in developing countries are still a challenge (Goel et al., 2021, Velusamy et al., 2021). These findings underscore the importance of increasing knowledge and literature in the context of NUS to improve our insights into them as alternative crops. The findings showed that 16 studies assessed crop phenology, 9 were on productivity, and 7 explored physiology using drone-acquired remotely sensed data. However, most of the retrieved studies focused on interrelated themes, which explains the high frequencies of studies on each crop attribute. Crop attributes, such as physiology, productivity, and phenology, are mutually dependent elements that determine crop development and health. According to Fageria et al. (2006), crop physiology in particular is a useful crop attribute that could be used to quantify crop growth for optimising crop yields.

The findings of this study showed that 11 NUS crop productivity elements, namely, crop yield, crop growth, crop health, chlorophyll content, biomass, LAI, canopy height, cover, leaf nitrogen, leaf water content elements, and stomatal conductance, were the most widely researched (Sobejano-Paz et al., 2020, Aboutalebi et al., 2018). These are the principal optical crop productivity and health elements; hence, they are anticipated to be covered extensively in the literature on agricultural remote sensing applications. The primary function of remote sensing applications is to optimise yield production and the supply of nutrient-rich foods (Sishodia et al., 2020). Additionally, all research efforts have been exerted towards optimising agricultural productivity (increasing yields) and addressing sustainable goals 1 and 2 on hunger and poverty (Van Wart et al., 2013, Duku et al., 2018, Mutanga et al., 2017, Jewan et al., 2022). Subsequently, yield is expected to be the most intensely researched NUS crop attribute based on drone and satellite-borne remotely sensed data (Van Wart et al., 2013, Jewan et al., 2022).

It must be noted that, in most instances, yield is synonymous with AGB. The findings of this study showed that 61% of drone-based remote sensing studies on NUS estimated crop AGB. AGB is an important parameter that can also be utilised to predict crop growth, yield. and productivity (Liu et al., 2022b). The findings of this study also showed that LAI is one of the most researched elements of NUS, featuring in 33% of the retrieved literature. This can be attributed to the fact that LAI is yet another accurate proxy of plant growth, as illustrated in Figure 2-7. It has been extensively proven to correlate with other plant growth indicators, including chlorophyll content, biomass, and, to some extent, yield (Ali and Imran, 2020, Buthelezi et al., 2023). LAI represents the structural attributes of the leaf components estimated by the area of the leaf per unit of ground surface area (Wu et al., 2022). The area covered by leaves per unit of the ground surface changes with the variations in a crop's growth stage. This variable can accurately represent the space available for photon interception across a crop's phenological stages, which can affect yield (Chapepa et al., 2020) (Blessing et al., 2020). Subsequently, LAI is a plausible indicator of canopy health and development that needs to be accurately mapped (Xue and Su, 2017). In addition, LAI can affect the surrounding canopy and the microclimate, e.g., radiation from the sun is intercepted by leaves, affecting transpiration and leaf surface temperature. This ultimately influences the photosynthetic nature of leaves and the stomatal conductance (Williams et al., 2022). In this regard, LAI was one of the most important NUS attributes in the retrieved literature.

The chlorophyll content is another predominant NUS attribute covered by 50% of the retrieved literature in this study (Raji et al., 2017, Singhal et al., 2019). The chlorophyll content of leaf tissue indicates a plant's physiological structure, nutritional composition, and health (Brewer et al., 2022, Tahir et al., 2018). The antenna pigments in chloroplasts absorb incoming solar radiation during photosynthetic activities (Monteoliva et al., 2021). The resulting radiation is then transferred to the

27

reaction centre pigments, which discharge electrons to activate the photochemical process (Monteoliva et al., 2021). Specifically, chlorophyll is a very relevant and optical indicator of crop health, since chlorophyll highly absorbs energy in the red (650–700 nm) and blue (400–500 nm) regions of the electromagnetic spectrum to increase photosynthesis. The types of chlorophyll responsible for the higher absorption within the visible spectrum are chlorophylls a and b (Monteoliva et al., 2021). In this regard, there is a positive relationship between the leaf total chlorophyll content (chlorophyll a+b), the solar radiation absorbed by the leaf tissues, and the photosynthetic rate of the crop (Monteoliva et al., 2021). Subsequently, a leaf's biophysical pigments and biochemical photosynthetic processes are linked to a plant's health and productivity. Hence it is considered a suitable proxy for crop health in the light of agricultural remote sensing applications (Tahir et al., 2018).

Meanwhile, the chlorophyll content has been widely proven to correlate positively with the nitrogen content in various crop species (Bojović and Marković, 2009, Musa et al., 2016, Blumenthal et al., 2020, Liu et al., 2019). Indeed, approximately 75% of the total nitrogen is stored within the leaf chloroplasts (Li et al., 2013). In this regard, the findings of this study revealed that 28% of the retrieved studies estimated nitrogen concentration using drone remotely sensed data, thus rendering the nitrogen content another sought-after attribute of NUS. An elevated nitrogen concentration is associated with an increased CO2 assimilation rate and stomatal conductance in the crop, which aids in producing chlorophyll and green pigments. For example, Muhammad et al. (2021) conducted a related study to evaluate the impact of various nitrogen and phosphorous levels and beneficial microbes on enhancing canola productivity. The results revealed that nitrogen applied at a rate of 180 kg ha^{-1} increased plant pods, seed pods, the seed-filling duration, seed weight, biological yield, and seed yield.

The findings of this review also showed that crop structural parameters, such as crop height, crop growth, and canopy cover, were explored in 39%, 72%, and 39% of drone- based studies, respectively. These crop structural parameters are related to AGB, LAI, and the chlorophyll content, which are measured and used to predict the yield. Hence, these parameters are directly linked to food and nutrition security. The crop height and growth attributes directly interact with the incident electromagnetic energy that is typically measured and used to model productivity. Furthermore, these physiological crop variables are sensitive to variations in environmental conditions. These include environmental (precipitation, temperature, soil type, etc.) and biochemical conditions (fertility, weeds, pests, and diseases). In this regard, these structural attributes are instrumental in monitoring the health of crops to optimise crop production; hence, significant research efforts were devoted to them.

This study showed that stomatal conductance was another optimal NUS health parameter assessed by 11% of the retrieved studies that utilised drone data. The stomatal conductance measures the degree of stomatal opening and can indicate leaf gas exchange (Iseki and Olaleye, 2020). The stomatal conductance is strongly associated with leaf transpiration rates, photosynthetic efficiency, chlorophyll concentration, and nitrogen concentration (Wijewardana et al., 2019). Specifically, periods of crop water stress or drought stress will be limited by the CO_2 concentration at carboxylation sites (Cc) inside the chloroplast. This is determined by the CO_2 diffusion components, i.e., stomatal conductance (gs) and mesophyll conductance (gm) (Ouyang et al., 2017). Particularly, the stomata control the CO_2 diffusion into the leaf tissue and water diffusion out of the plant. Therefore, it has been proven that, under water deficit conditions, plant stomata will close to prevent major water loss. This consequently decreases photosynthesis via the decreased influx of CO_2 (Ouyang et al., 2017).

In this regard, higher stomatal conductance and high photosynthetic efficiency are associated with limited moisture stress. Hence, these plants will be healthier, with a higher chlorophyll content and green pigment. In this regard, stomatal conductance was among the most researched crop attributes in the retrieved literature because it is an accurate proxy of moisture stress and the health status of crops (Sobejano-Paz et al., 2020, Iseki and Olaleye, 2020). In fact, the stomatal conductance aids in water use and irrigation scheduling as a pathway towards optimising food production. A study by Chai et al. (2016) measured the morpho-physiological traits of Bambara groundnut exposed to progressive mild

28

drought in a controlled environment. Drought stress reduced stomatal conductance significantly ($p < 0.01$). Furthermore, higher stomatal density and reduced leaf area were observed in drought-treated plants ($p < 0.01$). This suggests that NUS crops are more resistant to biotic and abiotic stresses, such as drought and water stress. Above all, this indicates the prospects of using stomatal conductance as a proxy for understanding crop water stress.

In most studies from the retrieved literature, there were strong correlations between the stomatal conductance and water relation status or leaf water content (Sobejano-Paz et al., 2020, Awais et al., 2022a, Awais et al., 2022b). Specifically, 17% of studies based on drone remote sensing researched the NUS leaf water content. Water content is an important indicator of crop health (Sobejano-Paz et al., 2020, Awais et al., 2022a, Awais et al., 2022b). A plant with higher water potential will produce greener pigmentation and have increased crop productivity. According to Ouyang et al. (2017), under water deficit or conditions of mild water stress, the stomatal conductance, internal CO_2 concentration, and net assimilation rate within a plant will decrease, and the A/G ratio will increase. Various studies assessed and reported that crop water stress allows for a decline in the total chlorophyll of various crops and a decline in plant productivity (Majid and Roza, 2012, Maes and Steppe, 2012, Pineda et al., 2021). This includes non-stomatal regulation of photosynthesis, a decline in light and the CO_2 concentration, a reduction in photochemistry, declining activity of photosynthetic enzymes, and lowered mesophyll conductance. For instance, Chibarabada (2018) assessed the stomatal conductance of three grain legume crops (groundnut, dry bean, and Bambara groundnut) grown under three water treatments. Their results indicated that, under varying water regimes, NUS crops adjusted to constrained soil water through stomatal regulation and reduced canopy size. Furthermore, Bambara groundnut showed a positive attribute under water-limited conditions. It had the lowest stomatal conductance under all watering regimes compared with the other crops. In the context of remote sensing, these plant conditions then impact the interaction between different sections of the EM spectrum and the various magnitudes of crop water stress (Bellvert et al., 2014). This example illustrates why stomatal conductance and foliar temperature were significantly considered in NUS production.

2.4.1.3. *Sensors and Platforms That Were Used in Remote Sensing NUS*

The dominance of drone-based remote sensing studies on NUS could be explained by the fact that most of these crop species are orphaned, neglected, and underutilised. In this regard, they are generally planted in smaller areas than mainstream crops, such as maize. On the other hand, very few freely accessible satellite-borne sensors offer finer spatial-resolution data suitable for capturing the variety of crops in fragmented smallholder croplands. Subsequently, the freely available datasets from moderate-spatial-resolution sensors, such as Landsat and Sentinel 2 MSI, cannot capture the dynamics of crops in smallholder farms when compared with UAVs. Drones offer rapid, ultra-fine-spatial resolution data, often to a sub-metre resolution, in a cost-effective manner (Gray et al., 2018).

Furthermore, the user determines the spatial and spectral resolution of the drone remotely sensed data, offering endless opportunities in crop phenotyping from the stand level to field scale. Sentinel-2 MSI was the most widely used satellite-borne sensor in mapping the spatial distribution, health, and productivity parameters of NUS crops. Sentinel 2 MSI has a minimum spatial resolution of 10 m and a spectral resolution that covers the red edge section of the electromagnetic spectrum, which is sensitive to crop health (Clevers and Gitelson, 2013). These attributes make Sentinel 2 MSI the second most suitable sensor among UAV-borne sensors in mapping NUS, often grown in small, fragmented fields. In terms of the drone sensors, our findings showed that the RGB and multispectral cameras (>three bands) were the most frequently used in the retrieved literature when compared with hyperspectral sensors (Figure 2-11). This could be explained by the exorbitant expenses associated with hyperspectral sensors to multispectral cameras. RGB and multispectral cameras generally cover the visible, including the red edge and the NIR, sections of the EM spectrum. This is usually in not more than six broader spectral band resolutions (i.e., MicaSense Altum) (Ndlovu et al., 2021).

Meanwhile, most hyperspectral sensors, such as the Cubert S185 hyperspectral sensors, cover a wavelength range between 450 and 950 nm. These are composed of 125 channels at a resolution of 8 nm at 532 nm, ranging from visible to near-infrared (450–950 nm) with a sampling interval of 4 nm (Zheng et al., 2020). Furthermore, the RGB type of sensors offers models with less accuracy when compared with multispectral or hyperspectral images covering a wider spectral range (Nyman, 2018). Hyperspectral sensors have been widely proven to offer robust narrow, relatively contiguous bands, although multicollinearity issues often impact them. Despite their exorbitant prices, these bands are more sensitive to subtle crop variations compared with broadband sensors (Marshall and Thenkabail, 2015, Thenkabail et al., 2013, Thenkabail et al., 2002).

The findings of this study also showed that very limited studies utilised cameras that captured data in the red edge section of the EM spectrum. The multispectral sensors that captured the red edge section in the retrieved studies were the MicaSense series, and Red-edge MX utilised in two and three studies, respectively. The red edge section has been vastly proven to be sensitive to minute variations in plant attributes associated with health and productivity, such as the LAI, chlorophyll content, stomatal conductance, AGB, and nitrogen content (Xue and Su, 2017). For instance, the increased chlorophyll content, LAI, and biomass generally result in increased absorption in the red region, pushing the red edge to longer wavelengths (Mafuratidze, 2010). Considering this phenomenon, the red edge has become one of the most sought-after sections of the EM spectrum in crop monitoring (Zhang et al., 2019b). In this regard, there is a need for more studies that assess the robustness of hyperspectral and red-edge sensors in mapping NUS attributes. This will improve the assessment and monitoring of the health elements of NUS if their productivity is optimised based on the information derived from remotely sensed data.

The findings of this study also showed that the multirotor drones were the most widely used platforms in the retrieved literature compared with fixed-wing drones (Figure 2-12). This could be explained by the fact that, despite the endurance associated with fixed-wing drones, they often require take-off and landing space. However, these requirements are not always available in experimental sites, where most retrieved studies have been conducted (Zaludin and Harituddin, 2019). Multirotor drones are characterised by vertical take-off and landing (VTOL), which makes them more suitable for utilisation in research areas with limited take-off space (Zaludin and Harituddin, 2019). These drones are relatively cheaper than fixed-wing drones (Sibanda et al., 2021b). This could also explain the high utilisation frequency of DJI drones in the retrieved literature (Figure 2-12). The advantage of DJI drones is that some are associated with an automated image acquisition procedure, making it easy to fly them, as they require less expertise in drone piloting. According to Sibanda et al. (2021b), the DJI platforms are generally compatible with many types of sensors from other platforms, which could also explain their wide utilisation in studies on the remote sensing of crops.

2.4.1.4. *Performance of Vegetation Indices, Classification, and Estimation Algorithms*

This review's findings also showed that vegetation indices (VIs), such as NDVI, NDRE, SR, GNDVI, CIgreen, and SAVI frequently mapped the spatial distribution of NUS and their health parameters. For instance, Li et al. (2020) deployed a quadcopter UAV to investigate its utility in crop identification from different land cover types based on VIs. The maximum likelihood classifier, in combination with optimal VIs, exhibited high classification accuracies in that study. This approach was accurate because VIs could partially overcome the influence of shadows and other noise in the background (Mutanga et al., 2023). A growing body of literature demonstrates the optimal performance of VIs (Suhairi et al., 2020, Lati et al., Liu et al., 2021). Specifically, VIs are robust because they can suppress background effects compared with bands (Thenkabail et al., 2013). Furthermore, VIs derive their strength from two or more sections of the EM spectrum. For instance, Vis, such as NDVI, NDRE, SR, GNDVI, CIgreen, and CIred-edge, derive their strength from sections of the EMS (i.e., red edge, NIR, and SWIR) that are more sensitive to crop elements, such as the chlorophyll content, LAI, ABG, nitrogen concentration,

30

and stomatal conductance (Brewer et al., 2022). Moreover, a large body of literature has proven that red-edge-based VIs are more robust than conventional vegetation indices, such as NDVI and SR (Sharifi, 2020, Ramírez et al., 2021). NDVI tends to be insensitive to increases in chlorophyll, LAI, and biomass (Cabrera-Bosquet et al., 2011, Mutanga et al., 2023). As aforementioned, the red edge is highly associated with plant physiological traits, such as the leaf angle distribution, chlorophyll concentration, and LAI, which directly influence vegetation spectral reflectance. Subsequently, red edge-derived vegetation harnesses this robust sensitivity to variations in LAI biomass and chlorophyll content, among others (Filella and Penuelas, 1994, Guyot et al., 1992, Mutanga and Skidmore, 2004, Mutanga et al., 2012, Mutanga et al., 2023)

As was suggested in many studies, the combinations of sensitive spectral variables with robust algorithms produce models with relatively optimal accuracies (Brewer et al., 2022). The findings of this study showed that the machine learning algorithms that were utilised in conjunction with drone-acquired remotely sensed data were primarily linear regressions (LR) (39%), followed by RF (28%), SVM (22%), and ANN (17%). Machine learning regression algorithms present a potential approach for generating adaptive, robust, and fast crop estimates. A growing body of literature demonstrates machine learning algorithms' efficiency and optimal performance in estimating crop biophysical parameters (Brewer, 2021, Wu et al., 2022, Sapkota et al., 2020). The high frequency of using regression models, such as RF, LR, and SVM, can be credited to the fact that they are simple to implement using various platforms. This ranges from Microsoft Excel to complex programming platforms, such as R Statistical Software and the Google Earth Engine platform. Despite their high frequency in the retrieved literature of this current study, LR models are parametric algorithms associated with data normality assumptions. However, these assumptions are often challenging to attain due to high spatial varieties in crop fields. Furthermore, these models are susceptible to overfitting and outliers (Gu et al., 2016).

Subsequently, more efforts have been channelled towards machine learning algorithms, such as SVM and RF. These algorithms are non-parametric, robust, and less prone to outliers, as they are not extremely affected by the data frequency distributions (Gu et al., 2016). Specifically, RF has (i) hyperparameters that are easy to adjust, (ii) is robust to outliers, overfitting, and data dimensionality, (iii) low bias and moderate to minimal variance due to the averaged trees, (vi) works well both continuous and categorical variables, (v) has a capability of discerning the importance of predictor variables, and (iv) it is relatively resistant to multicollinearity when tree depths are greater (Singh et al., 2022, Mutanga et al., 2012, Ehlers et al., 2022). This makes this algorithm suitable for mapping cropping attributes. Other than machine learning algorithms, numerous generic classification algorithms were utilised in the retrieved literature, such as maximum likelihood and minimum distance to mean classification algorithms (Zhang et al., 2018, Shirzadifar et al., 2020, Sengupta et al., 2022). Despite their optimal performance in the literature, these algorithms are less robust when compared with machine learning algorithms. For instance, maximum likelihood is also a traditional parametric algorithm that is often difficult to parametrise, despite the fact it is generally accessible through freely available GIS platforms.

2.4.2. Challenges in Mapping the Spatial Distribution and Health of NUS Using UAVs

Even though there is progress regarding the utility of drones in crop mapping and health quantification of NUS, several challenges impede their propagation, especially in Africa. Many African countries are battling to address various drone-related issues, such as privacy, public safety, and preventing the possession of malicious drones (Nguyen and Nguyen, 2021). Moreover, restrictive UAV or drone regulations across many developing regions, including Africa, hinder their utilisation. To utilise UAVs, users must seek permission from landowners and municipalities, and only operate in certain areas, among several other issues(Kemp et al., 2021). For example, the civil aviation authorities (CAAs) in many countries aim to prevent UAVs from entering the flight paths of manned aircraft. Moreover, CAAs are attempting to construct an inclusive system that accommodates UAVs into their respective

air navigation and surveillance systems (Grote et al., 2022) . To the best of our knowledge, only a few African countries, including Ghana, Kenya, South Africa, Rwanda, Zimbabwe, and Tanzania, have established complex legal requirements governing the use of UAVs in varied airspace practices. Some drone restrictions in South Africa (SA), for example, state that UAVs weighing more than 7 kg (15.4 pounds) are not permitted to operate (Kemp et al., 2021). In this regard, the regulation on the mass of UAVs at taking off tends to indirectly restrict the areal extent and the size of the camera to be mounted for research purposes (Sibanda et al., 2021b). Specifically, due to the weight restrictions, many of the sensor types that are frequently used tend to be lightweight, small, and general consumer grades with limited spectral resolution (Sibanda et al., 2021b). Also. this could explain why more studies are based on the VIS (RGB) spectra than other sections of the electromagnetic spectrum.

Furthermore, SACAA asserts that drone operators should maintain a continuous visual line of sight (VLOS) with their drones during flights. Moreover, remote-piloted aircraft (RPAs) are not permitted to fly beyond visual-line-of-sight in designated places (BVLOS) (Kemp et al., 2021). Sibanda et al. (2021b) stated that supporting regulations and the operationalisation of BVLOS drone technology applications will facilitate coverage of greater areas on a single mission. Covering a greater area in a single mission improves the cost-effectiveness of acquiring VHR imagery. Other restrictions include requiring drone operators to obtain an RPAS operator certificate (ROC) from the CAA before flying (Stopforth, 2017). UAV operators should obtain insurance to cover their liability in the case of committing physical or bodily harm to another individual while operating their drone (Stopforth, 2017). Aside from these regions, numerous African countries are still attempting to establish the necessary regulations that endorse UAV operations. As a result, these regulations are becoming increasingly complicated, while attaining RPAS is associated with high expenses. More notably, the cost of obtaining a drone pilot license is excessive, with estimates ranging from USD 1500 to USD 2000 in 2021 (Sibanda et al., 2021b). Furthermore, the value of drone platforms, including sensors, is prohibitively expensive for several minority groups or scholars, making these technologies unattainable for research purposes in the vast bulk of Sub-Saharan African countries (Sibanda et al., 2021b).

2.4.3. Research Gaps and Opportunities

The following gaps were noted in assessing the utility of drone-based remotely sensed data in mapping the spatial distribution and health of NUS crops:

- The observation of NUS crop health has garnered minimal research attention and interest from the scientific community. Further, few studies have sought to evaluate the utility of drone technology for characterizing crop dynamics, especially in the Global South. The limited research within this region means there are opportunities to innovate.
- Although NUS crops reportedly resist abiotic stresses, such as drought and heat stress, most of this information is anecdotal and inconsistent (Food and Organisation, 2021). This incomplete body of knowledge around drought and heat stress makes applying and validating RS techniques challenging. Hence, there is a requirement to generate more empirical information on the ecophysiology and morphology of NUS.
- Only a few research studies have sought to evaluate the effectiveness of robust ML algorithms in conjunction with VIs in predicting the spatial distribution and health of NUS crops. Further to this, few studies have attempted to assess and leverage the potential synergies between drone and satellite-borne datasets, especially considering the release of the freely accessible Planet Scope Sentinel 2 MSI and Landsat series.
- The application of UAV-based technology for estimating NUS' spatial extent and health has not attracted significant attention from the geospatial research community in practice. The spatial extent of NUS crops can be predicted at a granular scale using UAV-based modelling and classification. Such models will be useful for predicting crop yield, crop monitoring,

32

- predicting soil quality, and modelling evapotranspiration, precipitation, drought, and pest outbreaks.
- Modelling and predicting vegetation key variables, such as LAI, stomatal conductance, and AGB, are critical to understanding and quantifying NUS' morphological and phenological processes in the face of climate change.
- Optimal VIs, such as NDVI NDRE, and VARI, can aid smallholder farmers in analysing trends in plant health. Moreover, NDRE is useful in determining vegetative vigour late in the growing season.

It is, therefore, essential to research the prospects of these remote sensing technologies in monitoring these crops to promote their inclusion as mainstream crops within the agriculture sector.

2.4.4. Way Forward: Closing the Gaps in the Utilisation of Drone Technology in Mapping Spatial Distribution and Health Status of NUS Crops

Scholarly attention needs to be paid to promoting the application of UAVs for assessing NUS crops' spatial extent and health at the field scale. There is a need to increase and extend research efforts towards rainfed smallholder croplands in remotely sensing NUS. Hence, this will optimise their productivity while strengthening the livelihood and food security of marginalised subsistence farmers. UAVs are becoming increasingly common in agricultural research as relevant sources of high-temporal-resolution data for agricultural health monitoring, amongst other applications. This has been previously limited to a farm scale. UAVs provide immense opportunities by incorporating climate-smart and precision agriculture into smallholder farming. They deliver high-resolution imagery at user-defined temporal resolutions, which benefit crop health monitoring and independent decision-making. For example, the integration of multi-rotor drones, such as the DJI series, in conjunction with multispectral sensors, such as the Mica Sense RedEdgeMX Parrot Sequoia and MicaSense Altum cameras, has been demonstrated to deliver accurate models of crop health characteristics at the field scale. Additionally, the increasing adoption of cutting-edge narrow-band hyperspectral and LiDAR remote sensing technologies could provide the opportunity to assess diverse crop health parameters at high optical resolutions. This assessment would also allow for creating various optimal VIs. Hence, these are directly associated with NUS crop morphological and physiological characteristics, allowing for the quantification of their health status. Moreover, to improve research based on the application of UAVs to estimate NUS crop health, it is essential to identify and implement robust and reliable non-parametric ML algorithms. Algorithms that enhance prediction accuracies with fewer assumptions, such as the RF, seem to hold endless prospects. Using multi-fusion techniques based on the combination of ideal VIs and ML algorithms will achieve the best optimal accuracies. As a result, additional research is required to evaluate the utility of UAVs with distinct spectral characteristics for NUS. It would be valuable to research whether UAV sensors that measure spectral reflectance along the electromagnetic spectrum's thermal, SWIR, and NIR sections enhance the prediction of NUS water stress at the farm scale. Therefore, near-real-time-temporal-resolution spatially explicit information on NUS spatial extent and health can certainly assist smallholder farmers. This will assist in detecting variations in crop morphology to optimise yields. Near-real-time fine-resolution NUS information could be used to draw up early warning systems for smallholder farmers to prevent any damage or reduction to crop yields.

2.5. Limitations of This Study

Many possible sources of information on the spatial extent and health of NUS were disregarded throughout our search approach. We primarily searched for English-language sources and peer-reviewed articles included in Scopus, Web of Science, and Google Scholar. In conducting the literature review, some studies were inaccessible in full length and others were not written in English. This could have had a potentially negative effect on quantifying all the studies that focus on remote sensing the

spatial distribution and health status of NUS crops. More so, the exclusion of these studies has an impact on the spatial distribution of NUS studies. Since NUS crops research is highly under-represented and anecdotal, it was challenging to obtain research that focused on the health and spatial extent of NUS crops. Despite missed contributions, we believe that our findings are based on a sample that is adequate and diverse enough to offer meaningful insight and implications in the application of UAVs in the remote sensing of NUS crops in smallholder croplands. Another, limitation of the study was the fact that we limited our scope of research materials for the systematic review to only the Scopus, Web of Science, and Google Scholar databases. As such, we recommend that future work extend the sources to a larger number of databases.

2.6. Conclusions

The objective of this study was to systematically assess the literature on the progress, challenges, gaps, and opportunities in using drone-derived remotely sensed data to map the spatial distribution and health status of NUS. This study placed a special focus on classifying and measuring stomatal conductance in smallholder croplands in the Global South. From the reviewed literature, UAVs emerged as cutting-edge technology with a high potential to provide spatially explicit, timely, and reliable data for assessing the health of NUS. However, there is a noticeable scarcity of studies that have attempted to map the spatial distribution and stomatal conductance, along with other health attributes, of NUS in comparison with mainstream crops in smallholder croplands in the Global South. Several factors contribute to this scarcity, including the limited popularity of NUS, the prohibitive cost of drones and pilot licenses, a shortage of personnel with the necessary skills, and stringent regulations governing drone procurement and operation, among others. While acknowledging the substantial ownership costs associated with drones, our study advocates for the communal ownership of UAVs among smallholder farmers, which can significantly reduce operational expenses. This approach offers promising opportunities to integrate climate-smart agriculture into local farming systems through enhanced monitoring and mapping of crop health. It will equip farmers and, through extension, workers with valuable information for making informed decisions in the field. Additionally, it will enhance stress detection, improve irrigation scheduling, and boost crop productivity on a farm scale. Furthermore, improving the productivity of NUS and other crops presents an opportunity to revive local food culture and food systems, while simultaneously empowering smallholder farmers, who are often the stewards of this agrobiodiverse resource system. We also advocate for the use of UAVs to engage younger generations in agriculture, a critical priority in Sub-Saharan Africa. By delivering high-quality imagery and automating data collection, processing, and analysis at a low cost, the application of UAVs in local food systems can serve as a pathway to optimise food production among disadvantaged smallholder farmers.

References

Aboutalebi, M., Torres-Rua, A. F., & Allen, N. (2018). *Multispectral Remote Sensing for Yield Estimation Using High-Resolution Imagery from an Unmanned Aerial Vehicle* AUTONOMOUS AIR AND GROUND SENSING SYSTEMS FOR AGRICULTURAL OPTIMIZATION AND PHENOTYPING III,

Ali, A., & Imran, M. (2020). Evaluating the potential of red edge position (REP) of hyperspectral remote sensing data for real time estimation of LAI & chlorophyll content of kinnow mandarin (Citrus reticulata) fruit orchards. *Scientia Horticulturae*, *267*, 109326.

Ankrah, J., Monteiro, A., & Madureira, H. (2023). Shoreline Change and Coastal Erosion in West Africa: A Systematic Review of Research Progress and Policy Recommendation. *Geosciences*, *13*(2), 59.

Avneri, A., Aharon, S., Brook, A., Atsmon, G., Smirnov, E., Sadeh, R., Abbo, S., Peleg, Z., Herrmann, I. & Bonfil, D. J. 2023. UAS-based imaging for prediction of chickpea crop biophysical parameters and yield. *Computers and Electronics in Agriculture,* 205**,** 107581.

Awais, M., LI, W., Cheema, M., Zaman, Q., Shaheen, A., Aslam, B., Zhu, W., Ajmal, M., Faheem, M. & Hussain, S. 2022a. UAV-based remote sensing in plant stress imagine using high-resolution thermal sensor for digital agriculture practices: a meta-review. *International Journal of Environmental Science and Technology***,** 1-18.

Awais, M., LI, W., Cheema, M. J., Hussain, S., Shaheen, A., Aslam, B., LIu, C. & Ali, A. 2022b. Assessment of optimal flying height and timing using high-resolution unmanned aerial vehicle images in precision agriculture. *International Journal of Environmental Science and Technology,* 19**,** 2703-2720.

Azizan, F. A., Kiloes, A. M., Astuti, I. S., & Abdul Aziz, A. (2021). Application of optical remote sensing in rubber plantations: a systematic review. *Remote Sensing*, *13*(3), 429.

Bellvert, J., Zarco-Tejada, P. J., Girona, J., & Fereres, E. (2014). Mapping crop water stress index in a 'Pinot-noir' vineyard: comparing ground measurements with thermal remote sensing imagery from an unmanned aerial vehicle. *Precision Agriculture*, *15*(4), 361-376.

Blessing, C., Nhamo, M., & Rangarirai, M. (2020). The impact of plant density and spatial arrangement on light interception on cotton crop and seed cotton yield: an overview.

Blumenthal, J., Megherbi, D. B., & Lussier, R. (2020). Unsupervised machine learning via Hidden Markov Models for accurate clustering of plant stress levels based on imaged chlorophyll fluorescence profiles & their rate of change in time. *Computers and Electronics in Agriculture*, *174*, 105064.

Bojović, B., & Marković, A. (2009). Correlation between nitrogen and chlorophyll content in wheat (Triticum aestivum L.). *Kragujevac Journal of Science*, *31*(5827), 69-74.

Brewer, K., Clulow, A., Sibanda, M., Gokool, S., Naiken, V., & Mabhaudhi, T. (2022). Predicting the Chlorophyll Content of Maize over Phenotyping as a Proxy for Crop Health in Smallholder Farming Systems. *Remote Sensing*, *14*(3), 518. https://www.mdpi.com/2072-4292/14/3/518

Brewer, K. R. (2021). *Assessment of maize crop health and water stress based on multispectral and thermal infrared unmanned aerial vehicle phenotyping in smallholder farms* (Doctoral dissertation).

Buthelezi, S., Mutanga, O., Sibanda, M., Odindi, J., Clulow, A. D., Chimonyo, V. G. P., & Mabhaudhi, T. (2023). Assessing the Prospects of Remote Sensing Maize Leaf Area Index Using UAV-Derived Multi-Spectral Data in Smallholder Farms across the Growing Season. *Remote Sensing*, *15*(6), 1597. https://www.mdpi.com/2072-4292/15/6/1597

Butilă, E. V., & Boboc, R. G. (2022). Urban traffic monitoring and analysis using unmanned aerial vehicles (uavs): A systematic literature review. *Remote Sensing*, *14*(3), 620.

Cabrera-Bosquet, L., Molero, G., Stellacci, A., Bort, J., Nogués, S., & Araus, J. (2011). NDVI as a potential tool for predicting biomass, plant nitrogen content and growth in wheat genotypes subjected to different water and nitrogen conditions. *Cereal Research Communications*, *39*(1), 147-159.

Candiago, S., Remondino, F., De Giglio, M., Dubbini, M., & Gattelli, M. (2015). Evaluating Multispectral Images and Vegetation Indices for Precision Farming Applications from UAV Images. *Remote Sensing*, *7*(4), 4026-4047. https://doi.org/10.3390/rs70404026

Chai, H. H., Massawe, F., & Mayes, S. (2016). Effects of mild drought stress on the morpho-physiological characteristics of a bambara groundnut segregating population. *Euphytica*, *208*(2), 225-236.

Chapepa, B., Mudada, N. & Mapuranga, R. 2020. The impact of plant density and spatial arrangement on light interception on cotton crop and seed cotton yield: an overview. *Journal of Cotton Research,* 3**,** 18.

Che'Ya, N. N., Dunwoody, E., & Gupta, M. (2021). Assessment of Weed Classification Using Hyperspectral Reflectance and Optimal Multispectral UAV Imagery. *Agronomy-Basel*, *11*(7), Article 1435. https://doi.org/10.3390/agronomy11071435

Chibarabada, T. P. (2018). *Water use and nutritional water productivity of selected major and underutilised grain legumes* (Doctoral dissertation).

Clevers, J. G., & Gitelson, A. A. (2013). Remote estimation of crop and grass chlorophyll and nitrogen content using red-edge bands on Sentinel-2 and-3. *International Journal of Applied Earth Observation and Geoinformation*, *23*, 344-351.

Duarte, A., Borralho, N., Cabral, P., & Caetano, M. (2022). Recent advances in forest insect pests and diseases monitoring using UAV-based data: A systematic review. *Forests*, *13*(6), 911.

Duku, C., Zwart, S. J., van Bussel, L. G., & Hein, L. (2018). Quantifying trade-offs between future yield levels, food availability and forest and woodland conservation in Benin. *Science of The Total Environment*, *610*, 1581-1589.

Ehlers, D., Wang, C., Coulston, J., Zhang, Y., Pavelsky, T., Frankenberg, E., Woodcock, C., & Song, C. (2022). Mapping Forest Aboveground Biomass Using Multisource Remotely Sensed Data. *Remote Sensing*, *14*(5), 1115.

Everitt, J., Yang, C., Davis, M., Everitt, J., & Davis, M. (2007). Mapping wild taro with color-infrared aerial photography and image processing. *J. Aquat. Plant Manage*, *45*, 106-110.

Fageria, N. K., Baligar, V. C., & Clark, R. (2006). *Physiology of crop production*. crc Press.

Fan, S., & Rue, C. (2020). The role of smallholder farms in a changing world. *The role of smallholder farms in food and nutrition security*, 13-28.

Filella, I., & Penuelas, J. (1994). The red edge position and shape as indicators of plant chlorophyll content, biomass and hydric status. *International Journal of Remote Sensing*, *15*(7), 1459-1470.

Food, & Organisation, A. (2021). Small Family Farmers Produce a Third of the World's Food.

Funk, C., & Budde, M. E. (2009). Phenologically-tuned MODIS NDVI-based production anomaly estimates for Zimbabwe. *Remote Sensing of Environment*, *113*(1), 115-125.

Goel, R. K., Yadav, C. S., Vishnoi, S., & Rastogi, R. (2021). Smart agriculture–Urgent need of the day in developing countries. *Sustainable Computing: Informatics and Systems*, *30*, 100512.

Gray, P. C., Ridge, J. T., Poulin, S. K., Seymour, A. C., Schwantes, A. M., Swenson, J. J., & Johnston, D. W. (2018). Integrating drone imagery into high resolution satellite remote sensing assessments of estuarine environments. *Remote Sensing*, *10*(8), 1257.

Grote, M., Pilko, A., Scanlan, J., Cherrett, T., Dickinson, J., Smith, A., Oakey, A., & Marsden, G. (2022). Sharing airspace with Uncrewed Aerial Vehicles (UAVs): Views of the General Aviation (GA) community. *Journal of Air Transport Management*, *102*, 102218.

Grüner, E., Astor, T., & Wachendorf, M. (2021). Prediction of biomass and N fixation of legume–grass mixtures using sensor fusion. *FRONTIERS IN PLANT SCIENCE*, *11*, 603921.

Gu, Y., Wylie, B. K., Boyte, S. P., Picotte, J., Howard, D. M., Smith, K., & Nelson, K. J. (2016). An optimal sample data usage strategy to minimize overfitting and underfitting effects in regression tree models based on remotely-sensed data. *Remote Sensing*, *8*(11), 943.

Guyot, G., Baret, F., & Jacquemoud, S. (1992). *Imaging spectroscopy for vegetation studies* (Vol. 2). Kluwer Academic Publishers: Norwell, MA, USA.

Huang, Y., Reddy, K. N., Fletcher, R. S., & Pennington, D. (2018). UAV low-altitude remote sensing for precision weed management. *WEED TECHNOLOGY*, *32*(1), 2-6.

Iseki, K., & Olaleye, O. (2020). A new indicator of leaf stomatal conductance based on thermal imaging for field grown cowpea. *Plant Production Science*, *23*(1), 136-147.

Jewan, S. Y. Y., Pagay, V., Billa, L., Tyerman, S. D., Gautam, D., Sparkes, D., Chai, H. H., & Singh, A. (2022). The feasibility of using a low-cost near-infrared, sensitive, consumer-grade digital camera mounted on a commercial UAV to assess Bambara groundnut yield. *International Journal of Remote Sensing*, *43*(2), 393-423.

Joshi, B. K., Shrestha, R., Gauchan, D., & Shrestha, A. (2020). Neglected, underutilized, and future smart crop species in Nepal. *Journal of Crop Improvement*, *34*(3), 291-313.

Kemp, L., Roux, M., Kemp, M., & Kock, R. (2021). Application of drones and image processing for bridge inspections in South Africa. *Civil Engineering= Siviele Ingenieurswese*, *29*(8), 25-30.

Lati, R., Avneri, A., Aharon, S., Atsmon, G., Smirnov, E., Sadeh, R., Abbo, S., Peleg, Z., Herrmann, I., & Bonfil, D. J. Uav-Based Imaging for Prediction of Chickpea Crop Biophysical Parameters and Yield. *Available at SSRN 4123863*.

Li, K.-Y., Burnside, N. G., Sampaio de Lima, R., Villoslada Peciña, M., Sepp, K., Yang, M.-D., Raet, J., Vain, A., Selge, A., & Sepp, K. (2021). The application of an unmanned aerial system and machine learning techniques for red clover-grass mixture yield estimation under variety performance trials. *Remote Sensing*, *13*(10), 1994.

Li, L., Zheng, X. M., Zhao, K., Li, X. F., Meng, Z. G., & Su, C. H. (2020). Potential Evaluation of High Spatial Resolution Multi-Spectral Images Based on Unmanned Aerial Vehicle in Accurate Recognition of Crop Types. *Journal of the Indian Society of Remote Sensing*, *48*(11), 1471-1478. https://doi.org/10.1007/s12524-020-01141-4

Li, Y., Ren, B., Ding, L., Shen, Q., Peng, S., & Guo, S. (2013). Does chloroplast size influence photosynthetic nitrogen use efficiency? *Plos one*, *8*(4), e62036.

Liu, C., Liu, Y., Lu, Y., Liao, Y., Nie, J., Yuan, X., & Chen, F. (2019). Use of a leaf chlorophyll content index to improve the prediction of above-ground biomass and productivity. *PeerJ*, *6*, e6240.

Liu, Y., Feng, H., Yue, J., Fan, Y., Jin, X., Song, X., Yang, H. & Yang, G. 2022b. Estimation of Potato Above-Ground Biomass Based on Vegetation Indices and Green-Edge Parameters Obtained from UAVs. *Remote Sensing*, 14, 5323.

Liu, Y., Hatou, K., Aihara, T., Kurose, S., Akiyama, T., Kohno, Y., Lu, S., & Omasa, K. (2021). A robust vegetation index based on different UAV RGB images to estimate SPAD values of naked barley leaves. *Remote Sensing*, *13*(4), 686.

Mabhaudhi, T., Chimonyo, V. G., & Modi, A. T. (2017a). Status of underutilised crops in South Africa: Opportunities for developing research capacity. *Sustainability*, *9*(9), 1569.

Mabhaudhi, T., Chimonyo, V. G. P., & Modi, A. T. (2017b). Status of underutilised crops in South Africa: opportunities for developing research capacity. *Sustainability*, *9*(9), 1569.

Mabhaudhi, T., Modi, A., & Beletse, Y. (2013). Growth, phenological and yield responses of a bambara groundnut (Vigna subterranea L. Verdc) landrace to imposed water stress: II. Rain shelter conditions. *Water Sa*, *39*(2), 191-198.

Maes, W. H., & Steppe, K. (2012). Estimating evapotranspiration and drought stress with ground-based thermal remote sensing in agriculture: a review. *Journal of Experimental Botany*, *63*(13), 4671-4712. https://doi.org/10.1093/jxb/ers165

Mafuratidze, P. (2010). *Discriminating wetland vegetation species in an African savanna using hyperspectral data* (Doctoral dissertation).

Majid, K., & Roza, G. (2012). The effect of drought stress on leaf chlorophyll content and stress resistance in maize cultivars (Zea mays). *African Journal of Microbiology Research*, *6*(12), 2844-2848.

Malinao, R. M. L., & Hernandez, A. A. (2018). Classifying Breadfruit Tree using Artificial Neural Networks. Proceedings of the 6th ACM/ACIS International Conference on Applied Computing and Information Technology,

Marshall, M., & Thenkabail, P. (2015). Advantage of hyperspectral EO-1 Hyperion over multispectral IKONOS, GeoEye-1, WorldView-2, Landsat ETM+, and MODIS vegetation indices in crop biomass estimation. *Isprs Journal of Photogrammetry and Remote Sensing*, *108*, 205-218.

Mazarire, T., Ratshiedana, P., Nyamugama, A., Adam, E., & Chirima, G. (2020). Exploring machine learning algorithms for mapping crop types in a heterogeneous agriculture landscape using Sentinel-2 data. A case study of Free State Province, South Africa. *S. Afr. J. Geomat*, *9*, 333-347.

Mazarire, T. T., Ratshiedana, P. E., Nyamugama, A., Adam, E., & Chirima, G. (2020). Exploring machine learning algorithms for mapping crop types in a heterogeneous agriculture landscape using Sentinel-2 data. A case study of Free State Province, South Africa. *South African Journal of Geomatics*, *9*(2), 333-347.

Merkert, R., & Bushell, J. (2020). Managing the drone revolution: A systematic literature review into the current use of airborne drones and future strategic directions for their effective control. *Journal of air transport management*, *89*, 101929.

Monteoliva, M. I., Guzzo, M. C., & Posada, G. A. (2021). Breeding for drought tolerance by monitoring chlorophyll content.

Mugiyo, H., Chimonyo, V. G., Sibanda, M., Kunz, R., Nhamo, L., Masemola, C. R., Dalin, C., Modi, A. T., & Mabhaudhi, T. (2021). Multi-criteria suitability analysis for neglected and underutilised crop species in South Africa. *Plos one*, *16*(1), e0244734.

Muhammad, A., Alam, M., Ahmad, I., & Jalal, A. (2021). Role of beneficial microbes with nitrogen and phosphorous levels on canola productivity. *Brazilian Journal of Biology*, *82*.

Muruganantham, P., Wibowo, S., Grandhi, S., Samrat, N. H., & Islam, N. (2022). A systematic literature review on crop yield prediction with deep learning and remote sensing. *Remote Sensing*, *14*(9), 1990.

Musa, M., Massawe, F., Mayes, S., Alshareef, I., & Singh, A. (2016). Nitrogen fixation and N-balance studies on Bambara groundnut (Vigna subterranea L. Verdc) landraces grown on tropical acidic soils of Malaysia. *Communications in Soil Science and Plant Analysis*, *47*(4), 533-542.

Mutanga, O., Adam, E., & Cho, M. A. (2012). High density biomass estimation for wetland vegetation using WorldView-2 imagery and random forest regression algorithm. *International Journal of Applied Earth Observation and Geoinformation*, *18*(0), 399-406. https://doi.org/http://dx.doi.org/10.1016/j.jag.2012.03.012

Mutanga, O., Dube, T., & Galal, O. (2017). Remote sensing of crop health for food security in Africa: Potentials and constraints. *Remote Sensing Applications: Society and Environment*, *8*, 231-239.

Mutanga, O., Masenyama, A., & Sibanda, M. (2023). Spectral saturation in the remote sensing of high-density vegetation traits: A systematic review of progress, challenges, and prospects. *Isprs Journal of Photogrammetry and Remote Sensing*, *198*, 297-309.

Mutanga, O., & Skidmore, A. K. (2004). Narrow band vegetation indices overcome the saturation problem in biomass estimation. *International Journal of Remote Sensing*, *25*(19), 3999-4014.

Ndlovu, H. S., Odindi, J., Sibanda, M., Mutanga, O., Clulow, A., Chimonyo, V. G. P., & Mabhaudhi, T. (2021). A Comparative Estimation of Maize Leaf Water Content Using Machine Learning Techniques and Unmanned Aerial Vehicle (UAV)-Based Proximal and Remotely Sensed Data. *Remote Sensing*, *13*(20), 4091. https://www.mdpi.com/2072-4292/13/20/4091

Nguyen, H. P. D., & Nguyen, D. D. (2021). Drone application in smart cities: The general overview of security vulnerabilities and countermeasures for data communication. *Development and Future of Internet of Drones (IoD): Insights, Trends and Road Ahead*, 185-210.

Nyman, J. (2018). Pixel classification of hyperspectral images. In.

Opole, R. A. (2012). *Effect of environmental stress and management on grain and biomass yield of finger millet [Eleusine coracana (L.) Gaertn.]*. Kansas State University.

Ouyang, W., Struik, P. C., Yin, X., & Yang, J. (2017). Stomatal conductance, mesophyll conductance, and transpiration efficiency in relation to leaf anatomy in rice and wheat genotypes under drought. *Journal of Experimental Botany*, *68*(18), 5191-5205.

Parra, L., Mostaza-Colado, D., Yousfi, S., Marin, J. F., Mauri, P. V., & Lloret, J. (2021). Drone RGB images as a reliable information source to determine legumes establishment success. *Drones*, *5*(3), 79.

Pereira, F. d. S., de Lima, J., Freitas, R., Dos Reis, A. A., do Amaral, L. R., Figueiredo, G. K. D. A., Lamparelli, R. A., & Magalhães, P. S. G. (2022). Nitrogen variability assessment of pasture fields under an integrated crop-livestock system using UAV, PlanetScope, and Sentinel-2 data. *Computers and Electronics in Agriculture*, *193*, 106645.

Pineda, M., Baron, M., & Perez-Bueno, M. L. (2021). Thermal Imaging for Plant Stress Detection and Phenotyping. *Remote Sensing*, *13*(1), Article 68. https://doi.org/10.3390/rs13010068

Raji, S. N., Aparna, G. N., Mohanan, C. N., & Subhash, N. (2017). Proximal remote sensing of herbicide and drought stress in field grown colocasia and sweet potato plants by sunlight-induced

chlorophyll fluorescence Imaging. *Journal of the Indian Society of Remote Sensing*, *45*(3), 463-475.

Ramírez, D. A., Grüneberg, W., I Andrade, M., De Boeck, B., Loayza, H., S Makunde, G., Ninanya, J., Rinza, J., Heck, S., & Campos, H. (2021). Phenotyping of productivity and resilience in sweetpotato under water stress through UAV-based multispectral and thermal imagery in Mozambique. *Journal of Agronomy and Crop Science*.

Sankaran, S., Zhou, J., Khot, L. R., Trapp, J. J., Mndolwa, E., & Miklas, P. N. (2018). High-throughput field phenotyping in dry bean using small unmanned aerial vehicle based multispectral imagery. *Computers and Electronics in Agriculture*, *151*, 84-92.

Sapkota, B., Singh, V., Cope, D., Valasek, J., & Bagavathiannan, M. (2020). Mapping and Estimating Weeds in Cotton Using Unmanned Aerial Systems-Borne Imagery. *AGRIENGINEERING*, *2*(2), Article 24. https://doi.org/10.3390/agriengineering2020024

Sengupta, S., Mohinuddin, S., Arif, M., Sengupta, B., & Zhang, W. (2022). Assessment of agricultural land suitability using GIS and Fuzzy Analytical Hierarchy Process approach in Ranchi District, India. *Geocarto International*(just-accepted), 1-34.

Shao, Y., Liu, Y., Xuan, G., Wang, Y., Gao, Z., Hu, Z., Han, X., Gao, C., & Wang, K. (2020). Application of hyperspectral imaging for spatial prediction of soluble solid content in sweet potato. *RSC advances*, *10*(55), 33148-33154.

Sharifi, A. (2020). Remotely sensed vegetation indices for crop nutrition mapping. *Journal of the Science of Food and Agriculture*, *100*(14), 5191-5196. https://doi.org/10.1002/jsfa.10568

Shi, Y., Murray, S. C., Rooney, W. L., Valasek, J., Olsenholler, J., Pugh, N. A., Henrickson, J., Bowden, E., Zhang, D., & Thomasson, J. A. (2016). Corn and sorghum phenotyping using a fixed-wing UAV-based remote sensing system. Autonomous air and ground sensing systems for agricultural optimization and phenotyping,

Shirzadifar, A., Bajwa, S., Nowatzki, J., & Bazrafkan, A. (2020). Field identification of weed species and glyphosate-resistant weeds using high resolution imagery in early growing season. *Biosystems Engineering*, *200*, 200-214. https://doi.org/10.1016/j.biosystemseng.2020.10.001

Sibanda, M., Mutanga, O., Chimonyo, V. G., Clulow, A. D., Shoko, C., Mazvimavi, D., Dube, T. & Mabhaudhi, T. 2021b. Application of drone technologies in surface water resources monitoring and assessment: A systematic review of progress, challenges, and opportunities in the global south. *Drones,* 5, 84.

Singh, C., Karan, S. K., Sardar, P., & Samadder, S. R. (2022). Remote sensing-based biomass estimation of dry deciduous tropical forest using machine learning and ensemble analysis. *Journal of Environmental Management*, *308*, 114639.

Singhal, G., Bansod, B., Mathew, L., Goswami, J., Choudhury, B., & Raju, P. (2019). Estimation of leaf chlorophyll concentration in turmeric (Curcuma longa) using high-resolution unmanned aerial vehicle imagery based on kernel ridge regression. *Journal of the Indian Society of Remote Sensing*, *47*(7), 1111-1122.

Sishodia, R. P., Ray, R. L., & Singh, S. K. (2020). Applications of remote sensing in precision agriculture: A review. *Remote Sensing*, *12*(19), 3136.

Sobejano-Paz, V., Mikkelsen, T. N., Baum, A., Mo, X., Liu, S., Köppl, C. J., Johnson, M. S., Gulyas, L., & García, M. (2020). Hyperspectral and thermal sensing of stomatal conductance, transpiration, and photosynthesis for soybean and maize under drought. *Remote Sensing*, *12*(19), 3182.

Stopforth, R. (2017). Drone licenses-neccesities and requirements. *II Ponte*, *73*(1), 149-156.

Suhairi, T. A. S. T. M., Sinin, S. S. M., Wimalasiri, E. M., Nizar, N. M. M., Tharmandran, A. S., Jahanshiri, E., Gregory, P. J., & Azam-Ali, S. N. (2020). Use of Unmanned Aerial Vehicles (UAVs) Imagery in Phenotyping of Bambara Groundnut. *Journal of Agricultural Science*, *12*(6).

Tahir, M. N., Naqvi, S. Z. A., Lan, Y., Zhang, Y., Wang, Y., Afzal, M., Cheema, M. J. M., & Amir, S. (2018). Real time estimation of chlorophyll content based on vegetation indices derived from multispectral UAV in the kinnow orchard. *International Journal of Precision Agricultural Aviation*, *1*(1).

Thenkabail, P. S., Mariotto, I., Gumma, M. K., Middleton, E. M., Landis, D. R., & Huemmrich, K. F. (2013). Selection of hyperspectral narrowbands (HNBs) and composition of hyperspectral

39

twoband vegetation indices (HVIs) for biophysical characterization and discrimination of crop types using field reflectance and Hyperion/EO-1 data. *Selected Topics in Applied Earth Observations and Remote Sensing, IEEE Journal of*, *6*(2), 427-439.

Thenkabail, P. S., Smith, R. B., & De Pauw, E. (2002). Evaluation of narrowband and broadband vegetation indices for determining optimal hyperspectral wavebands for agricultural crop characterization. *Photogrammetric Engineering And Remote Sensing*, *68*(6), 607-622.

Van Wart, J., Kersebaum, K. C., Peng, S., Milner, M., & Cassman, K. G. (2013). Estimating crop yield potential at regional to national scales. *Field Crops Research*, *143*, 34-43.

Velusamy, P., Rajendran, S., Mahendran, R. K., Naseer, S., Shafiq, M., & Choi, J.-G. (2021). Unmanned Aerial Vehicles (UAV) in Precision Agriculture: Applications and Challenges. *Energies*, *15*(1), 217.

Wijewardana, C., Alsajri, F. A., Irby, J. T., Krutz, L. J., Golden, B., Henry, W. B., Gao, W., & Reddy, K. R. (2019). Physiological assessment of water deficit in soybean using midday leaf water potential and spectral features. *Journal of Plant Interactions*, *14*(1), 533-543.

Williams, T. B., Dodd, I. C., Sobeih, W. Y., & Paul, N. D. (2022). Ultraviolet radiation causes leaf warming due to partial stomatal closure. *Horticulture research*, *9*.

Wu, S., Deng, L., Guo, L., & Wu, Y. (2022). Wheat leaf area index prediction using data fusion based on high-resolution unmanned aerial vehicle imagery. *Plant Methods*, *18*(1), 1-16.

Xia, W., Luo, T., Zhang, W., Mason, A. S., Huang, D., Huang, X., Tang, W., Dou, Y., Zhang, C., & Xiao, Y. (2019). Development of high-density SNP markers and their application in evaluating genetic diversity and population structure in Elaeis guineensis. *FRONTIERS IN PLANT SCIENCE*, *10*, 130.

Xue, J., & Su, B. (2017). Significant remote sensing vegetation indices: A review of developments and applications. *Journal of Sensors*, *2017*.

Zaludin, Z., & Harituddin, A. S. M. (2019). Challenges and Trends of Changing from Hover to Forward Flight for a Converted Hybrid Fixed Wing VTOL UAS from Automatic Flight Control System Perspective. 2019 IEEE 9th International Conference on System Engineering and Technology (ICSET),

Zhang, L., Zhang, H., Niu, Y. & Han, W. 2019b. Mapping Maize Water Stress Based on UAV Multispectral Remote Sensing. *Remote Sensing,* 11**,** 605.

Zhang, Y., Teng, P., Aono, M., Shimizu, Y., Hosoi, F., & Omasa, K. (2018). 3D monitoring for plant growth parameters in field with a single camera by multi-view approach. *Journal of agricultural meteorology*, *74*(4), 129-139.

Zheng, Q., Huang, W., Ye, H., Dong, Y., Shi, Y., & Chen, S. (2020). Using continous wavelet analysis for monitoring wheat yellow rust in different infestation stages based on unmanned aerial vehicle hyperspectral images. *Applied Optics*, *59*(26), 8003-8013.

CHAPTER 3

ASSESSING THE POTENTIAL OF UAV ACQUIRED MULTISPECTRAL IMAGERY COMBINED WITH MACHINE LEARNING TECHNIQUES IN MAPPING THE SPATIAL DISTRIBUTION OF TARO AND SWEET POTATO IN SMALLER HOLDER FARMS.

Abstract: Taro and Sweet potato are Neglected and under-utilised crop species (NUS) that often suffer from a lack of research and market preference, which hinders their development and utilisation. However, recent advances in remote sensing and unmanned aerial vehicle (UAV) high-throughput phenotyping technologies offer promising opportunities to contribute significantly to the research and mapping of NUS in smallholder farms. This study sought to compare the capability of gradient boosting trees (GTB), support vector machines (SVM) and random forest (RF) in detecting and mapping the field boundaries and spatial distribution of sweet potato and taro crops within smallholder croplands using UAV acquired remotely sensed data. A comparative assessment of the contribution of bands, vegetation indices and both datasets combined was conducted. Results showed that ensemble classifiers, RF and GTB, outperformed SVM exhibiting overall accuracies above 80%. Specifically, SVM yielded overall accuracies ranging from (42% -74%). The application of combined data (Bands &VIs) produced the best accuracies. The optical spectral bands, specifically B1 (blue), B4 (Red edge), and Excess green index (EGI) played a pivotal role in influencing the classification performance. GTB and RF exhibited superior capabilities in mapping fragmented smallholder farms and delivering more precise area estimates when compared to SVM. Hence, the data derived from mapping the spatial distribution of neglected and underutilised crops holds paramount importance for biodiversity conservation, climate resilience, food security, and sustainable agriculture. The results of this study could offer local communities and smallholder farmers invaluable insights on how to better manage resources, make decisions, and optimise productivity, sustainability, food and nutrition security.

Keywords: Random Forest, Gradient tree boost, unmanned aerial vehicle, smallholder fields.

3.1. Introduction

Food security and sustainability are looming major global concerns due to population growth, climate change, and decreasing arable land (Vågsholm et al., 2020). The global population is predicted to rise to 9 billion by 2050, including 1.5 billion in SSA. In the year 2022, the African continent witnessed a notable surge in the number of malnourished individuals, which amounted to nearly 282 million, denoting a substantial escalation of 57 million people since the onset of the COVID-19 pandemic (FAO et al., 2023). Approximately 868 million people experienced moderate or severe food insecurity, highlighting the significant scale of the issue. Moreover, 78 percent of the African population were unable to afford a nutritionally adequate diet throughout the year 2021(FAO et al., 2023). As of 2023, progress toward achieving universal food and nutrition targets has been slow. Therefore, this amplifies the pressures on agricultural lands to meet the rising food demands that are already affected by the impact of climate change (Kumar et al., 2022). Smallholder farmers who supply most local food production are especially vulnerable as 80% of the crops they grow are rainfed (Fan and Rue, 2020). Therefore, it is crucial to identify and grow alternative drought-tolerant crops in smaller-holder farms to address nutrition issues (Mabhaudhi et al., 2017). Neglected and underutilised crops (NUS) like sweet potato and taro are stress-tolerant, nutrient-rich crops that can grow under adverse environmental conditions and are renowned to have a natural resistance and tolerance to pest, disease and drought

(Mabhaudhi et al., 2017). These NUS are also suitable for sustainable farming through adaptability, lower inputs, and diversification (El Bilali et al., 2023).

The incorporation of NUS crops into both commercial and subsistence food systems has been difficult partly due to a lack of knowledge on their spatial distribution and phenotypical attributes (Mabhaudhi et al., 2017). Furthermore, there are no clear criterion or spatially explicit techniques for assessing their spatial distribution and health within smallholder farms in developing countries. Therefore, it is imperative to develop accurate and time-effective quantitative spatial techniques for detecting and mapping their distribution. This information could support better resource management, decision making and ultimately increase productivity, sustainability, food and nutrition security through optimised production.

Generally, traditional field surveys have commonly been used to measure NUS crop spatial extent, suitability, growth, and morphology. However, such methods are time-consuming and expensive, making them impractical for continuous and effective crop monitoring (Ndlovu et al., 2021). Throughout several decades, satellite-based earth observation technologies have demonstrated their effectiveness in discriminating and mapping the spatial distribution of crops to optimise production. According to Wang et al. (2022), Sentinel-2 multispectral instrument (MSI) data with machine learning, for example, can differentiate alfalfa (*Medicago sativa L.*) from other crop types with overall accuracies over 90%. Moreover, Sharifi (2020) effectively combined Sentinel-2 MSI bands and vegetation indices to achieve accurate crop nutrition mapping. Nonetheless, even with advancements in satellite remote sensing applications, the effectiveness of satellite data in identifying and delineating the precise scope of NUS at farm scale is constrained by the relatively coarse spatial and temporal resolutions of openly accessible satellite remotely sensed datasets (Ndlovu et al., 2021). Satellite borne datasets such as Sentinel-2 MSI and Landsat typically have coarser spatial resolutions which often masks out the fine-scale variability within farms or individual plants. In recent years, the utilisation of unmanned aerial vehicles (UAVs) also known as drones have gain significant traction in the field of precision agriculture to remotely sense crops (Sun et al., 2021). UAVs equipped with advanced high-resolution sensors provide precise and timely data, which is well-suited for monitoring crops at the plot level (Ndlovu et al., 2021). They allow flexible altitude control, making them well-suited to assess the spatial distribution of crops at a farm scale. By flying at customised altitudes, UAVs can capture high-definition imagery enabling detailed analysis of minute crop formations at farm scale. Several studies have employed UAVs for proximal sensing in environmental applications (Everitt et al., 2007, Sankaran et al., 2018, Yang et al., 2012). For instance, Everitt et al. (2007) mapped the spatial distribution of wild taro using a Kodak color-infrared camera in combination with supervised image analysis techniques. This approach yieled kappa accuracies ranging from 83.3% to 100%. Although significant progress has been achieved in the utility of high-throughput phenotyping technologies for assessing crop distribution, very few studies have attempted to assess their accuracies in mapping and monitoring the spatial distribution of NUS crops, especially in typical smallholder croplands in the global south. It is suggested that the effective utilisation of high-resolution UAV data, in conjunction with robust classification algorithms, has the capability to accurately characterise the spatial distribution of NUS crops within smallholder fields.

A variety of classification techniques have been proposed for mapping crop spatial distributions. These techniques leverage various data sources like remote sensing imagery and ancillary data to differentiate crop types at different spatial scales. Machine learning and deep learning algorithms such as support vector machines (SVM), artificial neural networks (ANN), Random forests (RF) and Naïve Bayes (NB) are widely used due to their ability to accurately detect and quantify the spatial extent of crops (Sarker, 2021). These algorithms can learn complex patterns and relationships from training data and classify

pixels or objects into different crop classes. For instance, a study by Mazarire et al. (2020) explored the efficacy of SVM and RF in classifying crops within heterogenous landscapes in South Africa. SVM demonstrated the highest performance, achieving an overall accuracy of 95% and a kappa accuracy of 94%. Furthermore, Ayele and Tamiru (2020) designed a chickpea type classification model using ANN, SVM and decision tree (DT) algorithms. The experimental results demonstrated that the best algorithm was DT achieving 97.5% accuracy.

A large body of research has demonstrated that VIs like Normalized difference vegetation index (NDVI), Soil adjusted vegetation index (SAVI) and Normalized difference red-edge index (NDRE) often improve classification accuracies. For instance, Asgari and Hasanlou (2023) created a Vis mapping approach to accurately identify specific crop types, such as rapeseed, utilising phenological and spectral metrics extracted from Sentinel-2 MSI images. Among the various Vis employed for crop mapping, the Atmospherically Resistant Vegetation Index (ARVI) yielded superior accuracies. The RF, KNN, and GB models utilising the ARVI index achieved overall accuracies of 95%, 90%, and 88%, respectively.VIs are known to overcome the influence of shadows and other background noise (Mutanga et al., 2023). Although this has been demonstrated extensively based on satellite borne data, there is a need to expand research efforts toward cutting-edge sensors with ultra-high resolution specifically, UAV imagery to achieve the precise mapping of NUS crops such as taro and sweet potato in smaller holder farms.

Therefore, this study sought to comparatively assess the potential of advanced machine learning methods and UAV derived multispectral data in mapping the spatial distribution of taro and sweet potato amongst other crops in smaller holder farms of South Africa. To address this objective, the performance of Gradients Tree Boosting, Random Forest and Support Vector Machine were compared in mapping the spatial distribution of Sweet -potato and Taro in a smallholder cropland. Special attention was given to the classification model's ability to capture field boundaries. Also, the relative contributions of bands, vegetation indices and both datasets combined were assessed.

3.2. Methods and materials

3.2.1. Study Area

The research was conducted in Swayimane (29°31024" S and 30°41037" E), a small rural settlement located in UMshwathi Municipality, KwaZulu Natal Province. Swayimane experiences a sub-tropical climate whereby, summers are hot and humid and winters are relatively drier (Ndlovu et al., 2021). Mean temperatures ranges from 11.8 to 24 degrees Celsius (Ndlovu et al., 2021). Furthermore, rainfall is more common during the summer months. The region receives an average annual rainfall of around 600 to 1100 millimetres (Ndlovu et al., 2021). Swayimane is recognised for its fertile clay loam soils and holds a prestigious position within the top 2% of high productive lands in South Africa (Ndlovu et al., 2021). As a result, the favourable environmental conditions in Swayimane support the cultivation of a diverse range of grain and legume crops. The prevalent crops cultivated in the study area includes sugarcane, taro, sweet potato, spinach, maize. The region is recognised for its smallholder maize farms which are maintained and harvested by the local community. The Swayimane community partakes in traditional farming practices which include manual labour and the use of livestock manure as fertiliser.
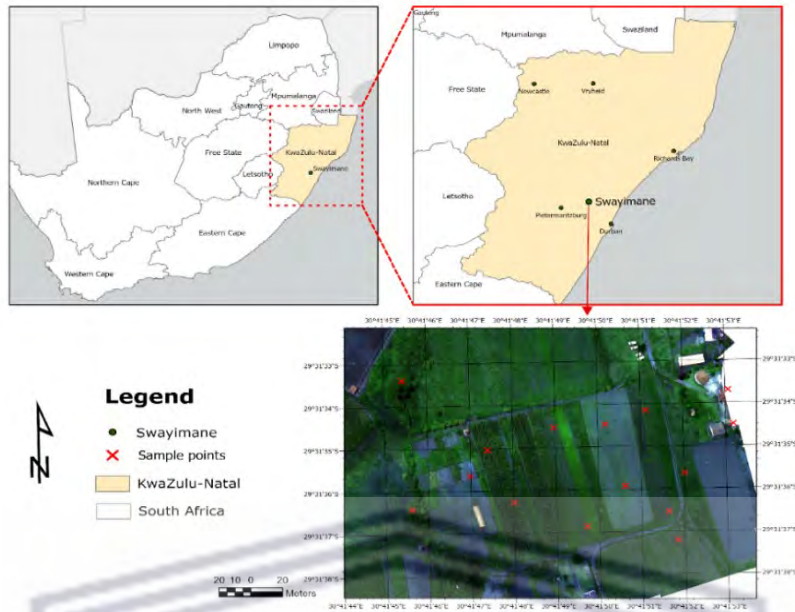
Figure 3-1: Location of the Swayimane study area, study site and smallholder crop field.

Figure 3-2, presents a flowchart outlining the key stages of this study, which include image data collection, image pre-processing, extraction of spectral traits, and subsequent statistical analysis.
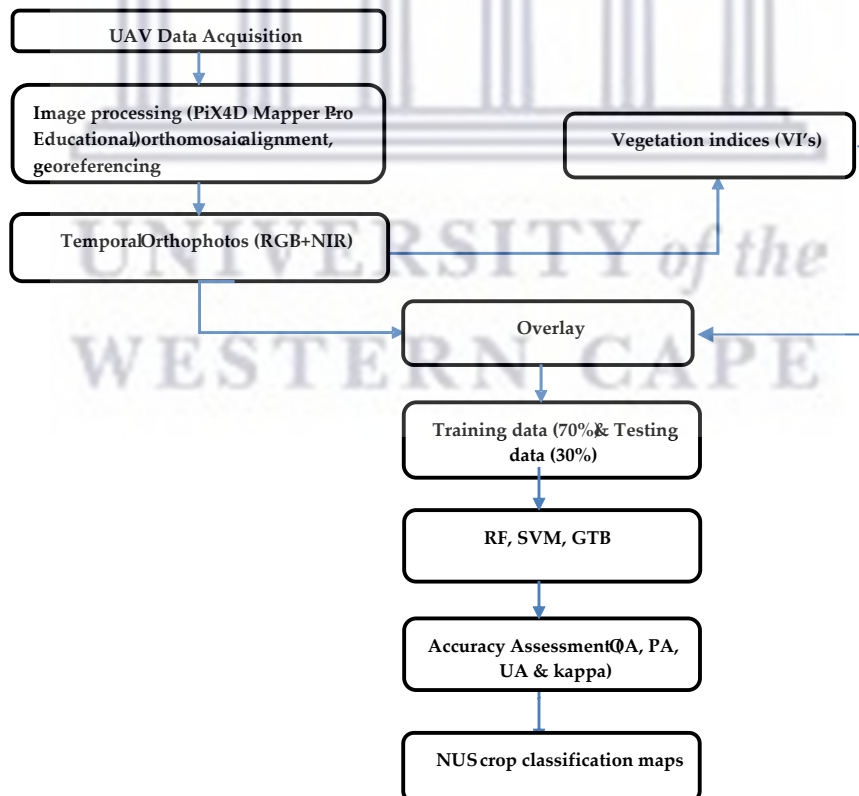
Figure 3-2: Flowchart of main processing steps in this study.

3.2.2.Data collection

Prior to capturing remotely sensed data, a field survey was conducted within the study area. A handheld Trimble Garmin GPS with an accuracy of ±1m was utilised to measure the location of different landuse land cover classes. Specifically, 8 classes were considered in this study. These were taro, sweet potato, natural vegetation, sugarcane, bare-land, buildup, maize growth stage one and maize growth stage two. A total of 310 points were collected in Google Earth Pro. The collected data was converted into a point map which was imported into Google Earth Engine for model training and validation.

A DJI Matrice (M300) quadcopter fitted with a Micasense Altum imaging sensor was utilised to capture images spanning the smallholder fields in this study. The DJI Matrice is an advanced high precision quadcopter that was fitted with a high accuracy Global Navigation Satellite System receiver (GNSS)(KEGA, 2021). The DJI has a maximum flight time of 55 minutes and maximum control range up to 15 kilometers, providing a wide operational range. The drone has a 1P45 rating which means it is protected against solid particles such as dust and water (KEGA, 2021). The Micasense Altum camera captures data in five spectral bands: red, green, blue, Red-edge (RE) and near-infrared (NIR). Additionally, it also includes a radiometric thermal sensor that operates within the 8–14 nm wavelength range. The Altum camera incorporates several features to enhance its functionality. Firstly, it is equipped with a solar irradiance sensor called DLS 2, which allows for accurate radiometric calibration by measuring the incident light conditions during image capture (KEGA, 2021). Additionally, the camera has a built-in GPS system, which enables georeferencing of the captured images (KEGA, 2021). The camera's Ground Sample Distance (GSD) is 5.2 cm per pixel when operated at a height of 120 meters above ground level (AGL) (KEGA, 2021). The multispectral bands of the camera have a sensor resolution of 3.2 cm per pixel, while the thermal band has a spatial resolution of 81 cm (KEGA, 2021).

To formulate a UAV flight plan, a shapefile defining the study area was created using the Google Earth Pro application. This shapefile was then transferred to the DJI matrice handheld console device. The formulated flight plan facilitated an autonomous drone mission, allowing for seamless aerial coverage of the study field and its surrounding regions. This automated flight mission was conducted at a flight height of 120 meters above ground level (AGL), with an image overlap of 80%. Images of the radiometric calibration target (CRP) and a white balance card were captured before and after the flights. The captured imagery was then pre-processed using Pix4D Fields photogrammetry software.

3.2.3.Data processing

In this stage, 3576 images were stitched together and adjusted for radiometric accuracy using Pix4Dfields 1.8.0 software, San Francisco, CA, USA. The radiometric correction process involved utilising CRP images which are captured before and after flights to account for atmospheric conditions and variations in indicent light conditions during image acquisition. This calibration process ensured accurate reflectance values in the image. After processing was completed an orthomosaic (high resolution aerial view) and digital eleveation model (DEM) GeoTIFF image was produced. Georeferencing of the orthomosaic was performed in ArcGIS 10.5 utilising ground reference points obtained from Google Earth Pro. This georeferencing stage yielded a root mean square error (RMSE) that is less than half the size of a pixel. The orthomosaic was aligned with the Universal Transverse Mercator (UTM zone 36S) projection. Thereafter, the drone orthomosaic of the smallholder crop field was imported into Google Earth Engine (GEE), a cloud-based platform for geospatial data analysis. Within GEE, the orthomosaic underwent classification using Gradient Tree Boost (GTB), Random Forest (RF), and Support Vector Machine (SVM) classifiers. These classifiers employ machine learning algorithms to classify pixels based on their spectral properties, enabling the identification and mapping

of various crops including sweet potato and taro. Three distinct datasets were used for this purpose within the study area.

A total of eleven Vis, which have been previously documented in literature, were chosen and evaluated to effectively differentiate NUS species. The VIs was derived by utilising the reflectance data obtained from the Altum multispectral and thermal bands. These indices typically relied on the red, red-edge, and near-infrared (NIR) segments of the electromagnetic (EM) spectrum. Table 3-1 presents a compilation of VIs that were chosen for this study, taking into consideration their direct and indirect correlation with image classification and crop health attributes, such as the NDVI, the NDRE, OSAVI and NDRGI.

Table 3-1: UAV-derived vegetation indices.

Vegetation Index	Abbreviation	Equation	Reference
Normalized difference vegetation index	NDVI	(NIR−RED)/(NIR+RED)	Xue and Su (2017)
Green normalized difference vegetation index	GNDVI	NIR−GREENNIR+GREEN	Gitelson et al. (1996)
Excess green index	EGI	2.5* (GREEN-RED)/(GREEN+RED+1)	(Qiu et al., 2020)
Normalized difference red-edge index	NDRE	NIR−RED EDGENIR+RED EDGE	(Fitzgerald et al., 2006)
Excess green index	EXG	2 * GREEN - RED – BLUE	Woebbecke et al. (1995)
Chlorophyll carotenoid index	CCI	(R - G) / (R + G)	(Jäger et al., 2022)
Optimized soil adjusted vegetation index	OSAVI	NIR−REDNIR+RED+0.16	Xue and Su (2017)
Enhanced vegetation index	EVI	(2.5 * (NIR+ RED) / (NIR + 6 * RED - 7.5* BLUE +1)	(Xing et al., 2019)
Normalised green, red difference index	NGRDI	(GREEN - RED) / (GREEN + RED)	Meyer and Neto (2008)
Simple ratio	SRI	NIR / RED	Jordan (1969)
Modified triangular vegetation index 1	MTVI1	1.2 ((1.2 ∗ (NIR − GREEN)) − (2.5 ∗ (RED − GREEN))	(Xing et al., 2019)

3.2.4. Image Classification

In the GEE platform three classification methods, that is Gradient tree boost, Support vector machine and Random Forest classifiers were implemented. These algorithms are renowned for their accuracy as they can effectively select spectral features for discriminating different cover classes (Judson et al., 2008). The training dataset utilised for image classification was derived by means of a meticulous visual examination of the orthomosaic, which had been acquired on February 12, 2021.Eight major land cover

46

classes were determined, and training data was acquired by identifying pixels that corresponded to these classes as outlined in Table 3-2. The sampled data was randomly split into 70% training ($n = 217$) and 30% validation ($n = 93$), for all classifiers. The training dataset was utilised for model development while the validation data was utilised to assess classification accuracy. An area computation was performed in GEE to estimate the number of pixels within each class, thereby determining the total areal extent for each landcover class.

Table 3-2: Training and testing data used for Pixel based image classification.

Class name	Code	Training (n)	Testing (n)
Taro	T	28	12
Sweet potato	SP	28	12
Natural Vegetation	NV	21	9
Sugarcane	SU	28	12
Bare land	BL	21	9
Built-up	BU	21	9
Maize growth stage 1	M1	35	15
Maize growth stage 2	M2	35	15

***Random Forest (RF)*:** RF is an ensemble machine learning method that incorporates bootstrap aggregation and binary recursive partitioning to grow multiple decision trees on randomly selected subsets of features and data. Groups of decision trees vote on the best class for each sample (Breiman, 2001). The algorithm was optimised using its hyper parameters that is the number of features randomly selected at each node (*mtry*) and the number of total trees (*ntree*). Specifically, the *ntree* was set to 300, the maximum depth of each tree (max Nodes), minimum samples required to split nodes (minSamples), and the randomization seed was set to default in GEE. The bag fraction, set at 0.5, facilitates the introduction of randomness during the construction of the tree-building process. According to (Mutanga et al., 2023), Random Forest (RF) has several advantageous characteristics:

    a. RF offers easily adjustable hyperparameters.
    b. The training process for RF is efficient, resulting in quick model training.
    c. RF exhibits robustness against outliers, overfitting, and high-dimensional data, making it suitable for various datasets.
    d. Due to the averaging of multiple trees, RF demonstrates low bias and moderate to minimal variance.
    e. RF is effective in handling both continuous and categorical variables.
    f. RF possesses the ability to assess the importance of predictor variables.
    g. RF shows a relative resistance to multicollinearity between predictor variables

These factors make it well-suited for mapping crop distributions in this study area. In this study all spectral bands and VIs derived from the drone composite were used as predictor variables.

47

***Support Vector Machine (SVM)*:** Support vector machines (SVMs) were initially developed for binary classification but have also proven their efficacy in regression problems (Zhao et al., 2020). For multiclass classification as in this study, SVMs uses a one-vs-all or one-vs-one approach with voting to determine the correct class. A radial basis function (RBF) kernel was used as it performed better than linear or polynomial kernels on this data. The two hyperparameters that were used to optimise SVM-RBF were cost C and gamma γ. Higher C increases penalty for misclassifications, while higher γ decreases variance. SVM is relatively insensitive to noisy inputs, reducing estimation errors and improving robustness (Singla et al., 2020). It performs well on high-dimensional datasets and is robust to outliers, making it advantageous for many problems (Hsu et al., 2003). Three parameters were tuned for the SVR model, namely the penalty parameter (C), precision parameter (ε), and kernel parameter (γ). Through this process, the SVR model achieved optimal performance with a C value of 10, ε value of 0.5, and the default γ value of 1 was maintained.

***Gradient tree boost (GTB)*:** Gradient Boosting Machines (GBMs) are a family of powerful ensemble machine learning techniques that fall under the category of sequential models. Each model in the sequence learns from the mistakes of previous models to incrementally improve overall performance (Natekin and Knoll, 2013). Unlike random forests which averages predictions, GBMs use a gradient descent approach to minimise error at each stage. GBMs are robust due to their flexibility in customising loss functions during model optimisation. This has led to their widespread success in real-world applications compared to single models. They rely on three main components - a loss function, weak learner models like decision trees, and an additive model that combines predictions from each weak learner (Natekin and Knoll, 2013). Importantly, tree based GBM algorithms were designed specifically to handle large datasets very efficiently. They can run over 10 times faster than other popular algorithms on large data, making them highly scalable for different scenarios. The GTB classifier has several adjustable parameters that require configuration, including the number of trees, shrinkage, sampling rate, maximum nodes, and seed values. The number of trees (*nTree*) was adjusted to 300. The maximum nodes, seeds, shrinkage and sampling parameters were set to default in GEE.

3.2.5. *Accuracy assessment*

An accuracy assessment was carried out on the multispectral UAV image, to assess the sensor's capability in effectively discriminate NUS crops at the plot level. Confusion matrices were generated to compute the overall accuracy (OA), kappa coefficient, F1 score, user and producer's accuracies for RF, GTB and SVM classifiers. A confusion matrix is an overly process that compares the classified classes with the reference points and provides a count of the correct and incorrect classifications for each class. It helps quantify the classification accuracy and identify patterns of misclassification. The overall accuracy (OA) metric was utilised to assess the efficiency of the algorithms employed in this study (Gxokwe, 2022). The producer's accuracy (PA) was employed to determine the likelihood of correctly classifying the reference data on the map. The user's accuracy (UA) was employed to assess probability that a classified pixel accurately correlates to the corresponding category on ground (Gxokwe, 2022).The kappa statistic, which ranges from 0 to 1, is used to measure the agreement between the classified map and the reference data. Values greater than 0.80 indicate a high level of agreement. In contrast, values below 0.40 indicate a weak level of agreement, whereas scores within the range of 0.40 to 0.80 indicate a moderate level of agreement (Dondofema et al., 2023). The F1 score harmonises the weighted averages of precision and recall metrics, making it a commonly used score for validating the accuracy of the classification process (Pham et al., 2023). As the values of the metrics increase, the model's confidence in accurately assigning the predefined classes in the study also increases. Furthermore, line plots and Jeffries-Matusita (JM) distances were employed in GEE to assess the spectral separability between landcover classes. This analysis involved examining the distances

between class means and the distribution of values derived from those means (Gxokwe, 2022). JM criterion is a parametric measure that ranges from 0 to 2 (Gxokwe, 2022). A value approaching 2 signifies a higher degree of spectral distinctiveness between two classes.

3.3. Results

3.3.1. *Spectral reflectance curve*

The spectral reflectance curve analysis revealed distinct separability among the classes, as depicted in Figure 3-3. The spectral responses of most of the classes exhibited notable distinctions in the NIR and RE regions of the electromagnetic spectrum. The Blue and Red regions of the EM spectrum exhibited limited discriminatory potential in distinguishing between different landcover classes. Sweet potato and Taro exhibited pronounced spectral distinctiveness compared to other classes, particularly in the RE and NIR segments of the EM spectrum (717 to 842 nm).
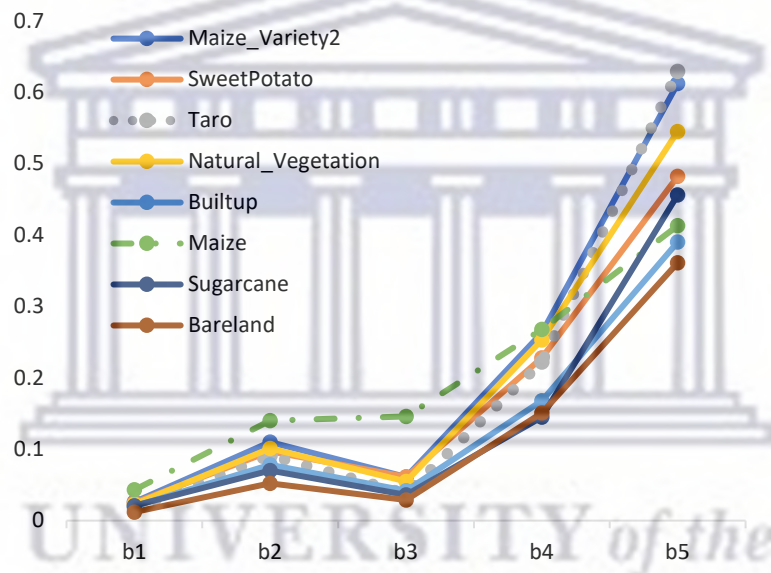
Figure 3-3: Spectral reflectance curve of all landcover classes

3.3.2. *Comparative classification of cropland using SVM, RF, GTB based on bands only.*

Land cover classification results using spectral bands as an independent dataset are shown in Table 3-3. The findings reveal that the RF and GTB models exhibited superior accuracies when utilising the raw spectral band dataset. These models achieved exceptional results in terms of OA, kappa, and F1 scores, surpassing 80 percent using optimal bands such as B1, B4 and B5. Consequently, these results demonstrate a noteworthy level of concurrence between the predicted and actual land cover categories, as visually depicted in Table 3-3. Moreover, the RF and GTB models also attained superior producer accuracies for most land cover classes (>75%) (supplementary Figure S2-3). Sweet potato and taro exhibited notably higher user accuracies, reaching >56 percent, with the RF and GTB models. These outcomes are further supported by Figure 3-3, as the spectral reflectance of sweet potato and taro are more discernible particularly within the Red-edge and NIR segments of the electromagnetic spectrum. In contrast, the SVM classifier yielded lower accuracies, with an OA of 0.42, kappa statistic of 0.32, and an F1 score of 0.31. The SVM user and producer accuracies were comparatively lower, with values ranging from 25- 60 percent.

Table 3-3: Overall accuracies, kappa statistics and F1 scores for RF, GTB and SVM

Analysis Stage	Variables	Accuracy unit	SVM	RF	GTB
1	Bands only	OA	0.42	0.86	0.83
		Kappa	0.32	0.84	0.80
		F1	0.31	0.84	0.80
2	VI's only	OA	0.74	0.84	0.83
		Kappa	0.70	0.81	0.80
		F1	0.71	0.82	0.81
3	Bands & VI'S	OA	0.71	0.86	0.88
		Kappa	0.67	0.84	0.85
		F1	0.66	0.80	0.84

The separabilities between all classes in the single image were investigated using the JM distances in Table 3-4. Most of the classes exhibited notable disparities among their respective outputs. The findings indicated that observable bands such as B1 demonstrated lower JM distances, suggesting a high degree of overlap between the classes. This was particularly notable for taro, sweet potato, and maize growth stage two, which were often confused with bareland and natural vegetation. In contrast, B4 and B5 exhibited higher separability (with JM distances ranging from 1.7 to 1.8) for classes such as taro, sweet potato, sugarcane, and maize growth stage one. This suggests that classification algorithms are likely to effectively distinguish these pairs of classes (supplementary tables S2-1 & S2-2). The results additionally showed that combining all auxiliary variables slightly decreased separability between sweet potato, bare land and the maize growth stages by 1-8% but increased separability between taro and natural vegetation.

Table 3-4: Band 1 JM distances

B1	Taro	SP	NV	SU	BL	BU	M1	M2
Taro	0	0.469	0.532	0.457	0.615	1.016	0.814	0.3542
SP	0.47	0	0.51	0.44	0.54	1.05	0.8	0.34
NV	0.53	0.51	0	0.71	0.45	0.85	0.64	0.58
SU	0.46	0.44	0.713	0.00	0.72	1.11	0.92	0.24
BL	0.62	0.54	0.45	0.72	0	0.95	0.58	0.61
BU	1.02	1.05	0.85	1.11	0.95	0	0.87	1.06
M1	0.81	0.8	0.64	0.91	0.58	0.87	0	0.84
M2	0.35	0.34	0.58	0.24	0.61	1.06	0.84	0

3.3.3. Comparative classification of croplands using SVM, RF, and GTB based vegetation indices only.

The utilisation of VIs in combination with RF, SVM, and GTB models resulted in superior outcomes, as indicated in Table 3-3. This superiority is evident from the variable importance scores, where EGI, EXG and GNDVI were identified as the most optimal performing variables (supplementary Figure S2-2). Notably, the SVM model exhibited a significant increase in the kappa statistic, rising from 0.32 to 0.74, upon incorporating VIs (Table 3-3). Regarding RF's performance, the inclusion of Vis led to a slight decrease of approximately 2% in the kappa statistic and accuracies. The GTB classifier demonstrated consistent high accuracy, equivalent to the band's dataset, with an overall accuracy (OA) of 0.83 and a kappa statistic of 0.80. There was a noticeable improvement in user accuracies for RF and GTB algorithms, with values ranging from 66% to 94% for the majority of classes. Similarly, SVM accuracies demonstrated an average increase of 10% to 26% across most classes. The combination of multiple bands such as Blue, Red-edge, and Near-Infrared contributed to the improved performance of vegetation indices. However, the highest overall accuracy was achieved when combining both spectral bands and VIs, indicating that their joint utilisation maximised the separability for this algorithm.

3.3.4. Comparative performance of spectral variables

The results indicate that the raw spectral bands underperformed compared to vegetation indices and the combined dataset across all models, as demonstrated by mean OA of 70 percent and a mean kappa statistic of 0.65 (Figure 3-4). This observation is further supported by the variable importance scores, whereby B2 and B4 ranked relatively lower (see supplementary Figure S2-1). Specifically, VIs outperformed the bands by 10 percent but yielded similar accuracies to the combined dataset (Table 3-3). The performance of optimal bands such as EGI, NDRE, and GNDVI significantly contributed to the improved performance of machine learning algorithms. Furthermore, the combined dataset exhibited the highest performance across all models, with a mean OA of 0.82 and a kappa statistic of 0.79. This is evident by the close alignment between the OA and the kappa statistic, indicating a strong agreement between the two measures.
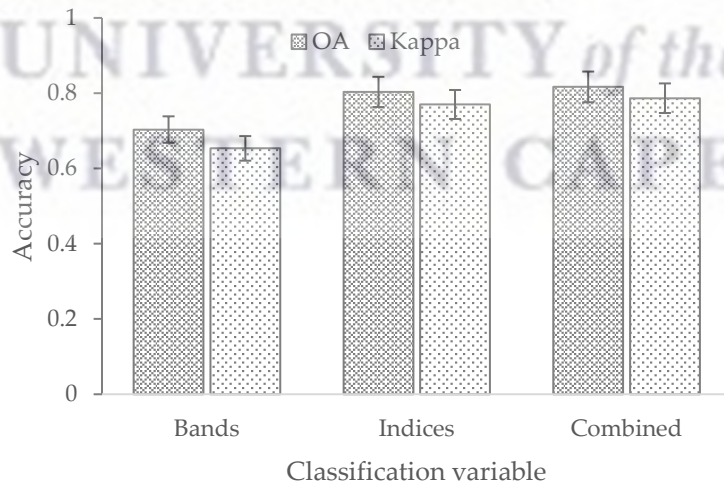
Figure 3-4: Comparative classification performance of bands, vegetation indices and combined data

3.3.5. Comparative classification performance of SVM, RF and GTB

The RF and GTB models achieved the highest overall performance based on classification mean OA and kappa statistics (Figure 3-5). RF and GTB produced accuracies >80% and mean kappa statistic values ranging from 0.80 to 0.85, demonstrating very good agreement between predicted and actual

land cover classes (Table 3-3). Furthermore, mean F1 scores ranged between 0.82 and 0.81 for RF and GTB, respectively. Contrastingly, the SVM classifier performed worse in comparison with a mean OA of 0.62 and kappa statistic of 0.56. Of all models tested, GTB showed the greatest increase (4% difference) in performance across input data, with accuracies sharply rising from 83% for the initial dataset to 88% with the combined dataset (Table 3-3). In comparison, RF displayed a smaller magnitude change in accuracy across datasets, decreasing slightly from bands-only to vegetation indices-only before increasing 2% with the combined dataset. The findings yielded by the GTB classifier illustrate that it can generate consistent results which are slightly better than those of RF.
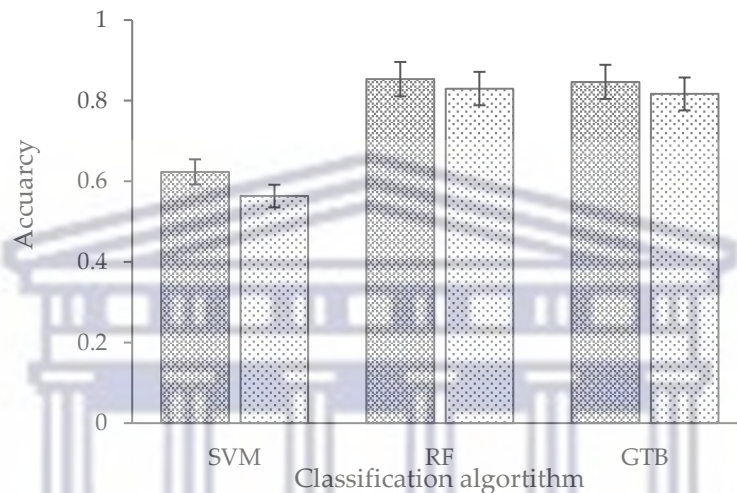
Figure 3-5: Comparative classification performance of Support vector machines (SVM), Random Forest (RF) and Gradient tree boosting algorithms (GTB)

3.3.6. Final classification of the cropland using combined data

The combination of spectral bands and VIs yielded the highest user's and producer's accuracies, ranging from 71.4% to 100%, for all classes, effectively representing the relationship between spectral data and land cover (Figure 3-6). The final RF classification, based on the combined data, achieved an OA of 0.86 and a kappa statistic of 0.84 (Table 3-3), utilising B1, NDRE, and EGI as the most optimal classification variables (Figure 3-7). Similarly, the GTB model showcased superior performance, achieving an OA of 0.88 and kappa statistic of 0.85 (Table 3-3) when utilising the B1, B3, and B5 variables. At the individual class level, RF and GTB most accurately mapped maize growth stage one and sugarcane (95-100% accuracy across datasets). Sweet potato, natural vegetation and built-up areas were most frequently misclassified (12.5-50% accuracy), suggesting weaker spectral representations of these classes. Specifically, maize had the highest classification accuracy when the RF and GTB models were used along with datasets two and three. SVM exhibited lower accuracies, with an OA of 0.71 and a kappa of 0.67 (Table 3-3). The SVM model experienced more misclassifications overall, struggling to effectively model the complex spectral-class relationships of the real-world environment (Figure 3-6C). Overall, the final classification models suggested that GTB could slightly outperform the RF ensemble.

52
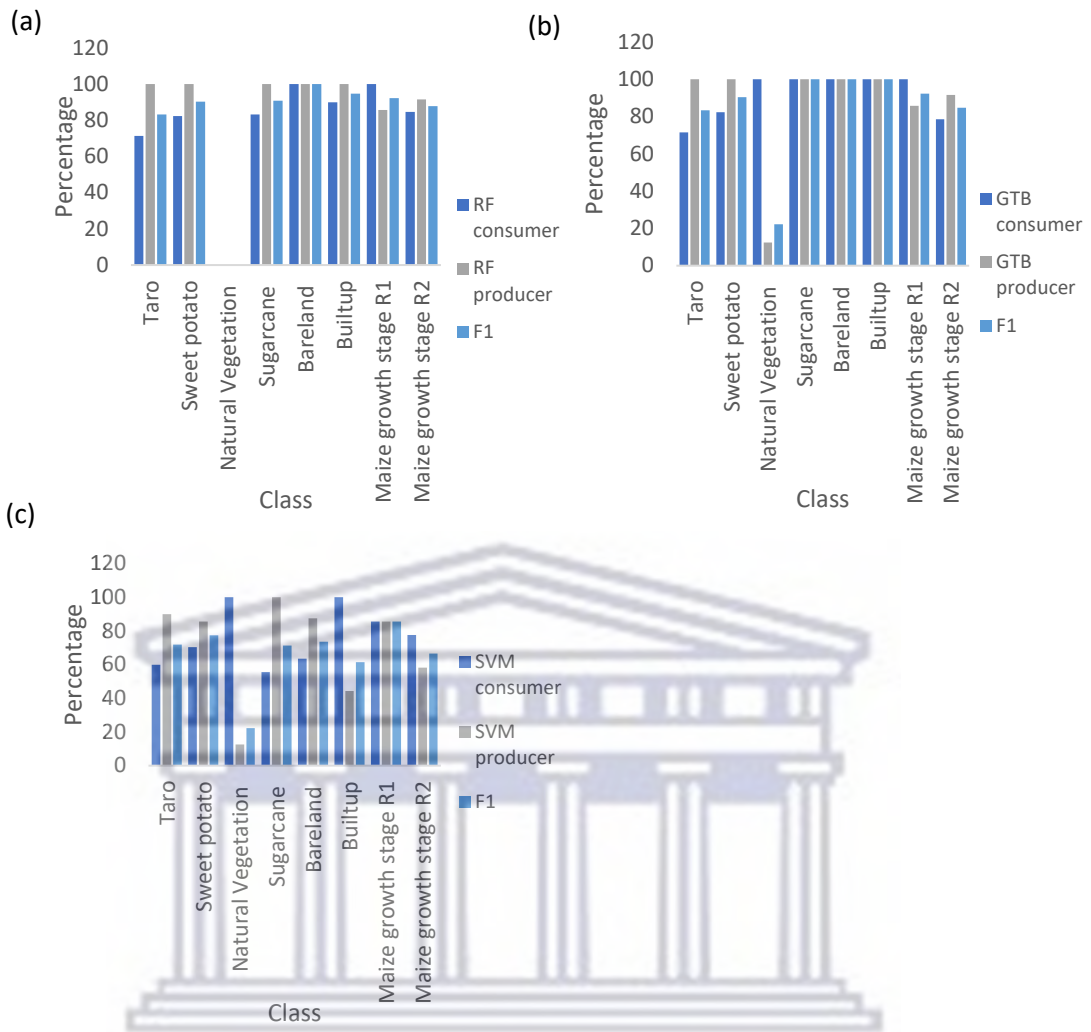
Figure 3-6 : user and producer accuracies of (a) RF, (b) GTB & (c) SVM in conjunction with dataset 3
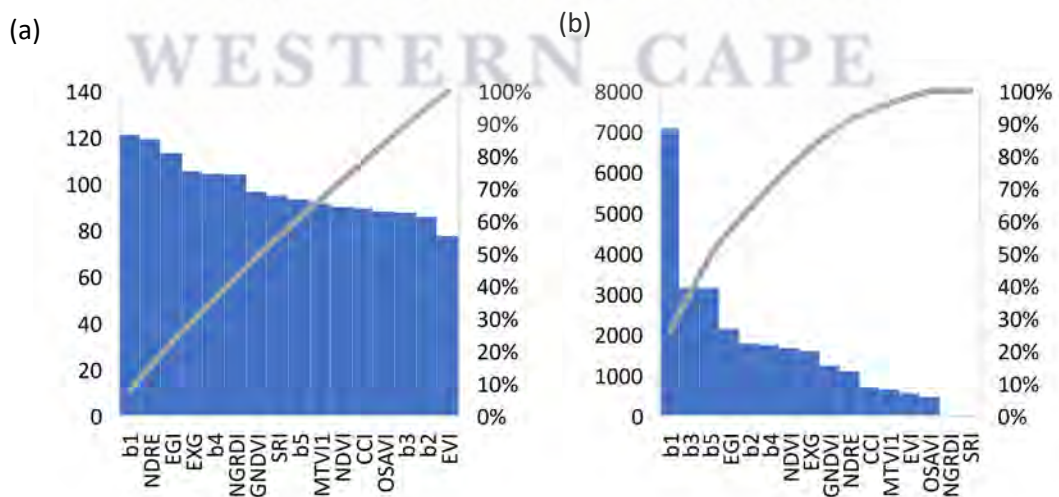
Figure 3-7: Variable importance scores of (a) RF and (b) GTB with dataset 3.

3.3.7. Spatial distribution of land cover types and their areal extents

Figures 3-8, present the percentage of the total pixel area occupied by each class, as determined by the selected classification approaches. Visual analysis of the classification maps reveals differences in how accurately the algorithms represented the spatial distribution of crops (Figure 3-9). The maps generated by the RF and GTB models exhibited distinct and accurate boundaries between sweet potato, maize, and taro, effectively capturing the shape of the fields. However, on the map classified using SVM, the depiction of crop boundaries was distorted. Field shapes were irregular and inaccurately represented. Pixel blocks were misclassified rather than capturing the fine-scale variability as RF and GTB achieved. Some crops like sweet potato appeared fragmented into separate small patches rather than compact field units. The transition zones between different crops appeared less clear, indicating a lack of precise delineation of adjacent fields by the SVM model. On the other hand, the RF and GTB models demonstrated a sharper and more distinct demarcation of fields located next to one another.
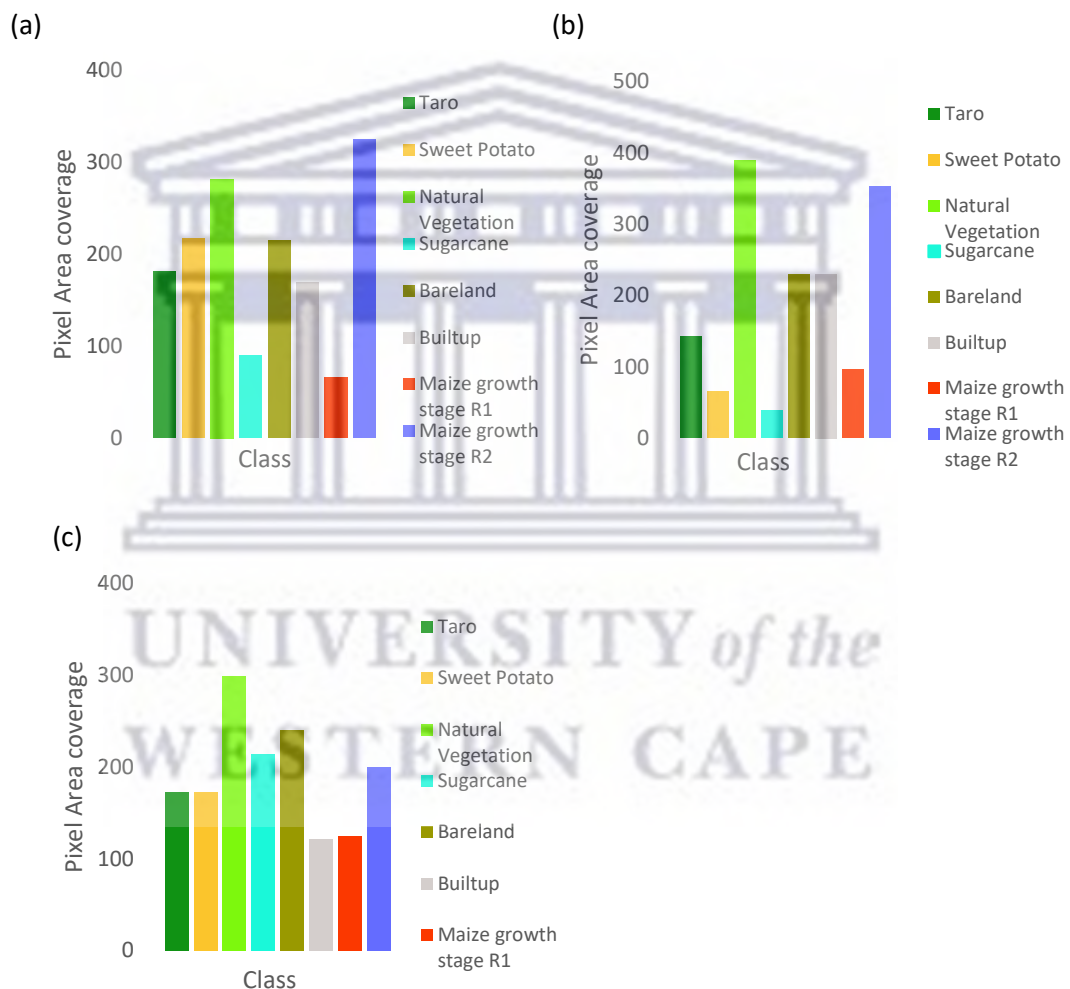
Figure 3-8: pixel area per class of (a) RF, (b) GTB, (c) SVM with dataset 3.
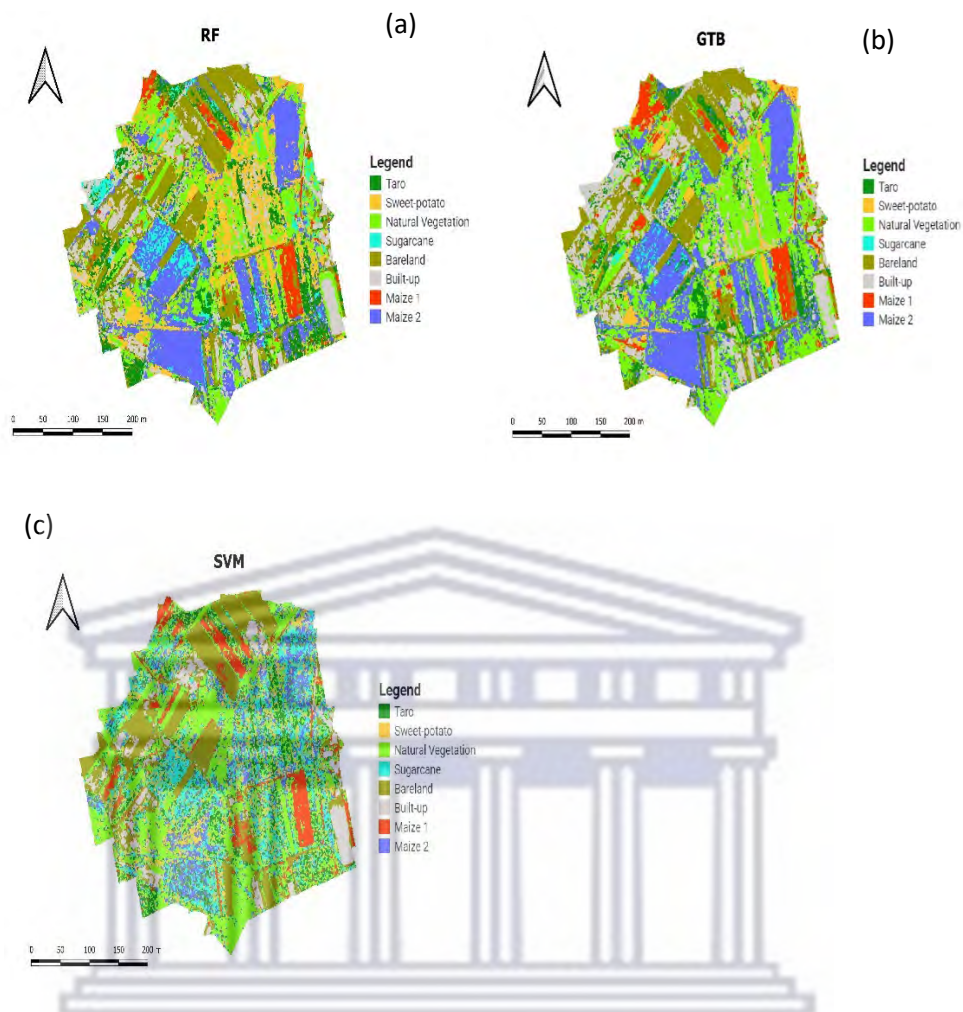
Figure 3-9: NUS crop distribution maps of (a) RF (b) GTB (c) SVM.

3.4. Discussion

3.4.1. Classification performance of raw spectral bands and vegetation indices in mapping the NUS in the smallholder cropland.

The results of this study indicated that both individual bands and vegetation indices can effectively map the spatial distributions of NUS crop species (Table 3-3). However, there were some notable differences in their predictive performance. Upon examining the variable importance graphs, it became apparent that certain bands, specifically band 1 (Blue), band 4 (Red-edge), and band 5 (NIR), consistently yielded higher classification accuracies compared to other individual raw spectral bands depicted (Figure 3-7). This is supported by the spectral separability between classes as measured by JM distances. The bands produced higher JM distances ranging from 1.5 to 1.7 for some classes like taro, sweet-potato and maize growth stage two, indicating better spectral separability (Table 3-4). However, the contribution of vegetation indices to classification algorithms was more effective than bands. This also suggests the VIs were effective in differentiating between crop types that exhibited similar spectral characteristics within homogeneous fields. The vegetation indices that exhibit the highest importance scores in both Random Forest (RF) and Gradient Boosting (GTB) models were RGB-based indices EGI, EXG, and

55

NDGRI. Among the vegetation indices, EGI consistently demonstrated the highest predictive capacity across all crop types (Figure 3-7).

It has been extensively demonstrated that VIs exhibit robustness in comparison to bands, as expected. Moreover, the utilisation of VIs led to a significant increase in both PA and UA results, surpassing the outcomes obtained in previous stages of analysis (analysis I). This improvement indicates an enhanced capacity of the dataset variables to distinguish specific classes from others, as depicted in Figure 3-6. The results of this study underscore the significance of integrating VIs in the process of mapping NUS crops within smallholder crop lands. The amalgamation of spectral bands and VIs contributed to an increase in OA, which can be attributed to the VIs' ability to mitigate the influence of soil background, sensor zenith angle, sun angle, and other atmospheric impurities (Zeng et al., 2022). Moreover, the incorporation of multiple spectral bands from different sections of the electromagnetic spectrum in computing vegetation indices enhances their resilience for image classification when compared to the influence of only one band from a single section of the EM spectrum. For example a study by Niederheiser et al. (2021) demonstrated that integrating different spectral and textural indices improved the accuracy of RF models in mapping vegetation cover. Asgari and Hasanlou (2023) also reported similar outcomes in their study, where they utilised Sentinel-2 MSI extracted vegetation indices to delineate various crop types, including rapeseed. The overall accuracy of RF, GTB, and k-nearest neighbours (KNN) models increased to 95%, 88%, and 90%, respectively, when employing the Atmospherically Resistant Vegetation Index (ARVI).

Specifically, VIs such as EGI and NDRE act as a robust proxy for leaf area, green biomass and general photosynthetic activity and all factors that influence crop spectral separability (Meyer and Neto, 2008). While other indices like EVI and NDVI incorporate additional bands and parameters, they did not substantially outperform NDRE, EXG, GNDVI for this application. These finding suggests that the NUS fields likely exhibited distinct spectral responses in the NIR, RE and Red bands, and the application of more complex adjustments provided limited additional predictive insight. Overall, both individual spectral bands and vegetation indices demonstrate their usefulness in mapping neglected crops through remote sensing techniques.

3.4.2. The comparative performance of machine learning algorithms in mapping the spatial distribution of neglected and underutilised crops species (NUS).

In evaluating the classification performance Support Vector machine (SVM), Random Forest (RF) and Gradient Tree Boost (GTB), in mapping the spatial distribution of NUS crop species in a smallholder cropland, results showed that RF and GTB achieved the highest classification accuracies based on all spectral variables. The optimal performance of RF can be attributed to its utilization of decision trees and the combination of their predictions, enabling accurate classifications (Sipper and Moore, 2021). The algorithm's ability to capture complex interactions and handle high-dimensional data contributed to its superior performance (Hornung and Boulesteix, 2022).

Furthermore, GTB algorithm, in conjunction with combined data, exhibited superior capabilities in detecting and mapping field boundaries of sweet potato and taro amongst others. Specifically, this combination produced the highest accuracy of 88%, kappa statistic of 0.85, and F1 score of 0.84 compared to the other models/datasets (Table 3-3). Moreover, the GTB classifier significantly demonstrated accuracy improvements from dataset 1 to dataset 3, outperforming the RF and SVM algorithms. GTB can identify subtle variations in spectral responses that may not be discernible using linear classifiers such as SVM (Ghimire et al., 2010). In a seminal study exploring land cover mapping with remote sensing data, Abdi (2020) found that the GTB algorithm outperformed the RF algorithm in

56

achieving more accurate results for mapping and detecting changes in land use and land cover types within a boreal (northern forest) landscape. GTB achieved higher overall and user accuracies, demonstrating a better predictive performance.

While Ensemble classifiers, in general, outperformed SVM in overall performance, there was no substantial difference in performance among the ensemble methods themselves. The mapped distributions of land cover classes revealed comparable spatial coverages for taro, bareland and maize at different growth stages as classified by GTB and RF. RF and GTB have an ability to capture complex patterns while controlling overfitting (Thenkabail and Lyon, 2016). Therefore, RF and GTB were better able to learn the intricate spectral signatures of different classes, hence accurately discriminating NUS crops at plot level from the remote sensing data. In contrast, the SVM results demonstrated divergent representations, with an exacerbated misclassification of some classes. This increased misassignment was prominently visible in the north-eastern and south-western regions of the map, highlighting disproportionate error in those areas relative to the other algorithms (Figure 3-9). SVM is relatively prone to overfitting and it is sensitive to noisy inputs further exacerbating its weakness in crop mapping in smallholder farms (Singla et al., 2020). Furthermore, according to Mountrakis et al. (2011), SVM models rely on finding a maximal margin hyperplane which can be heavily influenced by outliers and noisy samples. The comparable performance of GTB and RF suggests that ensemble decision tree methods excel in capturing and delineating the intricate relationships between predictor variables and crop classes (Aguilar et al., 2018). By combining many individual decision trees, they can model nonlinear interactions that aid in the differentiation of spectrally similar crops such as NUS (Saarela and Jauhiainen, 2021). Similarly, in their study, Yulianto et al. (2023) compared the performance of various algorithms for predicting and mapping land degradation using remote sensing techniques. Their results demonstrated the superiority and effectiveness of GTB and RF, both in achieving accuracies surpassing 85%, in contrast to the less effective performance of SVM. The superior performance metrics imply that these algorithms have the potential to create more reliable land cover maps with limited misclassifications.

Despite its ability to handle high-dimensional data and non-linear relationships, SVM might struggle to capture the complex patterns and interactions present in the spatial distribution of NUS. This indicates the crop classifications may not have been perfectly separable by simple hyperplanes in feature space (Gove and Faytong, 2012). SVM accuracies were slightly lower than RF and GTB accuracies, with a 42 to 72% OA across all datasets (Table 3-3). SVM classifier produced the lowest accuracies and kappa coefficients for all datasets, confirming its strong assumptions of independence between features are inappropriate for this remote sensing task. Furthermore, classes such as taro, natural vegetation, and maize at growth stage two were frequently misclassified hence lower user accuracies < 80%.

3.5. Conclusion

The objective of this study was to comparatively assess the classification performance of Gradient Tree Boosting, Random Forest and Support Vector Machine in mapping the field boundaries and the spatial distribution of Sweet -potato and Taro in a smallholder cropland using remotely sensed multispectral data acquired via UAV. In addressing this objective, relative contributions of bands and vegetation indices was also assessed. Grounded on the findings of this study it can be concluded that.

- GTB and RF could effectively discriminate the field boundaries of NUS and effectively map their spatial distribution in a smallholder cropland based on bands and indices derived from the Red-edge and the NIR amongst others.

- Specifically, the GTB algorithm, in conjunction with combined data, exhibited superior capabilities in detecting and mapping field boundaries of sweet potato and taro amongst other crops.
- Overall, the contribution of bands in classifying a smallholder cropland with NUS among other crops was found to be less significant than that of vegetation indices.

The precise identification and comprehension of distribution patterns of NUS crops play a pivotal role in enabling targeted interventions for conservation, cultivation, and utilisation. This, in turn, contributes significantly to enhancing food and nutrition security in Sub-Saharan Africa. In its entirety, this study adds to the effectiveness of advanced classification algorithms for mapping NUS in smallholder farming systems. The thematic maps depicting the distribution of NUS crops offer valuable insights for farm-scale management, while national departments can benefit from the implementation of robust classifiers to develop accurate and dependable agricultural landcover maps.

58

References

Abdi, A. M. (2020). Land cover and land use classification performance of machine learning algorithms in a boreal landscape using Sentinel-2 data. Giscience & Remote Sensing, 57(1), 1-20.

Aguilar, R., Zurita-Milla, R., Izquierdo-Verdiguier, E., & A. de By, R. (2018). A cloud-based multi-temporal ensemble classifier to map smallholder farming systems. Remote Sensing, 10(5), 729.

Asgari, S., & Hasanlou, M. (2023). A Comparative Study of Machine Learning Classifiers for Crop Type Mapping Using Vegetation Indices. ISPRS Annals of the Photogrammetry, Remote Sensing and Spatial Information Sciences, 10, 79-85.

Ayele, N. A., & Tamiru, H. K. (2020). Developing classification model for chickpea types using machine learning algorithms. International Journal of Innovative Technology and Exploring Engineering, 10(1), 5-11.

Breiman, L. (2001). Random forests. Machine learning, 45, 5-32.

Dondofema, F., Nethengwe, N., Taylor, P., & Ramoelo, A. (2023). Comparison of Satellite Platform for Mapping the Distribution of Mauritius Thorn (Caesalpinia decapetala) and River Red Gum (Eucalyptus camaldulensis) in the Vhembe Biosphere Reserve. Remote Sensing, 15(11), 2753.

El Bilali, H., Cardone, G., De Falcis, E., Naino Jika, A. K., Rokka, S., Diawara, A. B., Nouhou, B., & Ghione, A. (2023). Neglected and underutilised species (NUS): an analysis of strengths, weaknesses, opportunities and threats (SWOT).

Everitt, J., Yang, C., Davis, M., Everitt, J., & Davis, M. (2007). Mapping wild taro with color-infrared aerial photography and image processing. J. Aquat. Plant Manage, 45, 106-110.

Fan, S., & Rue, C. (2020). The role of smallholder farms in a changing world. The role of smallholder farms in food and nutrition security, 13-28.

FAO, AUC, ECA and WFP. 2023. Africa – Regional Overview of Food Security and Nutrition 2023: Statistics and trends. Accra, FAO. https://doi.org/10.4060/cc8743en

Fitzgerald, G., Rodriguez, D., Christensen, L., Belford, R., Sadras, V., & Clarke, T. (2006). Spectral and thermal sensing for nitrogen and water status in rainfed and irrigated wheat environments. Precision Agriculture, 7, 233-248.

Ghimire, B., Rogan, J., & Miller, J. (2010). Contextual land-cover classification: incorporating spatial dependence in land-cover classification models using random forests and the Getis statistic. Remote Sensing Letters, 1(1), 45-54.

Gitelson, A. A., Kaufman, Y. J., & Merzlyak, M. N. (1996). Use of a green channel in remote sensing of global vegetation from EOS-MODIS. REMOTE SENSING OF ENVIRONMENT, 58(3), 289-298.

Gove, R., & Faytong, J. (2012). Machine learning and event-based software testing: classifiers for identifying infeasible GUI event sequences. In Advances in computers (Vol. 86, pp. 109-135). Elsevier.

Gxokwe, S. 2022. Developing an integrated remotely sensed framework for the detection and monitoring of seasonally-flooded wetlands in semi-arid environments of southern Africa.

Hornung, R., & Boulesteix, A.-L. (2022). Interaction forests: Identifying and exploiting interpretable quantitative and qualitative interaction effects. Computational Statistics & Data Analysis, 171, 107460.

Hsu, C.-W., Chang, C.-C., & Lin, C.-J. (2003). A practical guide to support vector classification. In: Taipei, Taiwan.

Jäger, T., Mokos, A., Prasianakis, N. I., & Leyer, S. (2022). first_page settings Order Article Reprints Open AccessArticle Pore-Level Multiphase Simulations of Realistic Distillation Membranes for Water Desalination. Membranes.

Jordan, C. F. (1969). Derivation of leaf-area index from quality of light on the forest floor. Ecology, 50(4), 663-666.

Judson, R., Elloumi, F., Setzer, R. W., Li, Z., & Shah, I. (2008). A comparison of machine learning algorithms for chemical toxicity classification using a simulated multi-scale data model. BMC bioinformatics, 9(1), 1-16.

KEGA, S. (2021). EVALUATING THE POTENTIAL FOR INCREASED FORAGE PRODUCTIVITY AND SOIL CARBON SEQUESTRATION IN STRIP-THINNED SILVOPASTURES Department of Natural Resource Sciences, Thompson Rivers University].

Kumar, L., Chhogyel, N., Gopalakrishnan, T., Hasan, M. K., Jayasinghe, S. L., Kariyawasam, C. S., Kogo, B. K., & Ratnayake, S. (2022). Climate change and future of agri-food production. In Future Foods (pp. 49-79). Elsevier.

Mabhaudhi, T., Chimonyo, V. G., & Modi, A. T. (2017). Status of underutilised crops in South Africa: Opportunities for developing research capacity. Sustainability, 9(9), 1569.

Mazarire, T. T., Ratshiedana, P. E., Nyamugama, A., Adam, E., & Chirima, G. (2020). Exploring machine learning algorithms for mapping crop types in a heterogeneous agriculture landscape using Sentinel-2 data. A case study of Free State Province, South Africa. South African Journal of Geomatics, 9(2), 333-347.

Meyer, G. E., & Neto, J. C. (2008). Verification of color vegetation indices for automated crop imaging applications. Computers and Electronics in Agriculture, 63(2), 282-293.

Mountrakis, G., Im, J., & Ogole, C. (2011). Support vector machines in remote sensing: A review. Isprs Journal of Photogrammetry and Remote Sensing, 66(3), 247-259.

Mutanga, O., Masenyama, A., & Sibanda, M. (2023). Spectral saturation in the remote sensing of high-density vegetation traits: A systematic review of progress, challenges, and prospects. Isprs Journal of Photogrammetry and Remote Sensing, 198, 297-309.

Natekin, A., & Knoll, A. (2013). Gradient boosting machines, a tutorial. Frontiers in neurorobotics, 7, 21.

Ndlovu, H. S., Odindi, J., Sibanda, M., Mutanga, O., Clulow, A., Chimonyo, V. G., & Mabhaudhi, T. (2021). A comparative estimation of maize leaf water content using machine learning techniques and unmanned aerial vehicle (UAV)-based proximal and remotely sensed data. Remote Sensing, 13(20), 4091.

Niederheiser, R., Winkler, M., Di Cecco, V., Erschbamer, B., Fernández, R., Geitner, C., Hofbauer, H., Kalaitzidis, C., Klingraber, B., & Lamprecht, A. (2021). Using automated vegetation cover estimation from close-range photogrammetric point clouds to compare vegetation location properties in mountain terrain. Giscience & Remote Sensing, 58(1), 120-137.

Pham, H.-T., Nguyen, H.-Q., Le, K.-P., Tran, T.-P., & Ha, N.-T. (2023). Automated Mapping of Wetland Ecosystems: A Study Using Google Earth Engine and Machine Learning for Lotus Mapping in Central Vietnam. Water, 15(5), 854.

Qiu, Z., Xiang, H., Ma, F. & Du, C. 2020. Qualifications of rice growth indicators optimized at different growth stages using unmanned aerial vehicle digital imagery. Remote Sensing, 12, 3228.

Saarela, M., & Jauhiainen, S. (2021). Comparison of feature importance measures as explanations for classification models. Sn Applied Sciences, 3, 1-12.

Sankaran, S., Zhou, J., Khot, L. R., Trapp, J. J., Mndolwa, E., & Miklas, P. N. (2018). High-throughput field phenotyping in dry bean using small unmanned aerial vehicle based multispectral imagery. Computers and Electronics in Agriculture, 151, 84-92.

Sarker, I. H. (2021). Machine learning: Algorithms, real-world applications and research directions. SN computer science, 2(3), 160.

Sharifi, A. (2020). Remotely sensed vegetation indices for crop nutrition mapping. Journal of the Science of Food and Agriculture, 100(14), 5191-5196. https://doi.org/10.1002/jsfa.10568

Singla, M., Ghosh, D., & Shukla, K. K. (2020). Improved sparsity of support vector machine with robustness towards label noise based on rescaled α-hinge loss with non-smooth regularizer. Neural Processing Letters, 52(3), 2211-2239.

Sipper, M., & Moore, J. H. (2021). Conservation machine learning: a case study of random forests. Scientific reports, 11(1), 3629.

Sun, Z., Wang, X., Wang, Z., Yang, L., Xie, Y., & Huang, Y. (2021). UAVs as remote sensing platforms in plant ecology: review of applications and challenges. Journal of plant ecology, 14(6), 1003-1023.

Thenkabail, P. S., & Lyon, J. G. (2016). Hyperspectral remote sensing of vegetation. CRC Press.

Vågsholm, I., Arzoomand, N. S., & Boqvist, S. (2020). Food security, safety, and sustainability—getting the trade-offs right. Frontiers in Sustainable Food Systems, 16.

Wang, R., Shi, F. & Xu, D. 2022. The Extraction Method of Alfalfa (Medicago sativa L.) Mapping Using Different Remote Sensing Data Sources Based on Vegetation Growth Properties. *Land,* 11**,** 1996.

Woebbecke, D. M., Meyer, G. E., Von Bargen, K., & Mortensen, D. A. (1995). Color indices for weed identification under various soil, residue, and lighting conditions. Transactions of the ASAE, 38(1), 259-269.

Xing, N., Huang, W., Xie, Q., Shi, Y., Ye, H., Dong, Y., Wu, M., Sun, G., & Jiao, Q. (2019). A transformed triangular vegetation index for estimating winter wheat leaf area index. Remote Sensing, 12(1), 16.

Xue, J., & Su, B. (2017). Significant remote sensing vegetation indices: A review of developments and applications. Journal of Sensors, 2017.

Yang, C., Everitt, J. H., Du, Q., Luo, B., & Chanussot, J. (2012). Using high-resolution airborne and satellite imagery to assess crop growth and yield variability for precision agriculture. Proceedings of the Ieee, 101(3), 582-592.

Yulianto, F., Raharjo, P. D., Pramono, I. B., Setiawan, M. A., Chulafak, G. A., Nugroho, G., Sakti, A. D., Nugroho, S., & Budhiman, S. (2023). Prediction and mapping of land degradation in the Batanghari watershed, Sumatra, Indonesia: utilizing multi-source geospatial data and machine learning modeling techniques. Modeling Earth Systems and Environment, 1-22.

Zeng, Y., Hao, D., Huete, A., Dechant, B., Berry, J., Chen, J. M., Joiner, J., Frankenberg, C., Bond-Lamberty, B., & Ryu, Y. (2022). Optical vegetation indices for monitoring terrestrial ecosystems globally. Nature Reviews Earth & Environment, 3(7), 477-493.

Zhao, Y.-P., Wang, J.-J., Li, X.-Y., Peng, G.-J., & Yang, Z. (2020). Extended least squares support vector machine with applications to fault diagnosis of aircraft engine. ISA transactions, 97, 189-201.
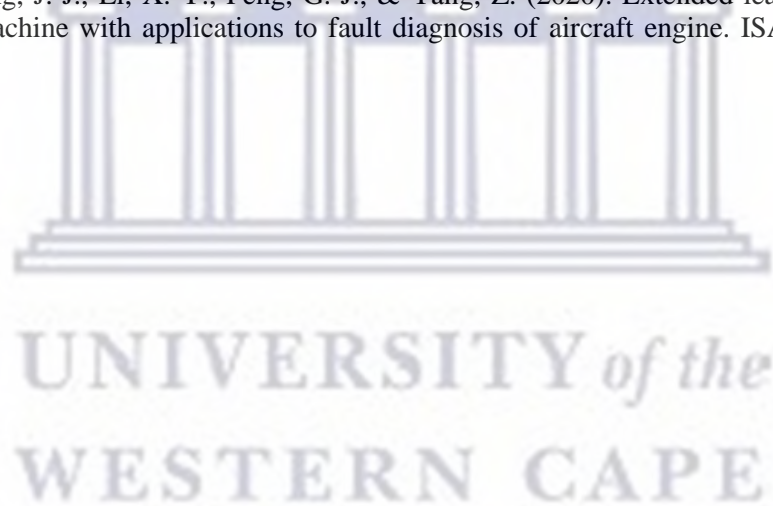
CHAPTER 4

EVALUATING UAV MULTISPECTRAL IMAGERY, MACHINE LEARNING, AND IMAGE ANALYSIS TECHNIQUES FOR MAPPING TARO AND SWEET POTATO IN A SMALLHOLDER CROPLAND IN SOUTHERN AFRICA.

Abstract: Mapping the spatial distribution of neglected and under-utilised crop species (NUS) crops in smallholder fields can be challenging due to their complex and minute formations, making it difficult to distinguish them from other spectrally similar crop types. Object-based image analysis has gained considerable recognition as a prominent classification approach suitable for accurately delineating diminutive, fragmented crop fields in smallholder croplands. However, very few studies have attempted to assess the robustness of UAV remotely sensed data in conjunction with object-based image analysis. In this context, this study aimed to assess the comparative performance of object-based (OBIA) and pixel-based image analysis (PBIA) Gradient Tree Boosting (GTB) ensembles in mapping the spatial distribution of sweet potato and taro in a typical smallholder cropland of Southern Africa using UAV acquired multi-spectral remotely sensed data. Additionally, a comparative assessment was conducted to evaluate the relative contribution of individual bands, vegetation indices, and combined data. The findings showed that OBIA-GTB and PBIA-GTB achieved mean overall accuracies of 80,6% and 84,6%, respectively, using the combined data. Conversely, the utilisation of individual spectral bands resulted in the least accurate classification outcomes. The PBIA-GTB approach was able to generate clear crop field-boundaries for sweet potato and taro among other crops. This demonstrates GTB's potential to improve NUS crop mapping accuracy in smallholder fields while reducing differences between OBIA and PBIA approaches.

Key words: Gradient tree boost, unmanned aerial vehicle, neglected and under-utilised crop species, smallholder fields.

4.1. Introduction

Neglected and underutilised species (NUS) emerge as a potential solution to the global challenge of providing a growing population with healthy and nutritious food, while concurrently mitigating adverse environmental impacts and adapting to a changing climate (Mabhaudhi et al., 2017). NUS are plant varieties that have received very little in terms of research attention, development in the agricultural stage, and are not widely preferred in commercial markets (Mabhaudhi et al., 2017). These agricultural crops play a significant role in traditional or local food systems. NUS crops have demonstrated a remarkable ability to adapt to harsh conditions such as drought, low soil fertility, and irregular rainfall, surpassing major commercial crops in resilience (Mabhaudhi et al., 2017). Having evolved under stress, they are naturally resilient to abiotic stresses faced by small-scale farmers in developing countries (Mabhaudhi et al., 2017). They are also suitable for cultivation in marginal agricultural lands. Given the innate stress tolerance of NUS crop species, it is indicative that they have the potential to play a significant role as the impacts of climate change exacerbate local growing conditions. Their nutrient density also makes NUS crops an attractive supplement to promote food and nutrition security within vulnerable communities across diverse agro-ecologies. To facilitate the expansion of NUS crop cultivation into both subsistence and commercial markets, it is imperative to map their spatial distributions and land suitability. Timely and accurate delineation of NUS areas, along with production

62

statistics is essential to optimise their production and enhance market participation at both the farm and industry levels (Chimonyo et al., 2022).

Traditional field surveys commonly employed for mapping NUS, are characterised by being time-consuming, expensive, and lacking spatial explicitness. An alternative is offered through earth observation facilities and data, which provide frequently acquired, spatially continuous data at varying resolutions (Ndlovu et al., 2021). Coarser resolution sensors like MODIS and AVHRR are suitable for large-scale daily monitoring due to their high temporal resolution of near daily. For instance, Zhang et al. (2022) utilised the MODIS multi-temporal enhanced vegetation index (EVI) in combination with SVM to accurately delineate maize cultivation across agricultural lands, achieving an impressive overall accuracy of 79%. However, spatial resolutions ranging from 250m-1km are inadequate for accurately delineating boundaries and estimating the area of smallholder farms, as intercropping and non-uniform planting/harvesting practices further complicate the difficulties associated with mapping at such resolutions (Persello et al., 2019). UAV remote sensing systems provide improved spatial and spectral imaging for smallholders with valuable multi/hyperspectral capabilities for species discrimination. For instance, UAV bands with a resolution of 2 meters, particularly in the red-edge spectrum, has shown improved capability in accurately mapping smallholder farm details (Tang et al., 2022). Nonetheless, the widespread adoption of high-resolution sensors is restricted due to their high costs and computational requirements.

For many years, pixel-based image analysis (PBIA) has emerged as the fundamental approach for image classification, particularly in third world nations where the availability of costly data and software is restricted. However, relying solely on spectral properties and neglecting other characteristics such as texture, shape, and size during the classification process can limit the reliability and precision of maps generated using PBIA as previous research has shown (Xiaoxia et al., 2005). In the last decade, OBIA has gained significant popularity among the geospatial research community. This is predominantly attributable to its capability to integrate spectral, spatial, textual, and contextual information, thereby resulting in enhanced precision in classification (Xiaoxia et al., 2005). While OBIA has demonstrated a slight advantage in mapping landscapes that are heterogeneous and fragmented, PBIA classifiers continue to be more commonly employed owing to their wider availability in both open-source and commercial software platforms, as opposed to OBIA classifiers which are primarily accessible through commercial means. Additionally, the difference in accuracy between the two methods is closely tied to the broad application of conventional PBIA classifiers like Maximum Likelihood. These classifiers have faced criticism for their inadequacies in dealing with imbalanced and small training datasets, leading to lower accuracies, as research has indicated (Xiaoxia et al., 2005).

In recent times, researchers have turned to more resilient machine-learning ensemble classifiers such as Gradient Tree boost (GTB) and Random Forest (RF) for classification (Ouma et al., 2023, Bayas et al., 2022). The efficacy of these classifiers has been proven to surpass that of the traditional probability-based classifiers in terms of accuracy (Kumar et al. 2016) and other machine-learning algorithms. For instance, Abdi (2020) found that GTB outperforms RF in accurately mapping land use land cover change within a boreal landscape. Unlike random forests with average predictions, GBMs use a gradient descent approach to minimise error at each stage. GBMs are robust due to their flexibility in customising loss functions during model optimisation. This has led to their widespread success in real-world applications compared to single models. They rely on three main components - a loss function, weak learner models like decision trees, and an additive model that combines predictions from each weak learner (Natekin and Knoll, 2013). Importantly, tree based GBM algorithms were designed specifically

63

to handle large datasets very efficiently. They can run over 10 times faster than other popular algorithms on large data, making them highly scalable for different scenarios.

Given the successful application of the Gradient Tree Boosting (GTB) classifier, this study aimed to leverage its capability in comparatively evaluating the performance of Pixel-Based Image Analysis (PBIA) and Object-Based Image Analysis (OBIA) for mapping NUS, sweet potato, and taro crop among other crops in a smallholder cropland in KwaZulu Natal, South Africa. To address this objective, the study assessed the relative influence of spectral bands, vegetation indices and the combination of both datasets.

4.2. Methods and materials

4.2.1. Study Area

The research was conducted in the Swayimane region, located in KwaZulu-Natal, South Africa, at coordinates (29°31024" S and 30°41037" E). This area falls under the jurisdiction of the uMshwathi Local Municipality. Swayimane is a small town situated in the northeastern direction from Pietermaritzburg, covering an approximate area of 36 km2 (Brewer et al., 2022). The local community in Swayimane primarily engages in semi-subsistence farming on their individual plots, which plays a crucial role in ensuring food and nutrition security. The prevalent crop types cultivated in this region include sugarcane, sweet potato, taro, tomatoes and white and yellow maize (Brewer et al., 2022). The smallholder farmers engage in the manual process of sowing crop seeds and fertilising croplands by utilising livestock manure (Brewer et al., 2022). The management of smallholder fields is entirely manual, i.e., plots are hand-weeded and maintained using backpack herbicide sprayers. Crop yields are also harvested by hand. The agricultural activities and crop production in Swayimane benefit from the region's climatic conditions characterised by warm and wet summers, as well as cool and dry winters (Brewer et al., 2022). The average temperatures in this area typically range from 12 ∘C to 24 ∘C. The annual precipitation averages between 600 and 1200 mm, with the majority of rainfall occurring during the summer season (Brewer et al., 2022). Consequently, rainwater serves as the primary source of irrigation for croplands in this area.
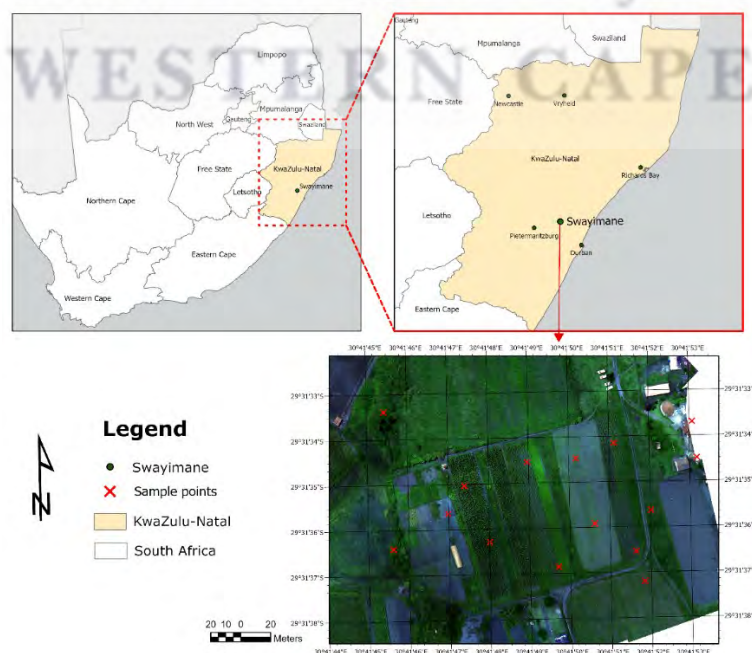
Figure 4-1 : Location of the Swayimane study area, study site and smallholder crop field

64
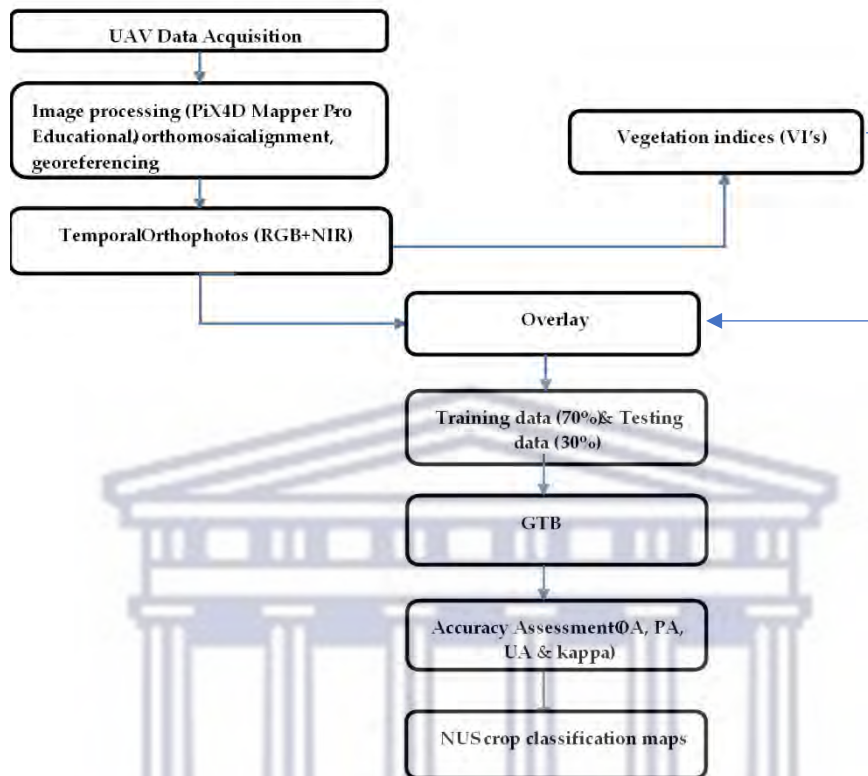
Figure 4-2: presents a flowchart that provides a concise overview of the key steps undertaken in this study, including image data collection and processing, spectral datasets utilised, and statistical analysis.

4.2.2. Data collection

Prior to remote data acquisition, a field survey was conducted within the study area. The coordinates for various land use/land cover classes were measured utilising a Trimble Garmin handheld GPS device with a positional accuracy of ±1 meter. Specifically, eight classes were examined as part of this study: taro, sweet potato, natural vegetation, sugarcane, bare land, built structures, maize at growth stage one, and maize at growth stage two. A total of three hundred and ten coordinate points were collected. These data were subsequently converted into a point map and imported into the Google Earth Engine (GEE) platform, where they were then leveraged for supervised classification of the processed remote sensing imagery.

Aerial-based flights over smallholder farms were conducted using the DJI Matrice 300 (DJI M-300) platform, equipped with a MicaSense Altum imaging device and Downwelling Light Sensor 2 (DLS-2). The rotary M-300 platform facilitates vertical take-off and landing (VTOL), via vertical hover technology. Key characteristics of the DJI M-300 platform includes a transmission range of 15 km, a maximum altitude of 7000 m, intelligent mapping around obstructions, advanced flight path planning and a locational position tracker (Brewer et al., 2022).The M-300 boasts an impressive maximum flight duration of 55 minutes (without payload) and remarkable operating velocity of 27 m/s, surpassing numerous drone platforms available in the market (Brewer et al., 2022). The MicaSense Altum camera is a highly sophisticated instrument that integrates the functionalities of multispectral and thermal

65

imaging. It encompasses five high-resolution channels, specifically blue, green, red, red-edge, and near-infrared. Additionally, a long-wave infrared thermal camera was used to capture thermal information (Ndlovu et al., 2021). This high-resolution camera facilitates the synchronised acquisition of multispectral and thermal images through the utilisation of a global shutter mechanism that offers a rapid one-second capture rate for accurate and properly aligned imagery (Hutton et al., 2020). The multispectral bands offer 2064 × 1544 sensor resolution at a distance of 120 meters per band (3.2 megapixels) and 5.2 cm ground sample distance at 120 meters flight altitude, suggesting this is optimal for acquiring high resolution crop images. Additionally, the camera possesses a field of view of 48° × 37°, along with an 8 mm focal length (Brewer et al., 2022).

The crop field boundaries were digitised using Google Earth Pro, converted into a shapefile and imported into the DJI M-300 smart console software. The shape-file was utilised within the console to create an autonomous flight plan that covers the desired study region.The flight path facilitated a hands-free image collection over the delineated field and proximate regions by the UAV system. The UAV underwent calibration before each flight utilising the MicaSense Altum calibrated reflectance panel (CRP). During the calibration procedure, an image was captured directly over the CRP without any shading. This allowed for the assessment and recording of the lighting conditions specific to the flight date, time, and location.

4.2.3. Data processing

A total of 3576 aerial images were subjected to a stitching and radiometric calibration process utilising the software application Pix4Dfields version 1.8.0, developed by Pix4d Inc., San Francisco, USA. The radiometric calibration process involved all captured images, including both pre-flight and post-flight CRP images (Brewer et al., 2022). A white balance card, known as the radiometric calibration target (the CRP), was utilised to establish the reflectance properties across various wavelengths of the camera's electromagnetic spectrum (Brewer et al., 2022). During this procedure, the software effectively calibrated and modified the reflectance values of the images, considering the prevailing weather conditions at the time of image acquisition. The utility of the CRP also served as an absolute reference, enabling the comparison of data from multiple flights by obtaining absolute reflectance values (Brewer et al., 2022). Subsequently, a final orthomosaic and a DEM GeoTIFF were produced. The orthomosaic was georeferenced in ArcGIS 10.5 by utilising ground control points obtained from Google Earth Pro. The Universal Transverse Mercator (UTM zone 36S) projection was used to reference the images. The drone orthomosaic of the smallholder crop field was transferred to GEE, where the process of classification was performed utilising the Random Forest (RF), Gradient Tree Boost (GTB), and Support Vector Machine (SVM) classifiers.

4.2.4. Vegetation Indices

A single-date image was employed to generate eleven vegetation indices using the equations available in GEE (Table 4-1). The selection and prioritisation of the near-infrared (NIR) and visible indices were based on their effectiveness in mapping NUS crops as documented in literature. The selection of the near-infrared (NIR) band was predicated upon its provision of valuable insights into both biomass and the vitality of vegetation (Xie et al., 2018).

Table 4-1: UAV-derived vegetation indices.

Vegetation Index	Abbreviation	Equation	Reference
Normalized difference vegetation index	NDVI	(NIR−RED)/(NIR+RED)	Xue and Su (2017)
Green normalized difference vegetation index	GNDVI	NIR−GREENNIR+GREEN	Gitelson et al. (1996)
Excess green index	EGI	2.5* (GREEN-RED)/(GREEN+RED+1)	(Qiu et al., 2020)
Normalized difference red-edge index	NDRE	NIR−RED EDGENIR+RED EDGE	(Fitzgerald et al., 2006)
Excess green index	EXG	2 * GREEN - RED – BLUE	Woebbecke et al. (1995)
Chlorophyll carotenoid index	CCI	(R - G) / (R + G)	(Jäger et al., 2022)
Optimized soil adjusted vegetation index	OSAVI	NIR−REDNIR+RED+0.16	Xue and Su (2017)
Enhanced vegetation index	EVI	(2.5 * (NIR+ RED) / (NIR + 6 * RED - 7.5* BLUE +1)	(Xing et al., 2019)
Normalised green, red difference index	NGRDI	(GREEN - RED) / (GREEN + RED)	Meyer and Neto (2008)
Simple ratio	SRI	NIR / RED	Jordan (1969)
Modified triangular vegetation index 1	MTVI1	$1.2\,((1.2*(NIR-GREEN))-(2.5*(RED-GREEN))$	(Xing et al., 2019)

4.2.5. Pixel based Classification.

Pixel based classification is a technique used in remote sensing image analysis which assigns a pixel to a landcover class by referring to the spectral similarities. Each individual image pixel is classified by comparing the spectral information it contains, with the spectral signatures of the selected landcover categories, which are acquired from reference data (Tassi et al., 2021). Within the GEE platform, the gradient tree boost algorithm was leveraged in conjunction with the PBIA technique. The sampled data was randomly divided into 70% training ($n = 217$) and 30% validation ($n = 93$) (Table 4-2). The training subset was utilised for developing the predictive model, while the validation subset served to assess the accuracy of the model in an independent context.

Table 4-2: Training and validation data used for PBIA classification.

Class name	Code	Training (*n*)	Testing (*n*)
Taro	T	28	12
Sweet potato	SP	28	12
Natural Vegetation	NV	21	9
Sugarcane	SU	28	12
Bare land	BL	21	9
Built-up	BU	21	9
Maize growth stage 1	M1	35	15
Maize growth stage 2	M2	35	15

Gradient tree boost (GTB): Gradient Boosting Machines (GBMs) are a family of powerful ensemble machine learning techniques that fall under the category of sequential models. Each model in the sequence learns from the mistakes of previous models to incrementally improve overall performance (Natekin and Knoll, 2013). The integrated model combines gradient, boosting, and decision tree techniques to address classification problems and make accurate predictions for regression tasks (Ye et al., 2021). Boosting refers to the offline aggregation of multiple weak classifiers to create a powerful classifier, and gradient refers to the improvement in flexibility and convenience when the model optimises the loss function (Ye et al., 2021). To reduce correlation among decision trees, a new tree is developed based on a randomly selected subset of training data. The GTB classifier involves several adjustable parameters that require configuration, including the number of trees, shrinkage, sampling rate, maximum nodes, and seed values. The number of trees (*nTree*) was adjusted to 300. The maximum nodes, seeds, shrinkage and sampling parameters were set to default in GEE.

4.2.6. *Object-Based Classification and segmentation*

For object-based classification, our initial step involved conducting image segmentation. The main objective of segmentation is to accurately extract and delineate the individual objects within an image. Google Earth Engine primarily supports G-means, K-means and Simple Non-Iterative Clustering (SNIC) for segmentation. The selection of the SNIC algorithm was based on its capability to be customised through user-defined parameters, as well as its exceptional performance in image segmentation tasks (Qu et al., 2021). It is non-recursive, ensures connectivity from the start, less memory intensive, and accuracy can be adjusted by configuring specific parameters (Gxokwe et al., 2022). SNIC is a super pixel boundary and image segmentation technique that divides an image into small, clusters of connected pixels called '*superpixels*' (Gxokwe et al., 2022). The image segmentation process using the SNIC algorithm begins by initialising centroid pixels on a regular grid within the image. Subsequently, the relationship between each pixel and the centroids is established by measuring its distance in a five-dimensional space, which is defined by colour and spatial coordinates (Gxokwe et al., 2022). Uniformly sized '*superpixels*' are developed by combining normalised spatial and colour distances using a distance calculation (Gxokwe et al., 2022). The selection of the candidate pixel is determined by identifying the shortest distance from the centroid (Gxokwe et al., 2022). The SNIC algorithm is optimised using four customisable parameters: connectivity, '*neighbourhoodSize*', compactness and seeds. Initially, the seeds are generated using the '*seedGrid*' technique, which

68

computes the spectral deviation and maximum distance between the mean value of the generated object and the source image. The parameters for compactness, connectivity, and neighbourhood size were set at 1, 4, and 128, respectively. Thereafter, the spectral attributes of all segmented objects within the study area were extracted, along with the average auxiliary feature values. A predictive model was developed by utilising the mean value within the object combined with the sample points. The SNIC algorithm was implemented using the provided source code '*ee.Algorithms.Image.Segmantation.SNIC* ' in the GEE platform. In this research, the same features applied in PBIA were utilised for OBIA, thereby ensuring an equitable assessment between the two methods (Table 4-2).

4.2.7. Accuracy assessment

An accuracy assessment was used to assess the efficiency of GTB in conjunction with OBIA and PBIA techniques. Confusion matrices were generated to calculate the overall accuracy, kappa coefficient, user/producer accuracies, and F1 scores for both techniques. A confusion matrix is an overly process that compares the classified classes with the reference points and provides a count of the correct and incorrect classifications for each class (Tiwari, 2022). It helps quantify the classification accuracy and identify patterns of misclassification. The overall accuracy (OA) is a metric of algorithmic efficiency, calculated as the proportion of correctly assigned samples to the total number of samples used for testing (Gxokwe, 2022). The producer's accuracy measures the likelihood of accurately classifying the ground truth sample on the thematic map (Gxokwe, 2022). Conversely, the user's accuracy evaluates the probability that a classified pixel in the landcover classification map accurately represents the corresponding landcover type on ground (Gxokwe, 2022).According to Bhunia et al. (2021) accuracy values greater than 70% is considered to be acceptable. Furthermore, the kappa statistic values range from 0 to 1, wherein values surpassing 0.80 signify a high agreement between the classified map and the ground truth. Conversely, values below 0.40 denote inadequate agreement. Kappa scores that fall within the range of 0.40 to 0.80 indicate a moderate level of concordance with the reference data (Dondofema et al., 2023). The F1 score combines the weighted averages of precision and recall measures and serves as a standardised measure for evaluating the accuracy/precision of classification techniques (Pham et al., 2023). As the metrics' values increase, so does the model's confidence in accurately assigning the designated classes within the study.

4.3. Results
4.3.1. Comparison of spectral bands and indices using PBIA and OBIA methods.

Upon reviewing the results presented in Table 4-3, it is apparent that dataset 1 (bands only) yielded the least accurate results compared to VIs and combined datasets. The evaluation of the OBIA-GTB model against datasets 2 and 3 observed a modest improvement in inter-rater reliability. Specifically, the kappa statistic was found to be approximately 3% higher with dataset 2, and approximately 6% higher when using dataset 3. The combined dataset exhibited superior performance for both models. However, the magnitude of change in accuracies between dataset 1 and dataset 3 is relatively smaller for the GTB-OBIA model. The results consistently fall within a range of 79-81% for OA, 0.76-0.82 for kappa statistics, and 0.74-0.79 for F1 scores, signifying a relatively consistent performance across the evaluations (Table 4-3). In contrast, there is an appreciable variation of 5 percent observed when comparing dataset 1 to dataset 3 with the PBIA model. The overall accuracy increases significantly from 83% to 88% with the inclusion of the combined dataset. This observation implies that the integration of bands and indices has significantly enhanced the accuracies and improved the models' capability to differentiate between classes with comparable spectral signatures.

4.3.2. Performance of PBIA-GTB and OBIA-GTB methods in mapping NUS crops

The GTB classifier demonstrated comparable results across the PBIA and OBIA classification approaches in terms of overall classification accuracy, kappa statistics and F1 scores, as seen in Table 4-3 and Figure 4-3. The mean kappa coefficient values obtained from the GTB classifier demonstrated favourable scores of 0.816 and 0.79 for the PBIA and OBIA approaches, respectively. Although both PBIA and OBIA approaches yielded good classification results overall, a direct comparison reveals that the PBIA approach surpassed the standard OBIA technique alone by a margin of 2-6% in terms of accuracy (Table 4-3). The most significant variables contributing to the peak performance of PBIA-GTB include B1, EGI and B4. The OBIA-GTB slightly underperformed in comparison to PBIA-GTB, with a mean accuracy of 80.6, kappa statistic of 0.79 and a F1 score of 0.77 (Table 4-3 & Figure 4-3). Hence, the PBIA-GTB combination can be considered a more optimal remote sensing classification framework based on these evaluation metrics.

Table 4-3: PBIA-GTB and OBIA-GTB overall accuracies, kappa statistics and F1 scores

Analysis Stage		Accuracies	PBIA-GTB	OBIA-GTB
1	Dataset 1(Bands only)	OA	0.83	0.80
		Kappa	0.80	0.76
		F1	0.80	0.78
2	Dataset 2 (VI's only)	OA	0.83	0.81
		Kappa	0.80	0.79
		F1	0.81	0.79
3	Dataset 3 (Bands & VI'S)	OA	0.88	0.81
		Kappa	0.85	0.82
		F1	0.84	0.74
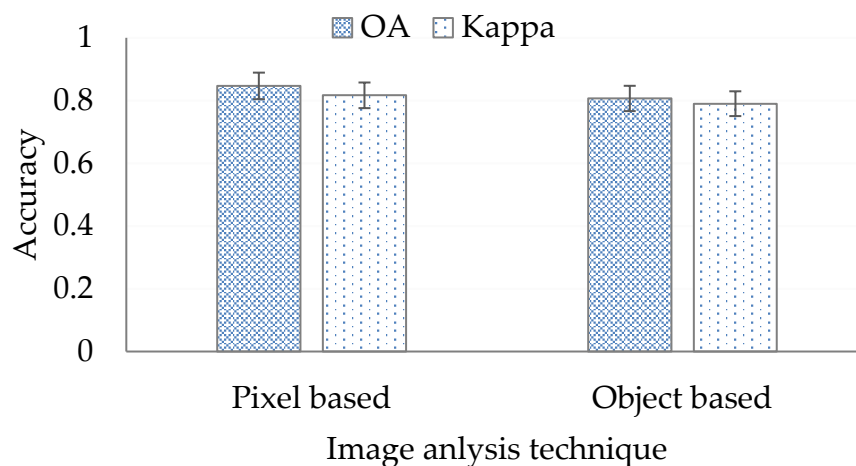
Figure 4-3: Mean accuracies (OA and Kappa) exhibited by PBIA-GTB and OBIA-GTB.

4.3.3. Comparative of all spectral datasets in classifying NUS among other crops in a smallholder cropland

The results indicate that the raw spectral bands slightly underperformed when compared to VIs and the combined dataset across all models, as demonstrated by mean OA of 81,5 percent and a mean kappa statistic of 0,78 (Table 4-3). This observation is further supported by the variable importance scores, whereby B4 and B5 ranked relatively lower (supplementary figures S3-1 & S3-2). Specifically, VIs outperformed the bands by 1-2% but yielded similar accuracies to the combined dataset (Table 4-3). The performance of optimal bands such as NDVI, GNDVI and EGI significantly contributed to the improved performance of machine learning algorithms. Furthermore, the combined dataset exhibited the highest performance across all models, with a mean OA of 84.5 and a kappa statistic of 83.5. When assessing Figure 4-4, it becomes apparent that the most optimal bands that contributed the most to the performance are B1, B3, and NDVI. In comparison, the bands in the combined dataset ranked lower compared to the indices.
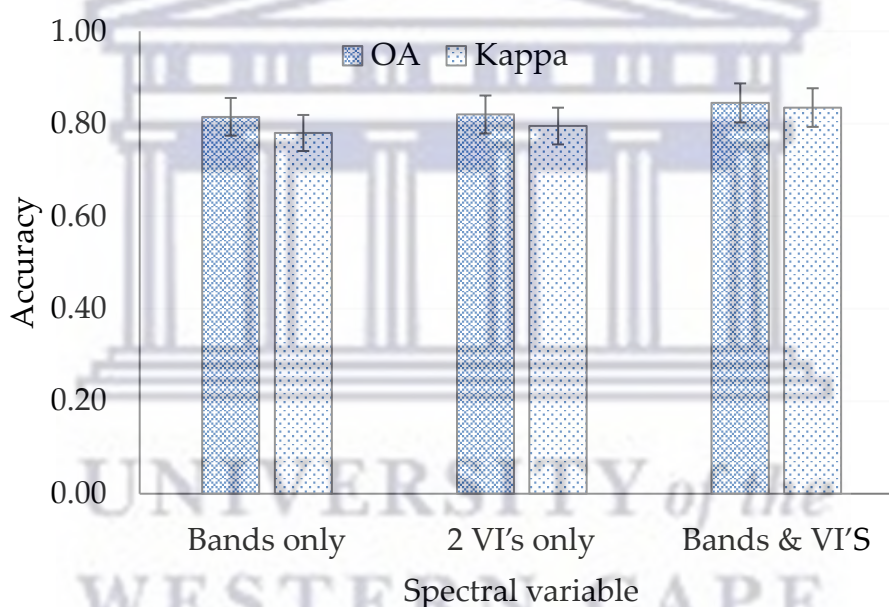
Figure 4-4: Mean accuracies (OA and Kappa) exhibited by PBIA-GTB and OBIA-GTB.

4.3.4. Final comparative assessment of GTB pixel based (PBIA) and object-based image analysis (OBIA-GTB) classifications for NUS among other crops in a smallholder cropland using a combination of selected datasets.

Utilising the combined datasets, both PBIA and OBIA classifications demonstrated relatively higher accuracies in the final results. PBIA had an OA of 0.88, kappa statistic of 0.85 and F1 score of 0.84 based on B1, NDVI, NDRE, B3, and GNDVI as influential classification variables listed in order of importance (Figure 4-5). OBIA exhibited a relatively lower OA of 0.81 and a kappa of 0.82 based B1, B2, B5 and EGI as optimal classification variables also listed in order of importance. Although PBIA was relatively higher than OBIA, both image analysis techniques exhibited very high classification accuracies.

71
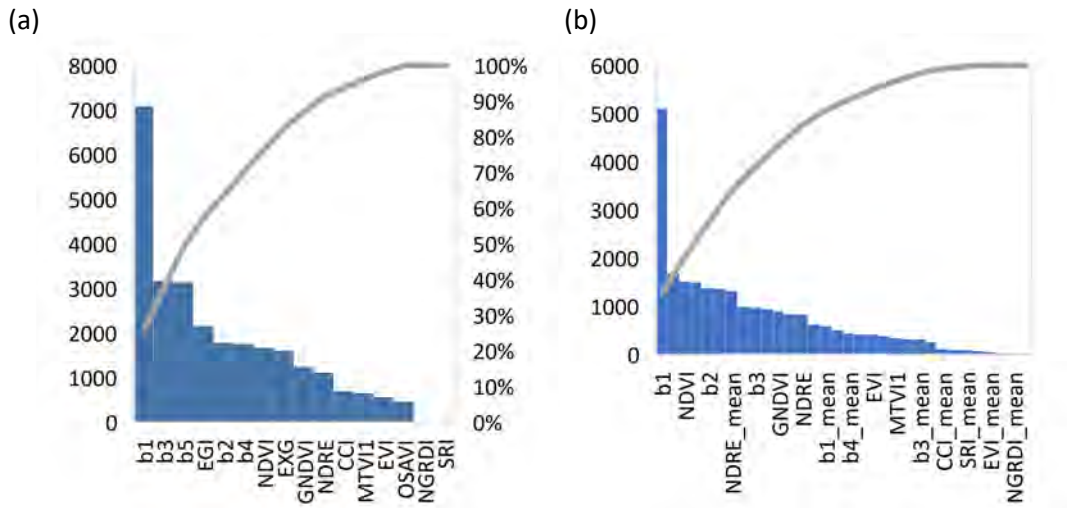
Figure 4-5: Variable importance scores of (a) PBIA-GTB, (b) OBIA-GTB with dataset 3

Collectively, GTB showcased a strong performance across both classification platforms, with five classes achieving PA and UA rates exceeding 70% (Figure 4-6). PBIA demonstrated an enhanced user accuracy in delineating the distribution of NUS crops when compared to OBIA- GTB. PBIA-GTB with dataset 3 yielded the highest UAs cross all classes, ranging from 71.4% to 100%, underscoring the remarkable capability of GTB in effectively modelling intricate decisions. In contrast, the OBIA approach yielded lower UA, with results ranging from 33% to 100%. Individually, when using the OBIA approach, the classification of natural vegetation exhibited the lowest PA at 20% and UA at 33%. However, higher PA and UA accuracies were observed for, sweet potato, sugarcane, built up and bare land and taro, and maize growth stage one when employing the PBIA method (supplementary Figure S3-3 & S3-4).
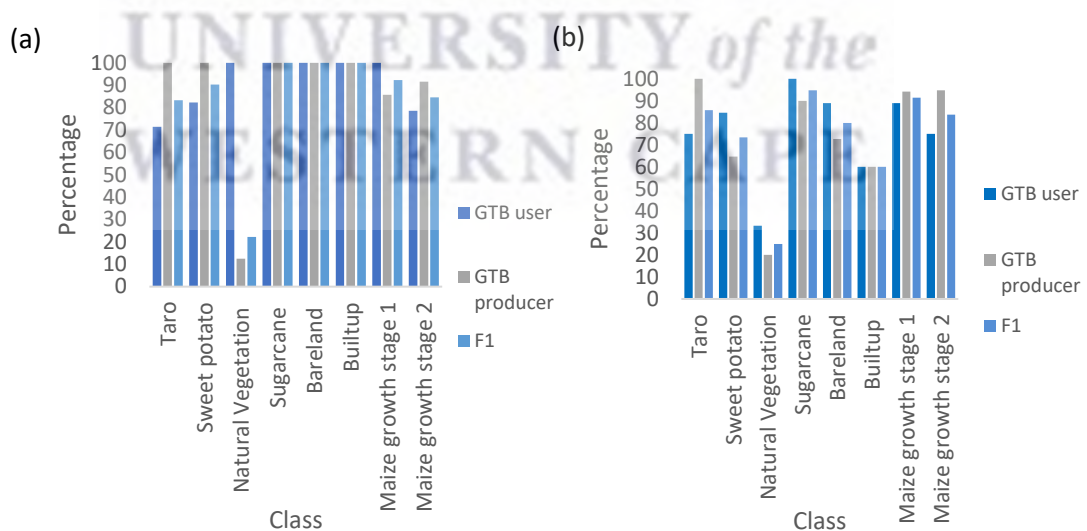
Figure 4-6: user, producer and F1 accuracies of (a) PBIA-GTB, (b) OBIA-GTB with dataset 3

4.3.5. *Classification results using the most optimal dataset (Bands & vegetation indices).*
Figure 4-7 displays the thematic maps that were produced through the application of the GTB algorithm with both PBIA and OBIA techniques. Visual inspection of GTB at both classification platforms

72

portrays similarities in terms of the NUS crops spatial coverage. Additionally, it is worth noting that traces of salt and pepper noise are present in the PBIA-GTB thematic map. Despite this noise, the map still effectively depicts the location of NUS crops, with the exception of taro, which is frequently misclassified towards the central section of the map. Moreover, the GTB-OBIA map often exhibits a higher incidence of misclassification when it comes to distinguishing between natural vegetation and maize growth stage two (Figure 4-7B). Table 4-4 and Figure 4-8, summarises the percentage areal extents derived from the thematic maps obtained through the classification using both PBIA and OBIA classification techniques. Based on Table 4-4, it is evident that there is a significant distinction in the areal extents between PBIA-GTB and OBIA-GTB (41 percent difference between all classes). It has been observed that OBIA tends to either underestimate or overestimate the extents of sugarcane, maize and sweet potato crops. In contrast, PBIA accurately depicts the distribution of landcover classes in relation to ground truth data. Significant differences in the areal extent coverage can be observed between classes, such as sugarcane and maize. This observation is further supported by the results of the PA and UA measures (Figure 4-6). Additionally, it has been observed that there is a smaller difference in the areal extents for classes such as taro, natural vegetation, built-up areas, and maize growth stage one (Table 4-4).
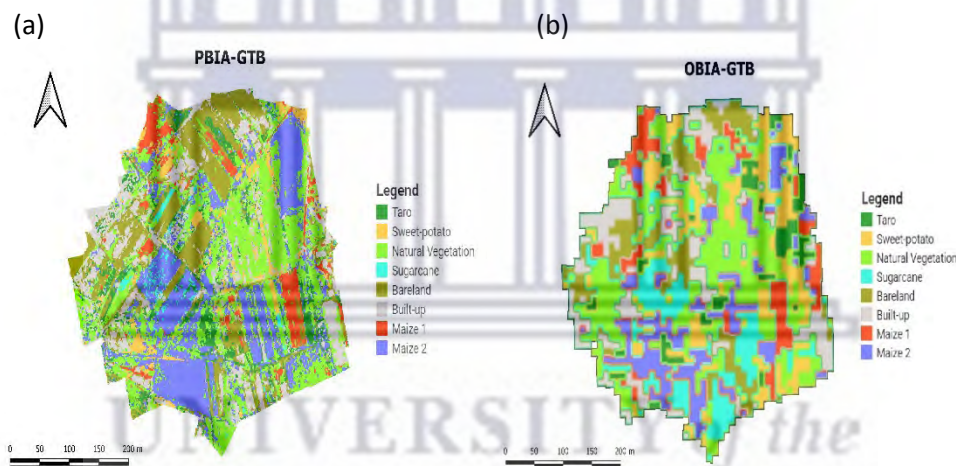
Figure 4-7: NUS crop distribution maps of (a) PBIA-GTB (b) and OBIA-GTB with dataset 3
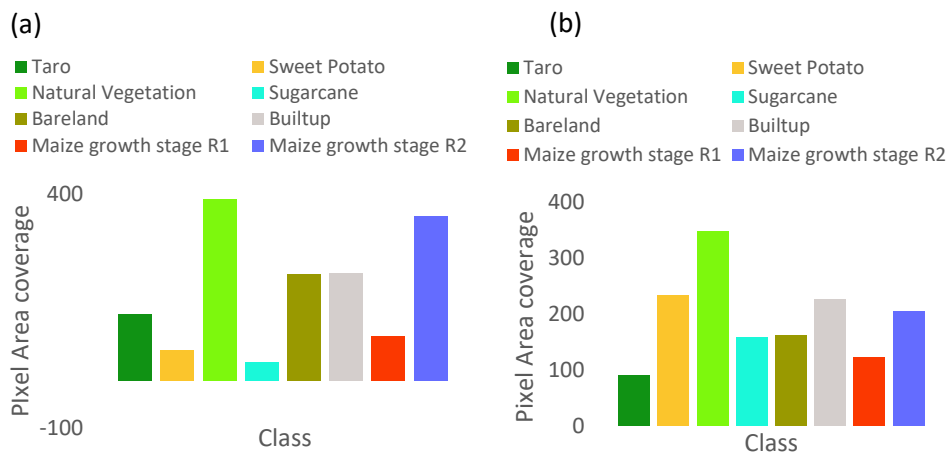
Figure 4-8: Pixel area per class of (a) PBIA-GTB, (b) OBIA-GTB with dataset 3.

73

Table 4-4: Areal extent map comparisons of PBIA-GTB and OBIA-GTB

Class	OBIA GTB %	PBIA GTB%	Percentage of change
Taro	5,83	9,26	3,43
Sweet Potato	15,08	4,21	10,87
Natural Vegetation	22,52	25,24	2,72
Sugarcane	10,29	2,52	7,76
Bareland	10,49	14,82	4,33
Builtup	14,63	14,89	0,25
Maize growth stage R1	7,90	6,21	1,68
Maize growth stage R2	13,27	22,85	9,58
Total	100	100	41

4.4. Discussion

4.4.1. Comparative performance of different spectral datasets in mapping NUS crops using PBIA and OBIA

The findings of this research indicate that the utilisation of UAV multispectral data, combined with pixel-based image analysis, can successfully identify, and map the spatial distribution of NUS among other crops in a smallholder cropland. Raw spectral bands yielded the lowest accuracies of OA=81,5, K=0,78 and F1= 0.79 (Table 4-3). Furthermore, raw spectral bands seem to rank relatively lower across variable importance scores (Figure 4-4). However, the combination of raw spectral bands with vegetation indices produced the highest overall classification accuracies, exceeding 80% based on B1, NDVI, NDRE, B3, and GNDVI as influential classification variables listed in order of importance. The B1 (blue) wavelength is commonly absorbed by plant leaves during the process of photosynthesis and exhibits a notable sensitivity to changes in plant biochemistry. The increased absorption of chlorophyll results in decreased reflectance in the blue wavelengths. Consequently, this characteristic enables a clear differentiation between healthy and unhealthy vegetation. This attribute of the blue band proves valuable in accurately mapping NUS crop boundaries and distinguishing vegetation with similar spectral properties.

The overall improvement in accuracy achieved by incorporating spectral bands and VIs can be attributed to the VIs' capability to mitigate the impacts of background soil effects, sensor zenith angle, sun angle, and other atmospheric influences (Liu et al., 2022a). This allows the combined use with spectral bands to increase performance. The findings align with prior research conducted by (Zeng et al., 2022), which reported the unique strength of incorporating VIs in distinguishing diverse land cover types. Furthermore, a recent study conducted by (Kazemi and Ghanbari Parmehr, 2023) showcased the potential of integrating UAV raw spectral bands with Vis for effectively classifying rice crop growth. Likewise, in another study conducted by (Wang et al., 2021), consistent results were obtained when employing a fusion of UAV spectral and textural data to estimate rice grain yield.

Moreover, the results also indicated a significant difference between the spectral bands dataset and VIs dataset. With PBIA-GTB exhibiting a 5 percent magnitude in change and OBIA with a 2 percent in

74

change (Table 4-3). Using bands and indices combinations introduce additional features/dimensions to the data compared to bands alone. This expanded feature space often allows models to better discriminate classes or patterns. The extra features from the combined dataset, such as texture, shape, or contextual relationships between pixels/objects, likely helped the classifiers make more informed decisions and improved their ability to accurately classify the data. For example a study by Li et al. (2023) used high dimensional data in combination with deep learning models to map the distribution of crops. Among various deep learning models, the 3D-CNN (Three-Dimensional Convolutional Neural Network) that integrates spectral, spatial, and temporal data emerged as the most accurate approach for crop classification. The additional data appears to have improved the ability of both the PBIA-GTB and OBIA-GTB classifiers to differentiate between spectrally similar but spatially distinct land cover types.

The findings of this study also demonstrated that there was no significant difference in the performance between bands and Vis (Figure 4-4). This situation could be attributed to the distinct characteristics of each vegetation index, the training data utilised, and the homogeneity of the agricultural settings. Interestingly, the classification accuracy achieved for all the investigated Vis in this study was not the highest, as reported by other authors in the literature (Zhang et al., 2020, Ustuner et al., 2014). This can also be attributed to the fact that vegetation indices, such as NDVI, predominantly rely on combinations of the preexisting spectral bands. Therefore, it is probable that they did not yield significantly novel or distinct information for distinguishing land cover classes beyond what was already attainable from the original spectral bands. Although vegetation indices can enhance the detection of subtle discrepancies in vegetation reflectance characteristics, the presence of both pixel-based and object-based classifiers that can already utilise the contextual relationships among neighbouring pixels or objects might render the redundant vegetation index features less effective in significantly improving classification accuracy. The OBIA and PBIA approaches demonstrated the capability to successfully identify vegetation patterns by utilising the robust spectral bands.

4.4.2. *The performance of PBIA-GTB and OBIA-GTB classification in mapping NUS crops spatial distribution.*

Results of this study showed that PBIA produced relatively higher accuracies ranging from 83%-88% when compared to OBIA which had accuracies that ranged between 80% and 81% in mapping the distribution of NUS crops (Table 4-3). This could be attributed to PBIA's ability to fully leverage the rich spectral detail information contained in multispectral remote sensing imagery in comparison to object-based classification techniques (Hao et al., 2015, Dorren et al., 2003). For instance, Hao et al. (2015) evaluated the performance of two hybrid techniques, namely multiple voting (M-voting) and probabilistic fusion (P-fusion), for crop classification using NDVI temporal data at both pixel and object levels. The results demonstrated that OBIA did not enhance the classification performance in comparison to PBIA, particularly in homogenous regions. Therefore, higher PBIA classification accuracies may be attributed, in part to the high dimensionality of pixel-level feature spaces in comparison to object features, as well as its capacity to detect fine-scale spectral changes between crop types (Mantripragada et al., 2022). Moreover, PBIA handles mixed pixels within homogenous regions more effectively than OBIA, which assigns them to whole objects. The segmentation process in OBIAs seeks to identify homogenous image objects but may struggle to accurately represent the complicated surroundings and fragmentation of some agricultural fields in the typical smallholder croplands of Southern Africa characterised by inter cropping (Hossain and Chen, 2019).

Furthermore, assessing Figure 4-7, it is evident that the PBIA classification was successfully able to distinguish minute variations (boundaries) between NUS and other crop types, as it incorporates spatial

and textural information. On average, the PBIA classifiers exhibited superior user and producer accuracies in-comparison to the OBIA classifiers. Specifically, landcover classes such as sweet potato and maize growth stage one has higher producer accuracies ranging between 75-100% in comparison to OBIA with ranges between 33%-100% (Figure 4-6). However, the PBIA-GTB classifier gave a higher overall accuracy (OA:88 %) than the OBIA classifier (OA:86%) for the combined dataset (16 variables). Furthermore, the PBIA classifier yielded a higher Kappa statistic estimate (k = 0.85) compared to the OBIA classifier (k = 0.84). The optimal performance of both PBIA and OBIA in this study can be assigned to the resilience of the GTB algorithm in discriminating the spectral signatures of smallholder crops. Additionally, the utilisation of UAV-acquired data with ultra-high spatial resolution further contributed to the optimal performance of the classifiers. The similarities in the areal extents between classes, such as natural vegetation, built-up areas, and maize growth stage one (as shown in Table 4-4), were also observed in both PBIA and OBIA, suggesting a strong overall spatial agreement between the two models. In a related study, Safari Khatouni et al. (2021)noted that the accuracy of a classification process is strongly influenced by the specific classifier employed. Therefore, this study proved that selecting GTB as the classifier positively influenced the overall accuracy for mapping the spatial distribution of NUS in smallholder fields, utilising UAV multispectral imagery.

4.5. Conclusion

The objective of this study was to evaluate the efficacy of object-based (OBIA) and pixel-based image analysis (PBIA) Gradient Tree Boosting (GTB) ensembles in mapping the spatial distribution of sweet potato and taro in a typical smallholder cropland in Southern Africa. This evaluation was carried out using multi-spectral remotely sensed data acquired through unmanned aerial vehicles (UAVs). Furthermore, a comparative examination was performed to determine the relative significance of individual bands, vegetation indices, and combined data in the mapping process. In light of the findings of this study, it can be inferred that both methods have a great potential in delineating NUS fields in smallholder croplands, especially in cases where different crops exhibit similar spectral characteristics.

- PBIA-GTB outperformed OBIA-GTB with a margin of 2-7 percent accuracy. However, it is worth noting that the the two methods did not perform significantly different.
- There was no significant difference in the performance of spectral bands and VIs as separate datasets, but both datasets combined improved the classification accuracies.
- A significant difference was observed between the performance of individual bands and the combined dataset. Bands & indices outperformed other datasets by 2-5percent.

This approach holds potential for further expansion in mapping smallholder fields that cultivate NUS. This is particularly valuable as there is a growing demand for techniques that can successfully estimate yields and determine the areas dedicated to NUS crops. Overall, this study makes a substantial contribution to the application of robust classification algorithms in precisely delineating small-scale farming systems. The generated thematic maps, depicting the distribution of NUS crops, can prove valuable for farm-level management and decision-making. Moreover, national agriculture departments can derive benefits from the adoption of robust classifiers to create dependable land-use/cover maps, facilitating effective planning and resource allocation.

References

Abdi, A. M. (2020). Land cover and land use classification performance of machine learning algorithms in a boreal landscape using Sentinel-2 data. Giscience & Remote Sensing, 57(1), 1-20.

Bayas, S., Sawant, S., Dhondge, I., Kankal, P., & Joshi, A. (2022). Land use land cover classification using different ml algorithms on sentinel-2 imagery. In Advanced Machine Intelligence and Signal Processing (pp. 761-777). Springer.

Bhunia, G. S., Chatterjee, U., & Shit, P. K. (2021). Land Reclamation and Restoration Strategies for Sustainable Development: Geospatial Technology Based Approach. Elsevier.

Brewer, K., Clulow, A., Sibanda, M., Gokool, S., Naiken, V., & Mabhaudhi, T. (2022). Predicting the Chlorophyll Content of Maize over Phenotyping as a Proxy for Crop Health in Smallholder Farming Systems. Remote Sensing, 14(3), 518.

Chimonyo, V. G. P., Chibarabada, T. P., Choruma, D. J., Kunz, R., Walker, S., Massawe, F., Modi, A. T., & Mabhaudhi, T. (2022). Modelling neglected and underutilised crops: a systematic review of progress, challenges, and opportunities. Sustainability, 14(21), 13931.

Dondofema, F., Nethengwe, N., Taylor, P., & Ramoelo, A. (2023). Comparison of Satellite Platform for Mapping the Distribution of Mauritius Thorn (Caesalpinia decapetala) and River Red Gum (Eucalyptus camaldulensis) in the Vhembe Biosphere Reserve. Remote Sensing, 15(11), 2753.

Dorren, L. K., Maier, B., & Seijmonsbergen, A. C. (2003). Improved Landsat-based forest mapping in steep mountainous terrain using object-based classification. Forest Ecology and Management, 183(1-3), 31-46.

Fitzgerald, G., Rodriguez, D., Christensen, L., Belford, R., Sadras, V., & Clarke, T. (2006). Spectral and thermal sensing for nitrogen and water status in rainfed and irrigated wheat environments. Precision Agriculture, 7, 233-248.

Gitelson, A. A., Kaufman, Y. J., & Merzlyak, M. N. (1996). Use of a green channel in remote sensing of global vegetation from EOS-MODIS. REMOTE SENSING OF ENVIRONMENT, 58(3), 289-298.

Gxokwe, S., Dube, T., & Mazvimavi, D. (2022). Leveraging Google Earth Engine platform to characterize and map small seasonal wetlands in the semi-arid environments of South Africa. SCIENCE OF THE TOTAL ENVIRONMENT, 803, 150139.

Hao, P., Wang, L., & Niu, Z. (2015). Comparison of hybrid classifiers for crop classification using normalized difference vegetation index time series: A case study for major crops in North Xinjiang, China. Plos one, 10(9), e0137748.

Hossain, M. D., & Chen, D. (2019). Segmentation for Object-Based Image Analysis (OBIA): A review of algorithms and challenges from remote sensing perspective. Isprs Journal of Photogrammetry and Remote Sensing, 150, 115-134.

Hutton, J., Lipa, G., Baustian, D., Sulik, J. & Bruce, R. 2020. High accuracy direct georeferencing of the altum multi-spectral uav camera and its application to high throughput plant phenotyping. *The International Archives of the Photogrammetry, Remote Sensing and Spatial Information Sciences,* 43**,** 451-456.

Jäger, T., Mokos, A., Prasianakis, N. I. & Leyer, S. 2022. first_page settings Order Article Reprints Open AccessArticle Pore-Level Multiphase Simulations of Realistic Distillation Membranes for Water Desalination. *Membranes*.

Jordan, C. F. (1969). Derivation of leaf-area index from quality of light on the forest floor. Ecology, 50(4), 663-666.

Kazemi, F., & Ghanbari Parmehr, E. (2023). Evaluation of RGB Vegetation Indices Derived from UAV Images for Rice Crop Growth Monitoring. ISPRS Annals of the Photogrammetry, Remote Sensing and Spatial Information Sciences, 10, 385-390.

Kumar, L., Chhogyel, N., Gopalakrishnan, T., Hasan, M. K., Jayasinghe, S. L., Kariyawasam, C. S., Kogo, B. K. & Ratnayake, S. 2022. Climate change and future of agri-food production. *Future foods*. Elsevier.

Li, M., Zang, S., Zhang, B., Li, S., & Wu, C. (2014). A review of remote sensing image classification techniques: The role of spatio-contextual information. European Journal of Remote Sensing, 47(1), 389-411.

Li, Q., Tian, J., & Tian, Q. (2023). Deep Learning Application for Crop Classification via Multi-Temporal Remote Sensing Images. Agriculture, 13(4), 906.

Liu, J., Fan, J., Yang, C., Xu, F., & Zhang, X. (2022). Novel vegetation indices for estimating photosynthetic and non-photosynthetic fractional vegetation cover from Sentinel data. International Journal of Applied Earth Observation and Geoinformation, 109, 102793.

Mabhaudhi, T., Chimonyo, V. G., & Modi, A. T. (2017). Status of underutilised crops in South Africa: Opportunities for developing research capacity. Sustainability, 9(9), 1569.

Mantripragada, K., Dao, P. D., He, Y., & Qureshi, F. Z. (2022). The effects of spectral dimensionality reduction on hyperspectral pixel classification: A case study. Plos one, 17(7), e0269174.

Meyer, G. E., & Neto, J. C. (2008). Verification of color vegetation indices for automated crop imaging applications. Computers and Electronics in Agriculture, 63(2), 282-293.

Natekin, A., & Knoll, A. (2013). Gradient boosting machines, a tutorial. Frontiers in neurorobotics, 7, 21.

Ndlovu, H. S., Odindi, J., Sibanda, M., Mutanga, O., Clulow, A., Chimonyo, V. G., & Mabhaudhi, T. (2021). A comparative estimation of maize leaf water content using machine learning techniques and unmanned aerial vehicle (UAV)-based proximal and remotely sensed data. Remote Sensing, 13(20), 4091.

Ouma, Y. O., Keitsile, A., Nkwae, B., Odirile, P., Moalafhi, D., & Qi, J. (2023). Urban land-use classification using machine learning classifiers: comparative evaluation and post-classification multi-feature fusion approach. European Journal of Remote Sensing, 56(1), 2173659.

Persello, C., Tolpekin, V., Bergado, J. R., & De By, R. (2019). Delineation of agricultural fields in smallholder farms from satellite images using fully convolutional networks and combinatorial grouping. REMOTE SENSING OF ENVIRONMENT, 231, 111253.

Pham, H.-T., Nguyen, H.-Q., Le, K.-P., Tran, T.-P., & Ha, N.-T. (2023). Automated Mapping of Wetland Ecosystems: A Study Using Google Earth Engine and Machine Learning for Lotus Mapping in Central Vietnam. Water, 15(5), 854.

Qiu, Z., Xiang, H., Ma, F. & Du, C. 2020. Qualifications of rice growth indicators optimized at different growth stages using unmanned aerial vehicle digital imagery. *Remote Sensing,* 12**,** 3228.

Qu, L. a., Chen, Z., Li, M., Zhi, J., & Wang, H. (2021). Accuracy improvements to pixel-based and object-based lulc classification with auxiliary datasets from Google Earth engine. Remote Sensing, 13(3), 453.

Safari Khatouni, A., Seddigh, N., Nandy, B., & Zincir-Heywood, N. (2021). Machine learning based classification accuracy of encrypted service channels: analysis of various factors. Journal of Network and Systems Management, 29, 1-27.

Tang, Z., Jin, Y., Alsina, M. M., McElrone, A. J., Bambach, N., & Kustas, W. P. (2022). Vine water status mapping with multispectral UAV imagery and machine learning. Irrigation Science, 40(4-5), 715-730.

Tassi, A., Gigante, D., Modica, G., Di Martino, L., & Vizzari, M. (2021). Pixel-vs. Object-based landsat 8 data classification in google earth engine using random forest: The case study of maiella national park. Remote Sensing, 13(12), 2299.

Tiwari, A. (2022). Supervised learning: from theory to applications. In Artificial intelligence and machine learning for EDGE computing (pp. 23-32). Elsevier.

Ustuner, M., Sanli, F. B., Abdikan, S., Esetlili, M. & Kurucu, Y. 2014. Crop type classification using vegetation indices of rapideye imagery. *The international archives of the photogrammetry, remote sensing and spatial information sciences,* 40**,** 195-198.

Wang, F., Yi, Q., Hu, J., Xie, L., Yao, X., Xu, T., & Zheng, J. (2021). Combining spectral and textural information in UAV hyperspectral images to estimate rice grain yield. International Journal of Applied Earth Observation and Geoinformation, 102, 102397.

Woebbecke, D. M., Meyer, G. E., Von Bargen, K., & Mortensen, D. A. (1995). Color indices for weed identification under various soil, residue, and lighting conditions. Transactions of the ASAE, 38(1), 259-269.

Xiaoxia, S., Jixian, Z., & Zhengjun, L. (2005). A comparison of object-oriented and pixel-based classification approachs using quickbird imagery. ISPRS STM, 281-284.

Xie, Q., Dash, J., Huang, W., Peng, D., Qin, Q., Mortimer, H., Casa, R., Pignatti, S., Laneve, G., & Pascucci, S. (2018). Vegetation indices combining the red and red-edge spectral information

for leaf area index retrieval. IEEE JOURNAL OF SELECTED TOPICS IN APPLIED EARTH OBSERVATIONS AND REMOTE SENSING, 11(5), 1482-1493.

Xue, J., & Su, B. (2017). Significant remote sensing vegetation indices: A review of developments and applications. Journal of Sensors, 2017.

Ye, Z., Sheng, Z., Liu, X., Ma, Y., Wang, R., Ding, S., Liu, M., Li, Z., & Wang, Q. (2021). Using machine learning algorithms based on GF-6 and Google Earth engine to predict and map the spatial distribution of soil organic matter content. Sustainability, 13(24), 14055.

Zeng, Y., Hao, D., Huete, A., Dechant, B., Berry, J., Chen, J. M., Joiner, J., Frankenberg, C., Bond-Lamberty, B., & Ryu, Y. (2022). Optical vegetation indices for monitoring terrestrial ecosystems globally. Nature Reviews Earth & Environment, 3(7), 477-493.

Zhang, C., Yang, Z., Di, L., Yu, E. G., Zhang, B., Han, W., Lin, L., & Guo, L. (2022). Near-real-time MODIS-derived vegetation index data products and online services for CONUS based on NASA LANCE. Scientific Data, 9(1), 477.

CHAPTER 5

SYNTHESIS AND CONCLUSIONS

5.1. *Introduction*

Neglected and underutilised crop species (NUS) hold promise and potential in addressing the challenges associated with reduced agricultural productivity and achieving food and nutrition security, especially in smallholder croplands of developing countries. Climate change is driving a shift in agricultural production due to variations in precipitation and temperatures globally. These climatic fluctuations have knock-on effects on the yields of staple crops such as maize. However, NUS face limited research focus and reduced commercial demand, constricting their potential for advancement and utilisation. Additionally, accurately determining the location and spatial distribution of these crops is made more difficult by the nature of their cultivation pattern. The fragmented and diverse arrangement of agricultural fields presents difficulties in accurately mapping and distinguishing distinctive plant varieties within the cropland for the purpose of making well-informed decisions. The advancement of remote sensing technologies, particularly data derived from unmanned aerial vehicles (UAVs), provides a valuable opportunity to obtain spatially explicit and multi-temporal information on NUS (Chivasa et al., 2021, Zhang et al., 2019a, Sibanda et al., 2021a). Therefore, gaining insight into how NUS develops, and how widely distributed they are, could aid in understanding their health, productivity, and ability to withstand stress under evolving climate conditions. Understanding the spatial arrangement of these crop species is thus a crucial factor for guaranteeing food and nutritional security in South Africa. In line with this objective, this study aimed to assess the utility of UAV-based proximal remote sensing in mapping the spatial distribution of NUS, with a specific focus on sweet potato and taro, among other crops, in a smallholder cropland area. This overarching objective, was addressed through the three following objectives; (1) to conduct a systematic literature review on the spatial distribution and health of NUS crops in sub-Saharan Africa (2) to evaluate the performance of three robust classifiers in mapping the spatial distribution NUS crops utilising multispectral UAV data and, (3) to assess the performance of OBIA and PBIA techniques combined with a GTB classifier in mapping and delineating the spatial distribution of NUS crops. This chapter serves as a reflection on the research aims and objectives, summarising the key findings, conclusions, and recommendations for future studies.

5.2. *Highlights of the findings*

5.2.1. *Reviewing the progress and challenges in mapping the spatial distribution of neglected and underutilised crops*

The first objective of this study was to conduct a systematic literature review on remote sensing (RS) the spatial distribution and health of NUS crops. The review aimed to assess the progress made, identify opportunities and challenges, and highlight any research gaps. To ensure a comprehensive analysis, a systematic review approach following the PRISMA framework was employed. A total of 171 peer-reviewed articles were gathered from reputable databases, including Scopus, Google Scholar and Web of Science. The findings of this study revealed that most of the research focusing on NUS crops was conducted in the United States (18 articles) and China (17 articles). Nonetheless, some notable contributions from regions in the Global South, such as Southern Africa, were also identified. The attributes of NUS that received the most extensive research attention include leaf area index (LAI), crop yield, growth, above-ground biomass (AGB), and chlorophyll content. However, the exploration of stomatal conductance and the spatial distribution of NUS crops was limited, accounting for only 29%

of the reviewed studies. Furthermore, findings revealed that more studies utilised satellite-borne sensors (twenty-one studies), while eighteen studies used UAV-borne sensors in conjunction with advanced remote sensing techniques to map the spatial distribution and health of NUS crops. The slow progress in the application of UAV technology for mapping NUS especially in the global South can be as result of the exorbitant purchasing and operating costs and regulatory restrictions. It is for this reason that future research should prioritise the integration of ML techniques and high resolution acquired UAV datasets to accurately delineate and discriminate NUS crops as to optimise food production and security in the Global South. The findings of the literature review played a crucial role in shaping the subsequent application chapters guiding the selection of the most suitable sensors, vegetation indices, and algorithms for evaluating the utility of UAV-based proximal remote sensing in mapping the spatial distribution NUS crops, specifically sweet potato and taro in smallholder cropland areas. Therefore, the literature findings underscored the value of employing combined image spectral datasets in combination with cutting-edge machine learning and classification techniques for discriminating NUS crop species in smallholder farms.

5.2.2. Comparing the performance of machine learning classifieds in mapping spatial distribution of NUS in smallholder fields using high resolution UAV imagery

In comparing the performance of Gradient Boosting (GTB), Support Vector Machines (SVM) and Random Forest (RF) ML classifiers for mapping the spatial distribution of NUS within smallholder croplands utilising high resolution UAV imagery, crop distribution maps were generated using each classifier in-combination with three different datasets: 1) spectral bands, 2) vegetation indices (VIs), and 3) bands combined with VIs. Results of the study indicated that RF and GTB classifiers outperformed the SVM classifier, with high overall accuracy rates ranging between 80% - 90%. The ensemble models demonstrated a clear capability to differentiate field boundaries between taro, and sweet potato among other crops when compared to the SVM model. However, the GTB classifier exhibited a greater degree of variation and improvement across multiple datasets compared to the other models. In comparing the performance of different datasets, results showed that vegetation indices only and combined datasets outperformed the bands only dataset. Overall, the superior classification accuracies achieved by utilising sophisticated ML algorithms underscore the effectiveness of applying robust approaches to define areas within smallholder NUS fields. The precise delineation of field boundaries and spatial extents of smallholder fields is crucial for making well-informed decisions related to the management of irrigation systems, planting schedules and harvest plans. These findings offer valuable insight into application of advanced machine learning methods for delineating the NUS boundaries amongst other crops in complex and fragmented smallholder croplands. Considering that the findings of this study pointed out that GTB was the most effective algorithm for mapping the spatial distribution of NUS specifically sweet potato and taro among other crops in a smallholder cropland area, it was then used in the following chapter.

5.2.3. To evaluate the performance of OBIA and PBIA classification techniques in mapping NUS crops spatial distribution in smallholder farms.

In comparatively assessing the performance of Object-Based Image Analysis (OBIA) and Pixel-Based Image Analysis (PBIA) for mapping the spatial distribution of NUS among other crops in a smallholder cropland area, GTB was utilised in conjunction with 1) spectral bands, 2) vegetation indices (VIs), and 3) bands combined with VIs. Results showed that the PBIA -GTB classification technique exhibited slightly higher classification accuracies in mapping NUS when compared to the performance of the

OBIA-GTB technique. The PBIA approach exhibited improved capability in distinguishing between the field boundaries of spectrally ambiguous NUS amongst other crop types in a fragmented smallholder cropland setting. Despite the relatively small margin of difference between PBIA and OBIA, the findings of this study suggested that pixel-based classification methods, leveraging ultrahigh spatial resolution and multi-spectral information, could be significantly robust in delivering superior classifications comparable to object-based segmentation techniques. The results provide meaningful insights into the selection of the most impactful remote sensing methods for detailed agricultural mapping within complex small-scale systems. This in turn, facilitates the planning and management of NUS crop production. These findings suggest that a pixel-based classifiers may perform comparably to object-based methods for detailed mapping of agriculture in smallholder systems, improving knowledge of NUS crop distributions to support management and food security goals.

5.3. *General Conclusion*

The overarching goal of this research study was to accurately map the spatial distribution and patterns of neglected and underutilised species (NUS) cultivation in a typically fragmented smallholder cropland of Southern Africa. The conclusions drawn from the findings indicate that;

- Ensemble methods, specifically RF and GTB, exhibited superior performance compared to SVM in accurately mapping the precise locations of NUS crops.
- The GTB classifier exhibited higher classification accuracies based on Band 1 (blue), Excess green vegetation (EXG) and Green Normalised Difference Vegetation Index (GNDVI) spectral variables.
- Both OBIA and PBIA demonstrated high classification accuracies in mapping sweet potato and taro among other crops in smallholder croplands. However, it was observed that PBIA slightly outperformed OBIA in accurately delineating the crop field boundaries.
- Combined data and vegetation indices exhibited the highest classification accuracies based on GTB and when combined with pixel and object-based image analysis techniques.

Most notably, the study findings indicate that UAV-acquired multispectral remotely sensed data could optimally map the spatial patterns and distributions of NUS, amongst others, with an extremely high level of precision and accuracy. The utility of UAV remote sensing allows researchers to optimally detect and locate even minor occurrences of NUS crops across complex smallholder agricultural systems. The advanced mapping capabilities of UAV data could provide complementary and informative insights into crop conditions, including health status, growth patterns over time, and ultimate yields. Such information can significantly assist smallholder farmers in enhancing their management practices and optimising productivity. The utilisation of UAV-multispectral solutions to facilitate better management of NUS crop varieties in challenging cropland areas has the potential to enhance rural food security and livelihoods. This, in turn, contributes to the overarching goals of poverty reduction and hunger alleviation as outlined in South Africa's national sustainable development goals.

5.4. *Recommendations for future research*

The present study employed UAV-derived imagery and utilised image analysis techniques in combination with advanced ML classifiers to map the spatial distribution of NUS crops. Further studies are required to evaluate the application of multi-temporal image compositing and time-series analysis to detect seasonal patterns and discriminate NUS from other rotation crops. This could offer valuable insights into NUS' phenological characteristics and temporal dynamics, aiding in their effective monitoring and management. Future studies should consider incorporating spatial, texture, and

climatic features and spectral information to effectively delineate NUS crops in smallholder farm settings. This will enable a comprehensive evaluation and comparison of different approaches, going beyond the scope of this study that focused on a fair comparison between OBIA and PBIA using solely single-date spectral information. For example, integrating LiDAR and digital elevation data to map topographic and terrain features influencing NUS growth should be considered by future studies. There is also a need to consider the combination of UAVs acquired data with satellite-borne instruments like synthetic aperture radar (SAR), especially when upscaling the applications. SAR data could be invaluable because weather conditions do not significantly impact sensors. Optical and radar data could provide a more comprehensive and nuanced view of NUS across smallholder fields.

Moreover, multi-fusion techniques that integrate diverse datasets are suggested to improve NUS crop mapping. This could include fusing optical, radar and other satellite datasets (e.g., DEM from LiDAR) using approaches like principal component analysis or inverse hyperbolic sine (IHS) transformation. This extracts complementary biophysical variables to enhance feature discrimination and map accuracy.

References

ABDI, A. M. 2020. Land cover and land use classification performance of machine learning algorithms in a boreal landscape using Sentinel-2 data. *GIScience & Remote Sensing,* 57**,** 1-20.

ABOUTALEBI, M., TORRES-RUA, A. F. & ALLEN, N. 2018. Multispectral Remote Sensing for Yield Estimation Using High-Resolution Imagery from an Unmanned Aerial Vehicle. *AUTONOMOUS AIR AND GROUND SENSING SYSTEMS FOR AGRICULTURAL OPTIMIZATION AND PHENOTYPING III.*

AGUILAR, R., ZURITA-MILLA, R., IZQUIERDO-VERDIGUIER, E. & A. DE BY, R. 2018. A cloud-based multi-temporal ensemble classifier to map smallholder farming systems. *Remote sensing,* 10**,** 729.

AHMAD, U., ALVINO, A. & MARINO, S. 2021. A Review of Crop Water Stress Assessment Using Remote Sensing. *Remote Sensing,* 13**,** 4155.

ALI, A. & IMRAN, M. 2020. Evaluating the potential of red edge position (REP) of hyperspectral remote sensing data for real time estimation of LAI & chlorophyll content of kinnow mandarin (Citrus reticulata) fruit orchards. *Scientia Horticulturae,* 267**,** 109326.

ANKRAH, J., MONTEIRO, A. & MADUREIRA, H. 2023. Shoreline Change and Coastal Erosion in West Africa: A Systematic Review of Research Progress and Policy Recommendation. *Geosciences,* 13**,** 59.

ASGARI, S. & HASANLOU, M. 2023. A Comparative Study of Machine Learning Classifiers for Crop Type Mapping Using Vegetation Indices. *ISPRS Annals of the Photogrammetry, Remote Sensing and Spatial Information Sciences,* 10**,** 79-85.

AVNERI, A., AHARON, S., BROOK, A., ATSMON, G., SMIRNOV, E., SADEH, R., ABBO, S., PELEG, Z., HERRMANN, I. & BONFIL, D. J. 2023. UAS-based imaging for prediction of chickpea crop biophysical parameters and yield. *Computers and Electronics in Agriculture,* 205**,** 107581.

AWAIS, M., LI, W., CHEEMA, M., ZAMAN, Q., SHAHEEN, A., ASLAM, B., ZHU, W., AJMAL, M., FAHEEM, M. & HUSSAIN, S. 2022a. UAV-based remote sensing in plant stress imagine using high-resolution thermal sensor for digital agriculture practices: a meta-review. *International Journal of Environmental Science and Technology***,** 1-18.

AWAIS, M., LI, W., CHEEMA, M. J., HUSSAIN, S., SHAHEEN, A., ASLAM, B., LIU, C. & ALI, A. 2022b. Assessment of optimal flying height and timing using high-resolution unmanned aerial vehicle images in precision agriculture. *International Journal of Environmental Science and Technology,* 19**,** 2703-2720.

AYELE, N. A. & TAMIRU, H. K. 2020. Developing classification model for chickpea types using machine learning algorithms. *International Journal of Innovative Technology and Exploring Engineering,* 10**,** 5-11.

AZIZAN, F. A., KILOES, A. M., ASTUTI, I. S. & ABDUL AZIZ, A. 2021. Application of optical remote sensing in rubber plantations: a systematic review. *Remote Sensing,* 13**,** 429.

BAYAS, S., SAWANT, S., DHONDGE, I., KANKAL, P. & JOSHI, A. 2022. Land use land cover classification using different ml algorithms on sentinel-2 imagery. *Advanced Machine Intelligence and Signal Processing.* Springer.

BELLVERT, J., ZARCO-TEJADA, P. J., GIRONA, J. & FERERES, E. 2014. Mapping crop water stress index in a 'Pinot-noir' vineyard: comparing ground measurements with thermal remote sensing imagery from an unmanned aerial vehicle. *Precision agriculture,* 15**,** 361-376.

BHUNIA, G. S., CHATTERJEE, U. & SHIT, P. K. 2021. *Land Reclamation and Restoration Strategies for Sustainable Development: Geospatial Technology Based Approach*, Elsevier.

BLESSING, C., NHAMO, M. & RANGARIRAI, M. 2020. The impact of plant density and spatial arrangement on light interception on cotton crop and seed cotton yield: an overview.

BLUMENTHAL, J., MEGHERBI, D. B. & LUSSIER, R. 2020. Unsupervised machine learning via Hidden Markov Models for accurate clustering of plant stress levels based on imaged chlorophyll fluorescence profiles & their rate of change in time. *Computers and Electronics in Agriculture,* 174**,** 105064.

BOJOVIĆ, B. & MARKOVIĆ, A. 2009. Correlation between nitrogen and chlorophyll content in wheat (Triticum aestivum L.). *Kragujevac Journal of Science,* 31**,** 69-74.

BREIMAN, L. 2001. Random forests. *Machine learning,* 45**,** 5-32.

BREWER, K., CLULOW, A., SIBANDA, M., GOKOOL, S., NAIKEN, V. & MABHAUDHI, T. 2022. Predicting the Chlorophyll Content of Maize over Phenotyping as a Proxy for Crop Health in Smallholder Farming Systems. *Remote Sensing,* 14**,** 518.

BREWER, K. R. 2021. *Assessment of maize crop health and water stress based on multispectral and thermal infrared unmanned aerial vehicle phenotyping in smallholder farms.*

BUTHELEZI, S., MUTANGA, O., SIBANDA, M., ODINDI, J., CLULOW, A. D., CHIMONYO, V. G. P. & MABHAUDHI, T. 2023. Assessing the Prospects of Remote Sensing Maize Leaf Area Index Using UAV-Derived Multi-Spectral Data in Smallholder Farms across the Growing Season. *Remote Sensing,* 15**,** 1597.

BUTILĂ, E. V. & BOBOC, R. G. 2022. Urban traffic monitoring and analysis using unmanned aerial vehicles (uavs): A systematic literature review. *Remote Sensing,* 14**,** 620.

CABRERA-BOSQUET, L., MOLERO, G., STELLACCI, A., BORT, J., NOGUÉS, S. & ARAUS, J. 2011. NDVI as a potential tool for predicting biomass, plant nitrogen content and growth in wheat genotypes subjected to different water and nitrogen conditions. *Cereal Research Communications,* 39**,** 147-159.

CANDIAGO, S., REMONDINO, F., DE GIGLIO, M., DUBBINI, M. & GATTELLI, M. 2015. Evaluating Multispectral Images and Vegetation Indices for Precision Farming Applications from UAV Images. *Remote Sensing,* 7**,** 4026-4047.

CHAI, H. H., MASSAWE, F. & MAYES, S. 2016. Effects of mild drought stress on the morpho-physiological characteristics of a bambara groundnut segregating population. *Euphytica,* 208**,** 225-236.

CHAPEPA, B., MUDADA, N. & MAPURANGA, R. 2020. The impact of plant density and spatial arrangement on light interception on cotton crop and seed cotton yield: an overview. *Journal of Cotton Research,* 3**,** 18.

CHE'YA, N. N., DUNWOODY, E. & GUPTA, M. 2021. Assessment of Weed Classification Using Hyperspectral Reflectance and Optimal Multispectral UAV Imagery. *AGRONOMY-BASEL,* 11.

CHIBARABADA, T. P. 2018. *Water use and nutritional water productivity of selected major and underutilised grain legumes.*

CHIMONYO, V. G. P., CHIBARABADA, T. P., CHORUMA, D. J., KUNZ, R., WALKER, S., MASSAWE, F., MODI, A. T. & MABHAUDHI, T. 2022. Modelling neglected and underutilised crops: a systematic review of progress, challenges, and opportunities. *Sustainability,* 14**,** 13931.

CHIMONYO, V. G. P., WIMALASIRI, E. M., KUNZ, R., MODI, A. T. & MABHAUDHI, T. 2020. Optimizing traditional cropping systems under climate change: a case of maize landraces and Bambara groundnut. *Frontiers in Sustainable Food Systems,* 4**,** 562568.

CHIVASA, W., MUTANGA, O. & BURGUENO, J. 2021. UAV-based high-throughput phenotyping to increase prediction and selection accuracy in maize varieties under artificial MSV inoculation. *Computers and Electronics in Agriculture,* 184**,** 106128.

CLEVERS, J. G. & GITELSON, A. A. 2013. Remote estimation of crop and grass chlorophyll and nitrogen content using red-edge bands on Sentinel-2 and-3. *International Journal of Applied Earth Observation and Geoinformation,* 23**,** 344-351.

DE LIMA, I. P., JORGE, R. G. & DE LIMA, J. L. P. 2021. Remote sensing monitoring of rice fields: Towards assessing water saving irrigation management practices. *Frontiers in Remote Sensing,* 2**,** 762093.

DONDOFEMA, F., NETHENGWE, N., TAYLOR, P. & RAMOELO, A. 2023. Comparison of Satellite Platform for Mapping the Distribution of Mauritius Thorn (Caesalpinia decapetala) and River Red Gum (Eucalyptus camaldulensis) in the Vhembe Biosphere Reserve. *Remote Sensing,* 15**,** 2753.

DORREN, L. K., MAIER, B. & SEIJMONSBERGEN, A. C. 2003. Improved Landsat-based forest mapping in steep mountainous terrain using object-based classification. *Forest Ecology and Management,* 183**,** 31-46.

DUARTE, A., BORRALHO, N., CABRAL, P. & CAETANO, M. 2022. Recent advances in forest insect pests and diseases monitoring using UAV-based data: A systematic review. *Forests,* 13**,** 911.

DUKU, C., ZWART, S. J., VAN BUSSEL, L. G. & HEIN, L. 2018. Quantifying trade-offs between future yield levels, food availability and forest and woodland conservation in Benin. *Science of the total environment,* 610**,** 1581-1589.

EHLERS, D., WANG, C., COULSTON, J., ZHANG, Y., PAVELSKY, T., FRANKENBERG, E., WOODCOCK, C. & SONG, C. 2022. Mapping Forest Aboveground Biomass Using Multisource Remotely Sensed Data. *Remote Sensing,* 14**,** 1115.

EL BILALI, H., CARDONE, G., DE FALCIS, E., NAINO JIKA, A. K., ROKKA, S., DIAWARA, A. B., NOUHOU, B. & GHIONE, A. 2023. Neglected and underutilised species (NUS): an analysis of strengths, weaknesses, opportunities and threats (SWOT).

EVERITT, J., YANG, C., DAVIS, M., EVERITT, J. & DAVIS, M. 2007. Mapping wild taro with color-infrared aerial photography and image processing. *J. Aquat. Plant Manage,* 45**,** 106-110.

FAGERIA, N. K., BALIGAR, V. C. & CLARK, R. 2006. *Physiology of crop production*, crc Press.

FAN, S. & RUE, C. 2020. The role of smallholder farms in a changing world. *The role of smallholder farms in food and nutrition security***,** 13-28.

FILELLA, I. & PENUELAS, J. 1994. The red edge position and shape as indicators of plant chlorophyll content, biomass and hydric status. *International Journal of Remote Sensing,* 15**,** 1459-1470.

FITZGERALD, G., RODRIGUEZ, D., CHRISTENSEN, L., BELFORD, R., SADRAS, V. & CLARKE, T. 2006. Spectral and thermal sensing for nitrogen and water status in rainfed and irrigated wheat environments. *Precision agriculture,* 7**,** 233-248.

FOOD & ORGANISATION, A. 2021. Small Family Farmers Produce a Third of the World's Food.

FUNK, C. & BUDDE, M. E. 2009. Phenologically-tuned MODIS NDVI-based production anomaly estimates for Zimbabwe. *Remote Sensing of Environment,* 113**,** 115-125.

GHIMIRE, B., ROGAN, J. & MILLER, J. 2010. Contextual land-cover classification: incorporating spatial dependence in land-cover classification models using random forests and the Getis statistic. *Remote Sensing Letters,* 1**,** 45-54.

GITELSON, A. A., KAUFMAN, Y. J. & MERZLYAK, M. N. 1996. Use of a green channel in remote sensing of global vegetation from EOS-MODIS. *Remote sensing of Environment,* 58**,** 289-298.

GOEL, R. K., YADAV, C. S., VISHNOI, S. & RASTOGI, R. 2021. Smart agriculture–Urgent need of the day in developing countries. *Sustainable Computing: Informatics and Systems,* 30**,** 100512.

GOVE, R. & FAYTONG, J. 2012. Machine learning and event-based software testing: classifiers for identifying infeasible GUI event sequences. *Advances in computers.* Elsevier.

GRAY, P. C., RIDGE, J. T., POULIN, S. K., SEYMOUR, A. C., SCHWANTES, A. M., SWENSON, J. J. & JOHNSTON, D. W. 2018. Integrating drone imagery into high resolution satellite remote sensing assessments of estuarine environments. *Remote Sensing,* 10**,** 1257.

GROTE, M., PILKO, A., SCANLAN, J., CHERRETT, T., DICKINSON, J., SMITH, A., OAKEY, A. & MARSDEN, G. 2022. Sharing airspace with Uncrewed Aerial Vehicles (UAVs): Views of the General Aviation (GA) community. *Journal of Air Transport Management,* 102**,** 102218.

GRÜNER, E., ASTOR, T. & WACHENDORF, M. 2021. Prediction of biomass and N fixation of legume–grass mixtures using sensor fusion. *Frontiers in Plant Science,* 11**,** 603921.

GU, Y., WYLIE, B. K., BOYTE, S. P., PICOTTE, J., HOWARD, D. M., SMITH, K. & NELSON, K. J. 2016. An optimal sample data usage strategy to minimize overfitting and underfitting effects in regression tree models based on remotely-sensed data. *Remote sensing,* 8**,** 943.

GUYOT, G., BARET, F. & JACQUEMOUD, S. 1992. *Imaging spectroscopy for vegetation studies*, Kluwer Academic Publishers: Norwell, MA, USA.

GXOKWE, S. 2022. Developing an integrated remotely sensed framework for the detection and monitoring of seasonally-flooded wetlands in semi-arid environments of southern Africa.

GXOKWE, S., DUBE, T. & MAZVIMAVI, D. 2022. Leveraging Google Earth Engine platform to characterize and map small seasonal wetlands in the semi-arid environments of South Africa. *Science of the Total Environment,* 803**,** 150139.

HALL, O., DAHLIN, S., MARSTORP, H., ARCHILA BUSTOS, M. F., ÖBORN, I. & JIRSTRÖM, M. 2018. Classification of maize in complex smallholder farming systems using UAV imagery. *Drones,* 2**,** 22.

HAO, P., WANG, L. & NIU, Z. 2015. Comparison of hybrid classifiers for crop classification using normalized difference vegetation index time series: A case study for major crops in North Xinjiang, China. *PloS one,* 10**,** e0137748.

HLOPHE-GININDZA, S. N. & MPANDELI, N. 2021. The Role of Small-Scale Farmers in Ensuring Food Security in Africa. *Food Secur. Afr.*

HORNUNG, R. & BOULESTEIX, A.-L. 2022. Interaction forests: Identifying and exploiting interpretable quantitative and qualitative interaction effects. *Computational Statistics & Data Analysis,* 171**,** 107460.

HOSSAIN, M. D. & CHEN, D. 2019. Segmentation for Object-Based Image Analysis (OBIA): A review of algorithms and challenges from remote sensing perspective. *ISPRS Journal of Photogrammetry and Remote Sensing,* 150**,** 115-134.

HSU, C.-W., CHANG, C.-C. & LIN, C.-J. 2003. A practical guide to support vector classification. Taipei, Taiwan.

HUANG, Y., REDDY, K. N., FLETCHER, R. S. & PENNINGTON, D. 2018. UAV low-altitude remote sensing for precision weed management. *Weed technology,* 32**,** 2-6.

HUTTON, J., LIPA, G., BAUSTIAN, D., SULIK, J. & BRUCE, R. 2020. High accuracy direct georeferencing of the altum multi-spectral uav camera and its application to high throughput plant phenotyping. *The International Archives of the Photogrammetry, Remote Sensing and Spatial Information Sciences,* 43**,** 451-456.

IFAD, U. 2013. Smallholders, food security and the environment. *Rome: International Fund for Agricultural Development,* 29.

ISEKI, K. & OLALEYE, O. 2020. A new indicator of leaf stomatal conductance based on thermal imaging for field grown cowpea. *Plant Production Science,* 23**,** 136-147.

JÄGER, T., MOKOS, A., PRASIANAKIS, N. I. & LEYER, S. 2022. first_page settings Order Article Reprints Open AccessArticle Pore-Level Multiphase Simulations of Realistic Distillation Membranes for Water Desalination. *Membranes.*

JEWAN, S. Y. Y., PAGAY, V., BILLA, L., TYERMAN, S. D., GAUTAM, D., SPARKES, D., CHAI, H. H. & SINGH, A. 2022. The feasibility of using a low-cost near-infrared, sensitive, consumer-grade digital camera mounted on a commercial UAV to assess Bambara groundnut yield. *International Journal of Remote Sensing,* 43**,** 393-423.

JINDO, K., KOZAN, O., ISEKI, K., MAESTRINI, B., VAN EVERT, F. K., WUBENGEDA, Y., ARAI, E., SHIMABUKURO, Y. E., SAWADA, Y. & KEMPENAAR, C. 2021. Potential utilization of satellite remote sensing for field-based agricultural studies. *Chemical and Biological Technologies in Agriculture,* 8**,** 1-16.

JORDAN, C. F. 1969. Derivation of leaf-area index from quality of light on the forest floor. *Ecology,* 50**,** 663-666.

JOSHI, B. K., SHRESTHA, R., GAUCHAN, D. & SHRESTHA, A. 2020. Neglected, underutilized, and future smart crop species in Nepal. *Journal of Crop Improvement,* 34**,** 291-313.

JUDSON, R., ELLOUMI, F., SETZER, R. W., LI, Z. & SHAH, I. 2008. A comparison of machine learning algorithms for chemical toxicity classification using a simulated multi-scale data model. *BMC bioinformatics,* 9**,** 1-16.

KAZEMI, F. & GHANBARI PARMEHR, E. 2023. Evaluation of RGB Vegetation Indices Derived from UAV Images for Rice Crop Growth Monitoring. *ISPRS Annals of the Photogrammetry, Remote Sensing and Spatial Information Sciences,* 10**,** 385-390.

KEATING, B. A., HERRERO, M., CARBERRY, P. S., GARDNER, J. & COLE, M. B. 2014. Food wedges: framing the global food demand and supply challenge towards 2050. *Global Food Security,* 3**,** 125-132.

KEGA, S. 2021. *EVALUATING THE POTENTIAL FOR INCREASED FORAGE PRODUCTIVITY AND SOIL CARBON SEQUESTRATION IN STRIP-THINNED SILVOPASTURES.* Department of Natural Resource Sciences, Thompson Rivers University.

KEMP, L., ROUX, M., KEMP, M. & KOCK, R. 2021. Application of drones and image processing for bridge inspections in South Africa. *Civil Engineering= Siviele Ingenieurswese,* 29**,** 25-30.

KUMAR, L., CHHOGYEL, N., GOPALAKRISHNAN, T., HASAN, M. K., JAYASINGHE, S. L., KARIYAWASAM, C. S., KOGO, B. K. & RATNAYAKE, S. 2022. Climate change and future of agri-food production. *Future foods.* Elsevier.

LATI, R., AVNERI, A., AHARON, S., ATSMON, G., SMIRNOV, E., SADEH, R., ABBO, S., PELEG, Z., HERRMANN, I. & BONFIL, D. J. Uav-Based Imaging for Prediction of Chickpea Crop Biophysical Parameters and Yield. *Available at SSRN 4123863*.

LI, K.-Y., BURNSIDE, N. G., SAMPAIO DE LIMA, R., VILLOSLADA PECIÑA, M., SEPP, K., YANG, M.-D., RAET, J., VAIN, A., SELGE, A. & SEPP, K. 2021. The application of an unmanned aerial system and machine learning techniques for red clover-grass mixture yield estimation under variety performance trials. *Remote Sensing,* 13**,** 1994.

LI, L., ZHENG, X. M., ZHAO, K., LI, X. F., MENG, Z. G. & SU, C. H. 2020. Potential Evaluation of High Spatial Resolution Multi-Spectral Images Based on Unmanned Aerial Vehicle in Accurate Recognition of Crop Types. *JOURNAL OF THE INDIAN SOCIETY OF REMOTE SENSING,* 48**,** 1471-1478.

LI, Q., TIAN, J. & TIAN, Q. 2023. Deep Learning Application for Crop Classification via Multi-Temporal Remote Sensing Images. *Agriculture,* 13**,** 906.

LI, Y., REN, B., DING, L., SHEN, Q., PENG, S. & GUO, S. 2013. Does chloroplast size influence photosynthetic nitrogen use efficiency? *PloS one,* 8**,** e62036.

LIU, C., LIU, Y., LU, Y., LIAO, Y., NIE, J., YUAN, X. & CHEN, F. 2019. Use of a leaf chlorophyll content index to improve the prediction of above-ground biomass and productivity. *PeerJ,* 6**,** e6240.

LIU, J., FAN, J., YANG, C., XU, F. & ZHANG, X. 2022a. Novel vegetation indices for estimating photosynthetic and non-photosynthetic fractional vegetation cover from Sentinel data. *International Journal of Applied Earth Observation and Geoinformation,* 109**,** 102793.

LIU, Y., FENG, H., YUE, J., FAN, Y., JIN, X., SONG, X., YANG, H. & YANG, G. 2022b. Estimation of Potato Above-Ground Biomass Based on Vegetation Indices and Green-Edge Parameters Obtained from UAVs. *Remote Sensing,* 14**,** 5323.

LIU, Y., HATOU, K., AIHARA, T., KUROSE, S., AKIYAMA, T., KOHNO, Y., LU, S. & OMASA, K. 2021. A robust vegetation index based on different UAV RGB images to estimate SPAD values of naked barley leaves. *Remote Sensing,* 13**,** 686.

MABHAUDHI, T., CHIMONYO, V. G. & MODI, A. T. 2017. Status of underutilised crops in South Africa: Opportunities for developing research capacity. *Sustainability,* 9**,** 1569.

MABHAUDHI, T., MODI, A. & BELETSE, Y. 2013. Growth, phenological and yield responses of a bambara groundnut (Vigna subterranea L. Verdc) landrace to imposed water stress: II. Rain shelter conditions. *Water Sa,* 39**,** 191-198.

MAES, W. H. & STEPPE, K. 2012. Estimating evapotranspiration and drought stress with ground-based thermal remote sensing in agriculture: a review. *JOURNAL OF EXPERIMENTAL BOTANY,* 63**,** 4671-4712.

MAFURATIDZE, P. 2010. *Discriminating wetland vegetation species in an African savanna using hyperspectral data.*

MAJAHA, J. 2023. The impact of drought in the South African agricultural sector and the skills implications.

MAJID, K. & ROZA, G. 2012. The effect of drought stress on leaf chlorophyll content and stress resistance in maize cultivars (Zea mays). *African Journal of Microbiology Research,* 6**,** 2844-2848.

MALINAO, R. M. L. & HERNANDEZ, A. A. Classifying Breadfruit Tree using Artificial Neural Networks. Proceedings of the 6th ACM/ACIS International Conference on Applied Computing and Information Technology, 2018. 27-31.

MANFREDA, S., MCCABE, M. F., MILLER, P. E., LUCAS, R., PAJUELO MADRIGAL, V., MALLINIS, G., BEN DOR, E., HELMAN, D., ESTES, L. & CIRAOLO, G. 2018. On the use of unmanned aerial systems for environmental monitoring. *Remote sensing,* 10**,** 641.

MANTRIPRAGADA, K., DAO, P. D., HE, Y. & QURESHI, F. Z. 2022. The effects of spectral dimensionality reduction on hyperspectral pixel classification: A case study. *PLoS One,* 17**,** e0269174.

MARSHALL, M. & THENKABAIL, P. 2015. Advantage of hyperspectral EO-1 Hyperion over multispectral IKONOS, GeoEye-1, WorldView-2, Landsat ETM+, and MODIS vegetation indices in crop biomass estimation. *ISPRS Journal of Photogrammetry and Remote Sensing,* 108**,** 205-218.

MAZARIRE 2020. Exploring machine learning algorithms for mapping crop types in a heterogeneous agriculture landscape using Sentinel-2 data. A case study of Free State Province, South Africa. *S. Afr. J. Geomat,* 9**,** 333-347.

MAZARIRE, T. T., RATSHIEDANA, P. E., NYAMUGAMA, A., ADAM, E. & CHIRIMA, G. 2020. Exploring machine learning algorithms for mapping crop types in a heterogeneous agriculture landscape using Sentinel-2 data. A case study of Free State Province, South Africa. *South African Journal of Geomatics,* 9**,** 333-347.

MERKERT, R. & BUSHELL, J. 2020. Managing the drone revolution: A systematic literature review into the current use of airborne drones and future strategic directions for their effective control. *Journal of air transport management,* 89**,** 101929.

MEYER, G. E. & NETO, J. C. 2008. Verification of color vegetation indices for automated crop imaging applications. *Computers and electronics in agriculture,* 63**,** 282-293.

MONTEOLIVA, M. I., GUZZO, M. C. & POSADA, G. A. 2021. Breeding for drought tolerance by monitoring chlorophyll content.

MOUNTRAKIS, G., IM, J. & OGOLE, C. 2011. Support vector machines in remote sensing: A review. *ISPRS journal of photogrammetry and remote sensing,* 66**,** 247-259.

MUGIYO, H., CHIMONYO, V. G., SIBANDA, M., KUNZ, R., NHAMO, L., MASEMOLA, C. R., DALIN, C., MODI, A. T. & MABHAUDHI, T. 2021. Multi-criteria suitability analysis for neglected and underutilised crop species in South Africa. *PloS one,* 16**,** e0244734.

MUHAMMAD, A., ALAM, M., AHMAD, I. & JALAL, A. 2021. Role of beneficial microbes with nitrogen and phosphorous levels on canola productivity. *Brazilian Journal of Biology,* 82.

MURUGANANTHAM, P., WIBOWO, S., GRANDHI, S., SAMRAT, N. H. & ISLAM, N. 2022. A systematic literature review on crop yield prediction with deep learning and remote sensing. *Remote Sensing,* 14**,** 1990.

MUSA, M., MASSAWE, F., MAYES, S., ALSHAREEF, I. & SINGH, A. 2016. Nitrogen fixation and N-balance studies on Bambara groundnut (Vigna subterranea L. Verdc) landraces grown on tropical acidic soils of Malaysia. *Communications in Soil Science and Plant Analysis,* 47**,** 533-542.

MUTANGA, O., ADAM, E. & CHO, M. A. 2012. High density biomass estimation for wetland vegetation using WorldView-2 imagery and random forest regression algorithm. *International Journal of Applied Earth Observation and Geoinformation,* 18**,** 399-406.

MUTANGA, O., DUBE, T. & GALAL, O. 2017. Remote sensing of crop health for food security in Africa: Potentials and constraints. *Remote Sensing Applications: Society and Environment,* 8**,** 231-239.

MUTANGA, O., MASENYAMA, A. & SIBANDA, M. 2023. Spectral saturation in the remote sensing of high-density vegetation traits: A systematic review of progress, challenges, and prospects. *ISPRS Journal of Photogrammetry and Remote Sensing,* 198**,** 297-309.

MUTANGA, O. & SKIDMORE, A. K. 2004. Narrow band vegetation indices overcome the saturation problem in biomass estimation. *International Journal of Remote Sensing,* 25**,** 3999-4014.

NATEKIN, A. & KNOLL, A. 2013. Gradient boosting machines, a tutorial. *Frontiers in neurorobotics,* 7**,** 21.

NDLOVU, H. S., ODINDI, J., SIBANDA, M., MUTANGA, O., CLULOW, A., CHIMONYO, V. G. & MABHAUDHI, T. 2021. A comparative estimation of maize leaf water content using machine learning techniques and unmanned aerial vehicle (UAV)-based proximal and remotely sensed data. *Remote Sensing,* 13**,** 4091.

NGUYEN, H. P. D. & NGUYEN, D. D. 2021. Drone application in smart cities: The general overview of security vulnerabilities and countermeasures for data communication. *Development and Future of Internet of Drones (IoD): Insights, Trends and Road Ahead***,** 185-210.

NIEDERHEISER, R., WINKLER, M., DI CECCO, V., ERSCHBAMER, B., FERNÁNDEZ, R., GEITNER, C., HOFBAUER, H., KALAITZIDIS, C., KLINGRABER, B. & LAMPRECHT, A. 2021. Using automated vegetation cover estimation from close-range photogrammetric point clouds to compare vegetation location properties in mountain terrain. *GIScience & remote sensing,* 58**,** 120-137.

NYMAN, J. 2018. Pixel classification of hyperspectral images.

OPOLE, R. A. 2012. *Effect of environmental stress and management on grain and biomass yield of finger millet [Eleusine coracana (L.) Gaertn.]*, Kansas State University.

OUMA, Y. O., KEITSILE, A., NKWAE, B., ODIRILE, P., MOALAFHI, D. & QI, J. 2023. Urban land-use classification using machine learning classifiers: comparative evaluation and post-classification multi-feature fusion approach. *European Journal of Remote Sensing,* 56**,** 2173659.

OUYANG, W., STRUIK, P. C., YIN, X. & YANG, J. 2017. Stomatal conductance, mesophyll conductance, and transpiration efficiency in relation to leaf anatomy in rice and wheat genotypes under drought. *Journal of Experimental Botany,* 68**,** 5191-5205.

PARRA, L., MOSTAZA-COLADO, D., YOUSFI, S., MARIN, J. F., MAURI, P. V. & LLORET, J. 2021. Drone RGB images as a reliable information source to determine legumes establishment success. *Drones,* 5**,** 79.

PEREIRA, F. D. S., DE LIMA, J., FREITAS, R., DOS REIS, A. A., DO AMARAL, L. R., FIGUEIREDO, G. K. D. A., LAMPARELLI, R. A. & MAGALHÃES, P. S. G. 2022. Nitrogen variability assessment of pasture fields under an integrated crop-livestock system using UAV, PlanetScope, and Sentinel-2 data. *Computers and Electronics in Agriculture,* 193**,** 106645.

PERSELLO, C., TOLPEKIN, V., BERGADO, J. R. & DE BY, R. 2019. Delineation of agricultural fields in smallholder farms from satellite images using fully convolutional networks and combinatorial grouping. *Remote sensing of environment,* 231**,** 111253.

PHAM, H.-T., NGUYEN, H.-Q., LE, K.-P., TRAN, T.-P. & HA, N.-T. 2023. Automated Mapping of Wetland Ecosystems: A Study Using Google Earth Engine and Machine Learning for Lotus Mapping in Central Vietnam. *Water,* 15**,** 854.

PINEDA, M., BARON, M. & PEREZ-BUENO, M. L. 2021. Thermal Imaging for Plant Stress Detection and Phenotyping. *REMOTE SENSING,* 13.

QIU, Z., XIANG, H., MA, F. & DU, C. 2020. Qualifications of rice growth indicators optimized at different growth stages using unmanned aerial vehicle digital imagery. *Remote Sensing,* 12**,** 3228.

QU, L. A., CHEN, Z., LI, M., ZHI, J. & WANG, H. 2021. Accuracy improvements to pixel-based and object-based lulc classification with auxiliary datasets from Google Earth engine. *Remote Sensing,* 13**,** 453.

RAJI, S. N., APARNA, G. N., MOHANAN, C. N. & SUBHASH, N. 2017. Proximal remote sensing of herbicide and drought stress in field grown colocasia and sweet potato plants by sunlight-induced chlorophyll fluorescence Imaging. *Journal of the Indian Society of Remote Sensing,* 45**,** 463-475.

RAMÍREZ, D. A., GRÜNEBERG, W., I ANDRADE, M., DE BOECK, B., LOAYZA, H., S MAKUNDE, G., NINANYA, J., RINZA, J., HECK, S. & CAMPOS, H. 2021. Phenotyping of productivity and resilience in sweetpotato under water stress through UAV-based multispectral and thermal imagery in Mozambique. *Journal of Agronomy and Crop Science*.

REN, T., XU, H., CAI, X., YU, S. & QI, J. 2022. Smallholder crop type mapping and rotation monitoring in mountainous areas with Sentinel-1/2 imagery. *Remote Sensing,* 14**,** 566.

SAARELA, M. & JAUHIAINEN, S. 2021. Comparison of feature importance measures as explanations for classification models. *SN Applied Sciences,* 3**,** 1-12.

SAFARI KHATOUNI, A., SEDDIGH, N., NANDY, B. & ZINCIR-HEYWOOD, N. 2021. Machine learning based classification accuracy of encrypted service channels: analysis of various factors. *Journal of Network and Systems Management,* 29**,** 1-27.

SANKARAN, S., ZHOU, J., KHOT, L. R., TRAPP, J. J., MNDOLWA, E. & MIKLAS, P. N. 2018. High-throughput field phenotyping in dry bean using small unmanned aerial vehicle based multispectral imagery. *Computers and Electronics in Agriculture,* 151**,** 84-92.

SAPKOTA, B., SINGH, V., COPE, D., VALASEK, J. & BAGAVATHIANNAN, M. 2020. Mapping and Estimating Weeds in Cotton Using Unmanned Aerial Systems-Borne Imagery. *AGRIENGINEERING,* 2.

SARKER, I. H. 2021. Machine learning: Algorithms, real-world applications and research directions. *SN computer science,* 2**,** 160.

SENGUPTA, S., MOHINUDDIN, S., ARIF, M., SENGUPTA, B. & ZHANG, W. 2022. Assessment of agricultural land suitability using GIS and Fuzzy Analytical Hierarchy Process approach in Ranchi District, India. *Geocarto International*, 1-34.

SHAO, Y., LIU, Y., XUAN, G., WANG, Y., GAO, Z., HU, Z., HAN, X., GAO, C. & WANG, K. 2020. Application of hyperspectral imaging for spatial prediction of soluble solid content in sweet potato. *RSC advances,* 10**,** 33148-33154.

SHARIFI, A. 2020. Remotely sensed vegetation indices for crop nutrition mapping. *JOURNAL OF THE SCIENCE OF FOOD AND AGRICULTURE,* 100**,** 5191-5196.

SHI, Y., MURRAY, S. C., ROONEY, W. L., VALASEK, J., OLSENHOLLER, J., PUGH, N. A., HENRICKSON, J., BOWDEN, E., ZHANG, D. & THOMASSON, J. A. Corn and sorghum phenotyping using a fixed-wing UAV-based remote sensing system. Autonomous air and ground sensing systems for agricultural optimization and phenotyping, 2016. SPIE, 46-53.

SHIRZADIFAR, A., BAJWA, S., NOWATZKI, J. & BAZRAFKAN, A. 2020. Field identification of weed species and glyphosate-resistant weeds using high resolution imagery in early growing season. *BIOSYSTEMS ENGINEERING,* 200**,** 200-214.

SIBANDA, M., MUGIYO, H. & CHIMONYO, V. 2021a. Evaluation of land suitability methods with reference to neglected and underutilised crop species: A scoping review.

SIBANDA, M., MUTANGA, O., CHIMONYO, V. G., CLULOW, A. D., SHOKO, C., MAZVIMAVI, D., DUBE, T. & MABHAUDHI, T. 2021b. Application of drone technologies in surface water resources monitoring and assessment: A systematic review of progress, challenges, and opportunities in the global south. *Drones,* 5**,** 84.

SINGH, C., KARAN, S. K., SARDAR, P. & SAMADDER, S. R. 2022. Remote sensing-based biomass estimation of dry deciduous tropical forest using machine learning and ensemble analysis. *Journal of Environmental Management,* 308**,** 114639.

SINGHAL, G., BANSOD, B., MATHEW, L., GOSWAMI, J., CHOUDHURY, B. & RAJU, P. 2019. Estimation of leaf chlorophyll concentration in turmeric (Curcuma longa) using high-resolution unmanned aerial vehicle imagery based on kernel ridge regression. *Journal of the Indian Society of Remote Sensing,* 47**,** 1111-1122.

SINGLA, M., GHOSH, D. & SHUKLA, K. K. 2020. Improved sparsity of support vector machine with robustness towards label noise based on rescaled α-hinge loss with non-smooth regularizer. *Neural Processing Letters,* 52**,** 2211-2239.

SIPPER, M. & MOORE, J. H. 2021. Conservation machine learning: a case study of random forests. *Scientific Reports,* 11**,** 3629.

SISHODIA, R. P., RAY, R. L. & SINGH, S. K. 2020. Applications of remote sensing in precision agriculture: A review. *Remote Sensing,* 12**,** 3136.

SOBEJANO-PAZ, V., MIKKELSEN, T. N., BAUM, A., MO, X., LIU, S., KÖPPL, C. J., JOHNSON, M. S., GULYAS, L. & GARCÍA, M. 2020. Hyperspectral and thermal sensing of stomatal conductance, transpiration, and photosynthesis for soybean and maize under drought. *Remote Sensing,* 12**,** 3182.

STOPFORTH, R. 2017. Drone licenses-neccesities and requirements. *II Ponte,* 73**,** 149-156.

SUHAIRI, T. A. S. T. M., SININ, S. S. M., WIMALASIRI, E. M., NIZAR, N. M. M., THARMANDRAN, A. S., JAHANSHIRI, E., GREGORY, P. J. & AZAM-ALI, S. N. 2020. Use of Unmanned Aerial Vehicles (UAVs) Imagery in Phenotyping of Bambara Groundnut. *Journal of Agricultural Science,* 12.

SUN, Z., WANG, X., WANG, Z., YANG, L., XIE, Y. & HUANG, Y. 2021. UAVs as remote sensing platforms in plant ecology: review of applications and challenges. *Journal of Plant Ecology,* 14**,** 1003-1023.

TAHIR, M. N., NAQVI, S. Z. A., LAN, Y., ZHANG, Y., WANG, Y., AFZAL, M., CHEEMA, M. J. M. & AMIR, S. 2018. Real time estimation of chlorophyll content based on vegetation indices derived from multispectral UAV in the kinnow orchard. *International Journal of Precision Agricultural Aviation,* 1.

TANG, Z., JIN, Y., ALSINA, M. M., MCELRONE, A. J., BAMBACH, N. & KUSTAS, W. P. 2022. Vine water status mapping with multispectral UAV imagery and machine learning. *Irrigation Science,* 40**,** 715-730.

TASSI, A., GIGANTE, D., MODICA, G., DI MARTINO, L. & VIZZARI, M. 2021. Pixel-vs. Object-based landsat 8 data classification in google earth engine using random forest: The case study of maiella national park. *Remote sensing,* 13**,** 2299.

THENKABAIL, P. S. & LYON, J. G. 2016. *Hyperspectral remote sensing of vegetation*, CRC Press.

THENKABAIL, P. S., MARIOTTO, I., GUMMA, M. K., MIDDLETON, E. M., LANDIS, D. R. & HUEMMRICH, K. F. 2013. Selection of hyperspectral narrowbands (HNBs) and composition of hyperspectral twoband vegetation indices (HVIs) for biophysical characterization and discrimination of crop types using field reflectance and Hyperion/EO-1 data. *Selected Topics in Applied Earth Observations and Remote Sensing, IEEE Journal of,* 6**,** 427-439.

THENKABAIL, P. S., SMITH, R. B. & DE PAUW, E. 2002. Evaluation of narrowband and broadband vegetation indices for determining optimal hyperspectral wavebands for agricultural crop characterization. *Photogrammetric Engineering and Remote Sensing,* 68**,** 607-622.

TIWARI, A. 2022. Supervised learning: from theory to applications. *Artificial intelligence and machine learning for EDGE computing.* Elsevier.

USTUNER, M., SANLI, F. B., ABDIKAN, S., ESETLILI, M. & KURUCU, Y. 2014. Crop type classification using vegetation indices of rapideye imagery. *The international archives of the photogrammetry, remote sensing and spatial information sciences,* 40**,** 195-198.

VÅGSHOLM, I., ARZOOMAND, N. S. & BOQVIST, S. 2020. Food security, safety, and sustainability—getting the trade-offs right. *Frontiers in Sustainable Food Systems***,** 16.

VAN WART, J., KERSEBAUM, K. C., PENG, S., MILNER, M. & CASSMAN, K. G. 2013. Estimating crop yield potential at regional to national scales. *Field Crops Research,* 143**,** 34-43.

VELUSAMY, P., RAJENDRAN, S., MAHENDRAN, R. K., NASEER, S., SHAFIQ, M. & CHOI, J.-G. 2021. Unmanned Aerial Vehicles (UAV) in Precision Agriculture: Applications and Challenges. *Energies,* 15**,** 217.

WANG, F., YI, Q., HU, J., XIE, L., YAO, X., XU, T. & ZHENG, J. 2021. Combining spectral and textural information in UAV hyperspectral images to estimate rice grain yield. *International Journal of Applied Earth Observation and Geoinformation,* 102**,** 102397.

WANG, R., SHI, F. & XU, D. 2022. The Extraction Method of Alfalfa (Medicago sativa L.) Mapping Using Different Remote Sensing Data Sources Based on Vegetation Growth Properties. *Land,* 11**,** 1996.

WIJEWARDANA, C., ALSAJRI, F. A., IRBY, J. T., KRUTZ, L. J., GOLDEN, B., HENRY, W. B., GAO, W. & REDDY, K. R. 2019. Physiological assessment of water deficit in soybean using midday leaf water potential and spectral features. *Journal of Plant Interactions,* 14**,** 533-543.

WILLIAMS, T. B., DODD, I. C., SOBEIH, W. Y. & PAUL, N. D. 2022. Ultraviolet radiation causes leaf warming due to partial stomatal closure. *Horticulture research,* 9.

WOEBBECKE, D. M., MEYER, G. E., VON BARGEN, K. & MORTENSEN, D. A. 1995. Color indices for weed identification under various soil, residue, and lighting conditions. *Transactions of the ASAE,* 38**,** 259-269.

WU, S., DENG, L., GUO, L. & WU, Y. 2022. Wheat leaf area index prediction using data fusion based on high-resolution unmanned aerial vehicle imagery. *Plant Methods,* 18**,** 1-16.

XIA, W., LUO, T., ZHANG, W., MASON, A. S., HUANG, D., HUANG, X., TANG, W., DOU, Y., ZHANG, C. & XIAO, Y. 2019. Development of high-density SNP markers and their application in evaluating genetic diversity and population structure in Elaeis guineensis. *Frontiers in plant science,* 10**,** 130.

XIAOXIA, S., JIXIAN, Z. & ZHENGJUN, L. 2005. A comparison of object-oriented and pixel-based classification approachs using quickbird imagery. *ISPRS STM***,** 281-284.

XIE, Q., DASH, J., HUANG, W., PENG, D., QIN, Q., MORTIMER, H., CASA, R., PIGNATTI, S., LANEVE, G. & PASCUCCI, S. 2018. Vegetation indices combining the red and red-edge spectral information for leaf area index retrieval. *IEEE Journal of selected topics in applied earth observations and remote sensing,* 11**,** 1482-1493.

XING, H., CHEN, B. & LU, M. 2022. A sub-seasonal crop information identification framework for crop rotation mapping in smallholder farming areas with time series sentinel-2 imagery. *Remote Sensing,* 14**,** 6280.

XING, N., HUANG, W., XIE, Q., SHI, Y., YE, H., DONG, Y., WU, M., SUN, G. & JIAO, Q. 2019. A transformed triangular vegetation index for estimating winter wheat leaf area index. *Remote Sensing,* 12**,** 16.

XUE, J. & SU, B. 2017. Significant remote sensing vegetation indices: A review of developments and applications. *Journal of Sensors,* 2017.

YANG, C., EVERITT, J. H., DU, Q., LUO, B. & CHANUSSOT, J. 2012. Using high-resolution airborne and satellite imagery to assess crop growth and yield variability for precision agriculture. *Proceedings of the IEEE,* 101**,** 582-592.

YE, Z., SHENG, Z., LIU, X., MA, Y., WANG, R., DING, S., LIU, M., LI, Z. & WANG, Q. 2021. Using machine learning algorithms based on GF-6 and Google Earth engine to predict and map the spatial distribution of soil organic matter content. *Sustainability,* 13**,** 14055.

YULIANTO, F., RAHARJO, P. D., PRAMONO, I. B., SETIAWAN, M. A., CHULAFAK, G. A., NUGROHO, G., SAKTI, A. D., NUGROHO, S. & BUDHIMAN, S. 2023. Prediction and mapping of land degradation in the Batanghari watershed, Sumatra, Indonesia: utilizing multi-source geospatial data and machine learning modeling techniques. *Modeling Earth Systems and Environment***,** 1-22.

ZALUDIN, Z. & HARITUDDIN, A. S. M. Challenges and Trends of Changing from Hover to Forward Flight for a Converted Hybrid Fixed Wing VTOL UAS from Automatic Flight Control System Perspective. 2019 IEEE 9th International Conference on System Engineering and Technology (ICSET), 2019. IEEE, 247-252.

ZENG, Y., HAO, D., HUETE, A., DECHANT, B., BERRY, J., CHEN, J. M., JOINER, J., FRANKENBERG, C., BOND-LAMBERTY, B. & RYU, Y. 2022. Optical vegetation indices for monitoring terrestrial ecosystems globally. *Nature Reviews Earth & Environment,* 3**,** 477-493.

ZHANG, C., YANG, Z., DI, L., YU, E. G., ZHANG, B., HAN, W., LIN, L. & GUO, L. 2022. Near-real-time MODIS-derived vegetation index data products and online services for CONUS based on NASA LANCE. *Scientific Data,* 9**,** 477.

ZHANG, H., KANG, J., XU, X. & ZHANG, L. 2020. Accessing the temporal and spectral features in crop type mapping using multi-temporal Sentinel-2 imagery: A case study of Yi'an County, Heilongjiang province, China. *Computers and Electronics in Agriculture,* 176**,** 105618.

ZHANG, L., GEER, T., SUN, X. X., SHOU, C. G. & DU, H. S. 2019a. APPLICATION OF HYPERSPECTRAL IMAGING TECHNIQUE IN AGRICULTURAL REMOTE SENSING. *Bangladesh Journal of Botany,* 48**,** 907-912.

ZHANG, L., ZHANG, H., NIU, Y. & HAN, W. 2019b. Mapping Maize Water Stress Based on UAV Multispectral Remote Sensing. *Remote Sensing,* 11**,** 605.

ZHANG, Y., TENG, P., AONO, M., SHIMIZU, Y., HOSOI, F. & OMASA, K. 2018. 3D monitoring for plant growth parameters in field with a single camera by multi-view approach. *Journal of agricultural meteorology,* 74**,** 129-139.

ZHAO, Y.-P., WANG, J.-J., LI, X.-Y., PENG, G.-J. & YANG, Z. 2020. Extended least squares support vector machine with applications to fault diagnosis of aircraft engine. *ISA transactions,* 97**,** 189-201.

ZHENG, Q., HUANG, W., YE, H., DONG, Y., SHI, Y. & CHEN, S. 2020. Using continous wavelet analysis for monitoring wheat yellow rust in different infestation stages based on unmanned aerial vehicle hyperspectral images. *Applied Optics,* 59**,** 8003-8013.

93

APPENDICES

Chapter 2 Appendix

Table S1: Drone acquired data VIs used in literature.

UAV Data Vegetation indices	References
Normalized difference vegetation index (NDVI)	[1], [2], [3], [4], [5], [6], [7], [8], [9], [10], [11], [12], [13], [14]
Normalized difference red edge index (NDRE)	[6], [8], [9], [11]
Renormalized difference vegetation index (RDVI)	[8], [11]
Normalized difference water index (NDWI)	[8]
Maximum difference water index (MDWI)	[8]
Excess green index (EGI)	[1], [4], [13]
Enhanced vegetation index (EVI2)	[2], [15]
green difference vegetation index (GDVI)	[10], [11], [14]
Difference Vegetation Index	[11]
Green normalized difference vegetation index (GNDVI)	[2], [9], [10], [11], [16], [14]
Normalized Green red difference index (NGRDI)	[8]
Simple ratio (SR)	[2], [10], [11], [14]
Modified Simple Ratio Index (MSRI)	[10], [11]
Modified SAVI 2	[11]
Soil-adjusted Vegetation Index (SAVI)	[11]
Optimized Soil-adjusted Vegetation Index (OSAVI)	[15], [8]
Green and Red ratio Vegetation Index (GRVI)	[9]
Red-Edge Simple Ratio (SRre)	[10]
Normalized difference photosynthetic vigor ratio	[5]
TCARI	[8]
Nutritional nitrogen index (NNI)	[17]
Crop water stress index	[8]
Chlorophyll Vegetation Index	[11]
Green Chlorophyll Index	[11]
Chlorophyll concentration index	[18]
Chlorophyll reflectance red-edge index	[12]
Modified Chlorophyll Absorption Index	[11]
Crop water stress index (CWSI).	[19]
Moisture stress index	[8]
Photochemical reflectance index	[8]
canopy difference	[19]
B1/B2	[10]
Green leaf index	[13]
Visible atmospherically resistant index	[13]

94

Table S2: Satellite data acquired VI's used in literature

Satellite (Vegetation indices)	References
NDVI	[20], [21], [22], [23], [24], [25], [26], [27], [28], [29], [30], [31]
DEV NDVI	[20]
normalized difference red edge index	[21]
enhanced vegetation index (EVI2)	[30], [32], [33]
Difference Vegetation Index	[24]
green normalized difference vegetation index (GNDVI)	[25], [26], [31]
simple ratio (SR)	[21]
Ratio Vegetation Index (RVI)	[24]
Soil-adjusted Vegetation Index (SAVI)	[23], [25], [26], [28]
Vegetation Condition Index (VCI)	[20]
Simple ratio red edge	[21]
TCARI	[21]
nutritional nitrogen index (NNI)	[17]
Chlorophyll Vegetation Index	[21]
Green Chlorophyll Index	[21]
chlorophyll reflectance red-edge index	[21]
Modified Chlorophyll Absorption Index	[21]
Triangular vegetation index (TVI)	[21]
modified triangular index 2	[21]
Normalized Difference Water Index	[30] ,[31]

Table S3: Drone platforms used in mapping specific NUS crop attributes other than stomatall conductance.

Drone sensor type	Crop Type	Research domain	Reference
DJI Phantom 4 Pro, M600 Pro	Palmer amaranth	Modelling, Phenology/growth, Monitoring, Regression and prediction	[1]
DJI Phantom 4 Pro	Bambara groundnut	Modelling, Production/crop yield, Phenology/growth, Regression and prediction	[2]
MikroKopter JR11X	Sorghum & Amaranth	Modelling, Phenology/growth, Regression and prediction	[3]
DJI S1000 UAV, DJI Phantom 4 Pro	Amaranthus	Classification, Phenology/growth	[34]
DJI Phantom 4 Pro	Cotton & Palmer amaranth	Classification, Land suitability, Production/crop yield, Phenology/growth,	[4]
Quadcopter G-Q45	Ruzi grass & Millet	Modelling, Production/crop yield, Phenology/growth, Regression and prediction	[17]
Hexacopter UAV, M600 Pro	Tumeric	Modelling, Physiology, Phenology/growth, Regression and prediction	[18]
	Sorghum	Phenotyping, growth, production	[35]
DJI Phantom 4 Pro	Bambara groundnut	Modelling, Phenotyping/crop genetics, Physiology, Phenology/growth, Regression and prediction	[36]
DJI 100	Alfalfa	Phenotyping/crop genetics, Phenology/growth	[9]
Parrot Bebop 2 Pro,	Chickpea & Lentil	Classification, Physiology and crop vigour, Phenology/growth	[10]

Sensefly eBee RTK	Red clover	Land suitability, Modelling, Phenology/growth	[14]
DJI Phantom 4 Pro	Legumes	Modelling, Climate adaptation, Production/crop yield, Physiology, Phenology/growth.	[11]
Octocopter	Dry bean	Phenotyping/crop genetics, Production/crop yield, Phenology/growth	[16]
DJI Inspire 1	Sweet potato	Phenotyping/crop genetics, Climate adaptation, Production/crop yield, Physiology, Phenology/growth	[12]
Cessna	Taro	Classification, Land suitability, Production/crop yield	[37]
DJI S1000 UAV	Sweet potato	Modelling, Production/crop yield, Physiology, Phenology/growth	[38]
Mavic Mini	Chickpea	Modelling, Climate adaptation, Physiology, Phenology/growth, Regression and prediction	[13]

Table S4: Drone platforms used to map the spatial distribution of various NUS crops.

Drone used in study	**Crop assessed**
Octocopter	Dry bean [16]
Hexacopter UAV	Tumeric [18]
Cessna	Taro [37]
Parrot Bebop 2 Pro	Chickpea and Lentil [10]
DJI Inspire 1	Sweet potato [12]
DJI 100	Alfalfa (Medicago sativa L) [9]
DJI S1000 UAV	Amaranthus [34], Sweet potato[38]
DJI Phantom 4 Pro	Palmer amaranth [1], Bamara groundut [2], Amaranthus [34], Palmer amaranth (Amaranthus palmeri S. Watson) [4] , Bamara groundut [7] Legume [11].
M600 Pro	Palmer amaranth [1], Tumeric [18]
Mavic Mini	Chickpea [13]
quadcopter G-Q45	Ruzi grass and Millet [17]
Sensefly eBee RTK	Red clover [14]
MikroKopter JR11X	sorghum and amaranth *[3]*

Table S5: Satellite borne sensors used to assess NUS crops.

Reference	**Satellite Sensor**	**Crop type**	**Research domain**
[28]	Landsat Thematic mapper	Chickpea, lentil, vetch	Classification, Regression and prediction, Climate adaptation, Production/crop yield, Phenology/growth, Regression and prediction
[22]	Landsat 7	Sorghum	Regression and prediction, Land suiitability, Climate adaptation, Physiology and crop vigour, Phenology
[20]	MODIS	Teff, haricot beans, sweet potato (Ipomoea batatas) and taro (Colocasia esculenta).	Land suiitability, Modelling, Climate adaptation, Production/crop yield, Phenology, Regression and prediction
[33]	MODIS	C3 and C4 crops	Regression and prediction, Land suiitability, Modelling, Climate adaptation, Production
[17]	Planet	Ruzi grass & Millet	Modelling, Production/crop yield, Phenology/growth, regression
[17]	Sentinel-2	Ruzi grass & Millet	Modelling, Production/crop yield, Phenology/growth, regression
[21]	Sentinel-2	Cotton & Sugar beet	Modelling, Production/crop yield, Physiology, Phenology/growth, regression

96

[23]	Sentinel-2	Sorghum, alfalfa,	Land suiitability, Modelling, Climate adaptation, Production/crop yield, Phenology, Regression and prediction
[39]	Sentinel-2	Chickpea, faba bean, field pea, lentil, vetch	Classification, land suitability, Phenology/growth
[25]	Sentinel-2	Sweet potato	Phenotyping, Climate adaptation, Phenology/growth, Regression, and prediction
[26]	Sentinel-2	Sweet potato	Classification, Regression and prediction, Climate adaptation, Production/crop yield, Phenology
[27]	Sentinel-2	Legumes	Modelling, Climate adaptation, Physiology, Phenology/growth, regression
[30]	Sentinel-2	Sorghum, Alfalfa, and dry beans	Classification, land suitability, Climate adaptation,Phenology/growth
[29]	Worldview 2	Sweet potato	Classification, land suitability, Climate adaptation,Phenology/growth
[24]	LiDAR	Sorghum	Phenotyping/crop genetics, Phenology
[40]	LiDAR	Cassava	Regression and prediction,Phenotyping/crop genetics, Physiology, Phenology,
[41]	LiDAR	Sweet potato	Regression and prediction, Physiology, Phenology,
[33]	Global Ozone Monitoring Experiment-2 satellite	C3 and C4 crops	Regression and prediction, Land suitability, Modelling, Climate adaptation, Production
[31]	Landsat 8	Alfalfa	Classification,, Land suitability, Production/crop yield, Climate adaptation, Phenology

Table S6: Satellites Datasets used by different institution to assess various research domains of NUS.

Satellite sensor articles and Institutions					
Author	Article title	Publication	Area	Crop Type	Institutions
[20]	Assessing the spatio-temporal variability of NDVI and VCI as indices of crops productivity in Ethiopia: a remote sensing approach	2021	Ethiopia	Teff, haricot beans, sweet potato (Ipomoea batatas) and taro (Colocasia esculenta).	Copperbelt University, Kitwe, Zambia; b Institute of Climate and Society, Mekelle University, Mekelle, Ethiopia. University of Nigeria, Nsukka, Enugu, Nigeria. Ghent University, Ghent, Belgium.
[17]	Nitrogen variability assessment of pasture fields under an integrated crop-livestock system using UAV, PlanetScope, and Sentinel-2 data	2022	Brazil	Ruzi grass & Millet	Federal Institute of Education, Science and Technology of Alagoas, 57120-000 Satuba, Alagoas, Brazil.. University of Campinas, 13083-896 Campinas, Sao ˜ Paulo, Brazil.
[21]	Remotely sensed vegetation indices for crop nutrition mapping	2020	Iran	Cotton & Sugar beet	Shahid Rajaee Teacher Training University, Tehran, 16785-136, Iran. E-mail: a_sharifi@sru.ac.ir
[23]	Optimized land use through integrated land suitability and gis approach in west el-minia governorate, upper Egypt	2021	Egypt	Sorghum & alfalfa,	Ain-Shams University, Cairo 11241, Egypt. National Authority for Remote Sensing and Space Sciences, Cairo 11769, Egypt; National Authority for Remote Sensing and Space Sciences (NARSS),

[22]	Water requirement and crop coefficients of sorghum in apodi plateau [Necessidade hídrica e coeficientes de cultivo do sorgo nas condições da chapada do apodi]	2021	Brazil	Sorghum	Research developed at Empresa de Pesquisa Agropecuária do Rio Grande do Norte, Apodi, RN, Brazil Faculdade UNINASSAU, Caruaru, PE, Brazil Universidade Federal Rural do Semi-Árido/Centro de Ciências Agrárias/Departamento de Ciências Agronômicas e Florestais, Mossoró, RN, Brazil
[39]	Needle in a haystack: Mapping rare and infrequent crops using satellite imagery and data balancing methods	2019	Australia	Chickpea, faba bean, field pea, lentil, vetch	CSIRO Agriculture & Food, St Lucia, QLD 4067, Australia CSIRO Data61, Docklands, VIC 3008, Australia CSIRO Agriculture & Food, Floreat, WA 6014, Australia
[24]	Crop 3D—a LiDAR based platform for 3D high-throughput crop phenotyping	2018	China	Sorghum	University of Chinese Academy of Sciences, Beijing China. Beijing Normal University, Beijing 100875, China.
[33]	Improving the monitoring of crop productivity using spaceborne solar-induced fluorescence	2016	USA	C3 and C4 crops	Stanford University, Stanford, CA 94305,USA Nanjing University, Nanjing 210023, China, German Research Center for Geosciences (GFZ), Telegrafenberg A17, 14473 Potsdam, Germany, National Aeronautics and Space Administration Goddard Space Flight Center, Greenbelt, MD 20771, USA
[25]	Use of remote sensing to characterize the phenological development and to predict sweet potato yield in two growing seasons	2021	Brazil	Sweet potato	Sao ˜ Paulo State University. Federal University Lavras, Brazil. Taquaritinguense Institute of Higher Education, Brazil
[26]	Predicting on multi-target regression for the yield of sweet potato by the market class of its roots upon vegetation indices	2021	Brazil	Sweet potato	Sao ˜ Paulo State University.
[40]	Prediction of aboveground biomass of three cassava (manihot esculenta) genotypes using a terrestrial laser scann	2021	Colombia	Cassava	Texas A&M University, College Station, TX, USA International Center for Tropical Agriculture, Santiago de Cali 6713, Colombia
[27]	Application of Sentinel-2A data for pasture biomass monitoring using a physically based radiative transfer model	2018	England	Legumes	University of Reading, Reading RG6 6UR, UK
[28]	Biophysical and yield information for precision farming from near-real-time and historical Landsat TM images	2003	Syria	Chickpea, lentil, vetch	Yale University, New Haven.
[41]	Estimating Leaf Water Content through Low-Cost LiDAR	2022	Japan	Sweet potato	Chiba University, 648, Matsudo, Matsudo-shi 271-8510, Japan.
[29]	Parcel-level mapping of crops in a smallholder agricultural area: A case of central China using single-temporal VHSR imagery	2020	China	Sweet potato,	China University of Geosciences (CUG), Wuhan 430074, PR China. University of Connecticut, Storrs, CT 06269, USA. Key Laboratory of Rule of Law Research, Ministry of Natural Resources, Wuhan 430074, PR China
[31]	Crop type detection using an object-based classification method and multi-temporal Landsat satellite images,Paddy and Water Environment	2022	Iran	Alfalfa	Department of Water Resources Study and Research, Water Research Institute, Tehran, Iran
[30]	Exploring machine learning algorithms for mapping crop types in a heterogeneous agriculture landscape using Sentinel-2 data. A case study of Free State Province, South Africa	2020	South Africa	Sorghum, Alfalfa and dry beans	Geo-information Division, Institute for soil water and climate, Agricultural Research Council. University of Witwatersrand. Private Bag x3, Wits 2050, Johannesburg, South Africa.

Table S7: Institutions that utilized UAV borne sensors to assess NUS crops.

UAV articles and Institutions					
Author	Article title	Publication	Area	Crop Type	Institutions
[1]	Seed rain potential in late-season weed escapes can be estimated using remote sensing	2021	United States	Palmer amaranth	Texas A&M University, College Station, TX, USA;
[2]	The feasibility of using a low-cost near-infrared, sensitive, consumer-grade digital camera mounted on a commercial UAV to assess Bambara groundnut yield	2022	Malaysia	Bamara groundut	University of Nottingham Malaysia Campus, Semenyih, Malaysia. The University of Adelaide, Glen Osmond, Australia. Charles Darwin University, Casuarina, Australia. University of Nottingham, Nottingham, UK.
[3]	Assessment of Weed Classification Using Hyperspectral Reflectance and Optimal Multispectral UAV Imagery	2021	Australia	sorghum and amaranth	The University of Queensland, Gatton Campus, QLD 4343, Australia. University Putra Malaysia, Serdang 43400, Selangor, Malaysia
[34]	Field identification of weed species and glyphosate-resistant weeds using high resolution imagery in early growing season	2020	USA	Amaranth	Shiraz University, Shiraz, Iran. North Dakota State University, Fargo, ND, USA. Montana State University, Bozeman, MT, USA. Yazd University, Yazd, Iran
[4]	Mapping and Estimating Weeds in Cotton Using Unmanned Aerial Systems-Borne Imagery	2020	United States	Cotton, Palmer amaranth (Amaranthus palmeri S. Watson)	Texas A&M University, College Station, TX 77843, USA.
[17]	Nitrogen variability assessment of pasture fields under an integrated crop-livestock system using UAV, PlanetScope, and Sentinel-2 data	2022	Brazil	Ruzi grass & Millet	Federal Institute of Education, Science and Technology of Alagoas, 57120-000 Satuba, Alagoas, Brazil. University of Campinas, 13083-896 Campinas, Sao ˜ Paulo, Brazil.
[35]	Corn and sorghum phenotyping using a fixed-wing UAV-based remote sensing system	2016	United States	Sorghum	
[7]	Use of Unmanned Aerial Vehicles (UAVs) Imagery in Phenotyping of Bambara Groundnut	2020	Selangor	Bambara groundnut	Semenyih, Selangor, Malaysia. University of Nottingham Malaysia. University of Reading, Early Gate, Reading, UK
[9]	Phenomics-Assisted Selection for Herbage Accumulation in Alfalfa (Medicago sativa L.)	2021	United States	Alfalfa (Medicago sativa L)	University of Florida, Gainesville, FL, United States. EMBRAPA-ACRE, Rio Branco, Brazil.
[10]	Drone RGB Images as a Reliable Information Source to Determine Legumes Establishment Success	2021	Spain	Chickpea & Lentil	Universitat Politècnica de València. Instituto Madrileño de Investigación y Desarrollo Rural, Agrario y Alimentario (IMIDRA), Finca "El Encin". Areaverde MG Projects SL. C/Oña, 43, 28933 Madrid, Spain.
[14]	The Application of an Unmanned Aerial System and Machine Learning Techniques for Red Clover-Grass Mixture	2021	Estonia	Red clover	Estonian University of Life Sciences, Kreutzwaldi 5, EE-51006 Tartu, Estonia.

99

|				
	Yield Estimation under Variety Performance Trials				University of Brighton, Lewes Road, Brighton BN2 4JG, UK. Agricultural Research Center, 4/6 Teaduse St., 75501 Saku, Estonia. National Chung Hsing University, Taichung 402, Taiwan.
[11]	Prediction of Biomass and N Fixation of Legume-Grass Mixtures Using Sensor Fusion	2021	Germany	Legume	Universität Kassel, Witzenhausen, Germany
[16]	High-throughput field phenotyping in dry bean using small unmanned aerial vehicle based multispectral imagery	2018	United States	Dry bean	Washington State University, United States. University of Missouri, 211 Agricultural Engineering Building, Columbia, MO, United States. USDA–ARS, Grain Legume Genetics and Physiology Research Unit, 24106 N. Bunn Rd., Prosser, WA, United States
[12]	Phenotyping of productivity and resilience in sweetpotato under water stress through UAV-based multispectral and thermal imagery in Mozambique	2021	Mozambique	Sweet potato	International Potato Center (CIP), Lima, Peru Universidad Nacional Agraria La Molina (UNALM), Lima, Peru. International Potato Center (CIP), Maputo, Mozambique. International Potato Center (CIP), Nairobi, Kenya.
[37]	Mapping wild taro with color-infrared aerial photography and image processing	2007	United States	Taro	USDA-ARS, Integrated Farming and Natural Resources Research Unit, 2413 E. Highway 83, Weslaco.
[38]	Estimation of ground surface and accuracy assessments of growth parameters for a sweet potato community in ridge cultition	2019	Japan	Sweet potato	The University of Tokyo, Graduate School of Agricultural and Life Sciences,1-1-1 Yayoi, Bunkyo, Tokyo 113-8657, Japan. National Institute for Environmental Studies, 16. Takasaki University of Health and Welfare, 54 Nakaorui-machi, Takasaki, Gunma 370-0033, Japan.
[13]	Uav-Based Imaging for Prediction of Chickpea Crop Biophysical Parameters and Yield	2022	Israel	Chickpea	Newe Ya'ar Research Center, Agricultural Research Organization (ARO) - Volcani Center, Ramat Yishay 30095, Israel. The Hebrew University of Jerusalem, Rehovot 7610001, Israel. Field Crops and Natural Resources Department, Agricultural Research Organization (ARO) – Gilat Research Center, Gilat 8531100, Israel
[42]	Classifying Breadfruit Tree using Artificial Neural Networks	2018	China	Breadfruit	Technological Institute of the Philippines, Manila Philippines.

100
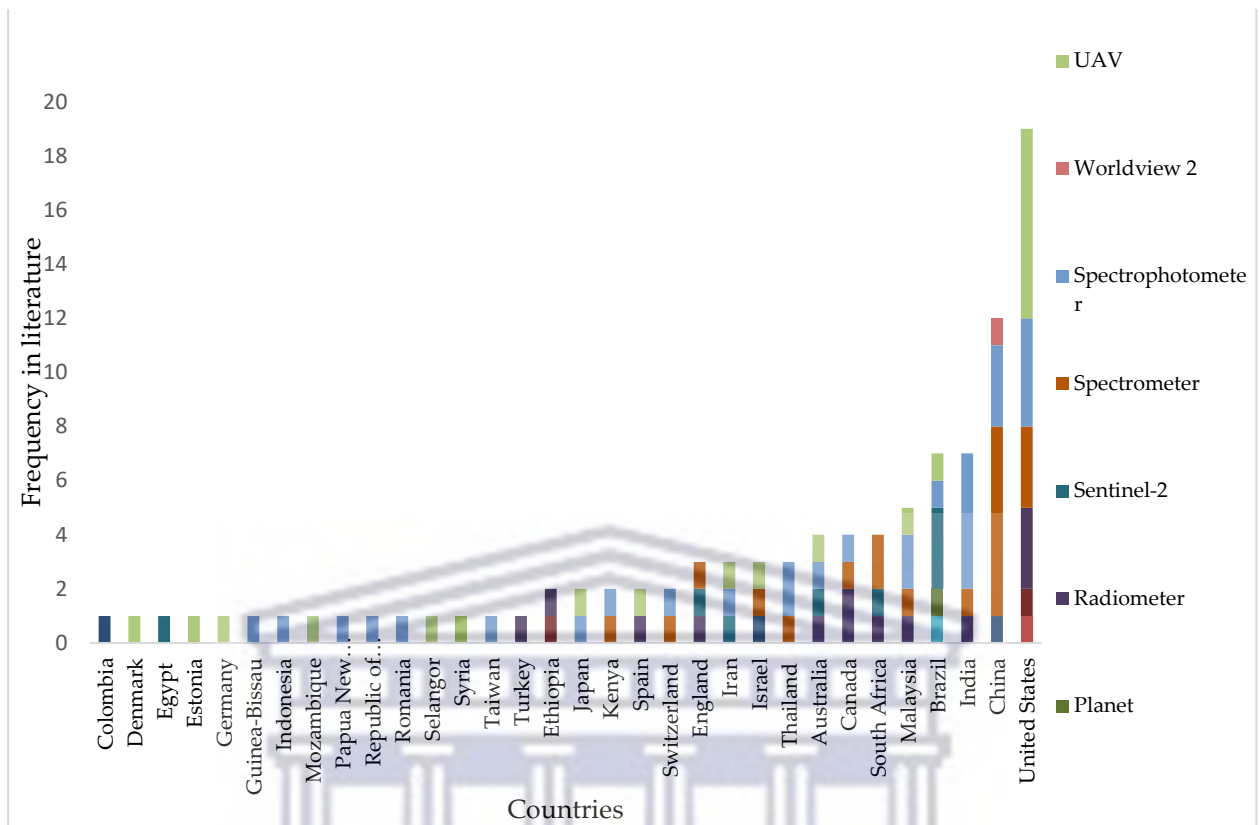
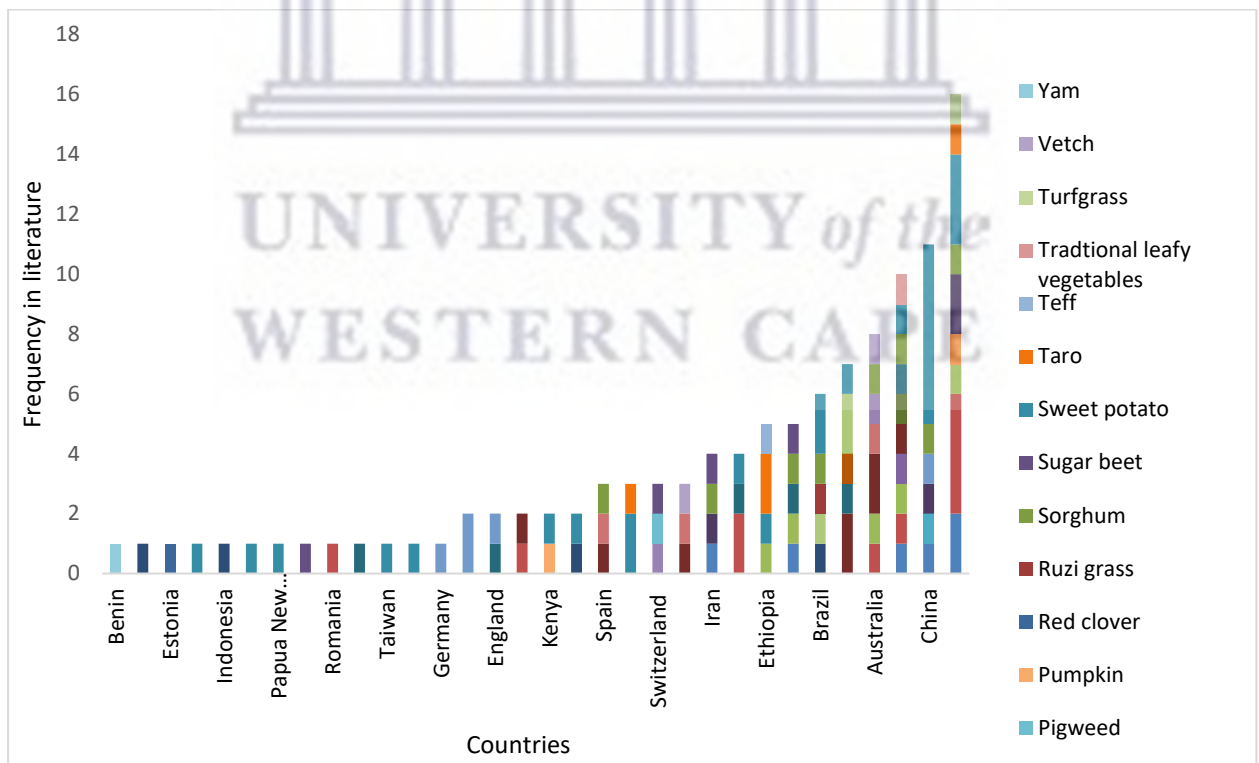Figure S1: Countries and various sensors they used to assess NUS.

Figure:S2 Countries which assessed various NUS crops.

101

References

1. Kutugata, M.; Hu, C.; Sapkota, B.; Bagavathiannan, M. Seed rain potential in late-season weed escapes can be estimated using remote sensing. *Weed Sci.* **2021**, *69*, 653–659.

2. Jewan, S.Y.Y.; Pagay, V.; Billa, L.; Tyerman, S.D.; Gautam, D.; Sparkes, D.; Chai, H.H.; Singh, A. The feasibility of using a low-cost near-infrared, sensitive, consumer-grade digital camera mounted on a commercial UAV to assess Bambara groundnut yield. *Int. J. Remote Sens.* **2022**, *43*, 393–423. https://doi.org/10.1080/01431161.2021.1974116.

3. Che'Ya, N.N.; Dunwoody, E.; Gupta, M. Assessment of Weed Classification Using Hyperspectral Reflectance and Optimal Multispectral UAV Imagery. *Agronomy* **2021**, *11*, 1435. https://doi.org/10.3390/agronomy11071435.

4. Sapkota, B.; Singh, V.; Cope, D.; Valasek, J.; Bagavathiannan, M. Mapping and Estimating Weeds in Cotton Using Unmanned Aerial Systems-Borne Imagery. *Agriengineering* **2020**, *2*, 24. https://doi.org/10.3390/agriengineering2020024.

5. Huang, Y.B.; Reddy, K.N.; Fletcher, R.S.; Pennington, D. UAV Low-Altitude Remote Sensing for Precision Weed Management. *Weed Technol.* **2018**, *32*, 2–6. https://doi.org/10.1017/wet.2017.89.

6. Li, L.; Zheng, X.; Zhao, K.; Li, X.; Meng, Z.; Su, C. Potential Evaluation of High Spatial Resolution Multi-Spectral Images Based on Unmanned Aerial Vehicle in Accurate Recognition of Crop Types. *J. Indian Soc. Remote Sens.* **2020**, *48*, 1471–1478.

7. Suhairi, T.A.S.T.M.; Sinin, S.S.M.; Wimalasiri, E.M.; Nizar, N.M.M.; Tharmandran, A.S.; Jahanshiri, E.; Gregory, P.J.; Azam-Ali, S.N. Use of Unmanned Aerial Vehicles (UAVs) Imagery in Phenotyping of Bambara Groundnut. *J. Agric. Sci.* **2020**, *12*. https://doi.org/10.5539/jas.v12n6p12

8. Awais, M.; Li, W.; Cheema, M.; Zaman, Q.; Shaheen, A.; Aslam, B.; Zhu, W.; Ajmal, M.; Faheem, M.; Hussain, S. UAV-based remote sensing in plant stress imagine using high-resolution thermal sensor for digital agriculture practices: A meta-review. *Int. J. Environ. Sci. Technol.* **2022**, *20*, 1135–1152.

9. Biswas, A.; Andrade, M.H.M.L.; Acharya, J.P.; de Souza, C.L.; Lopez, Y.; De Assis, G.; Shirbhate, S.; Singh, A.; Munoz, P.; Rios, E.F. Phenomics-Assisted Selection for Herbage Accumulation in Alfalfa (Medicago sativa L.). *Front. Plant Sci.* **2021**, *12*, 756768.

10. Parra, L.; Mostaza-Colado, D.; Yousfi, S.; Marin, J.F.; Mauri, P.V.; Lloret, J. Drone RGB images as a reliable information source to determine legumes establishment success. *Drones* **2021**, *5*, 79.

11. Grüner, E.; Astor, T.; Wachendorf, M. Prediction of biomass and N fixation of legume–grass mixtures using sensor fusion. *Front. Plant Sci.* **2021**, *11*, 603921.

12. Ramírez, D.A.; Grüneberg, W.; Andrade, M.I.; De Boeck, B.; Loayza, H.; Makunde, G.S.; Ninanya, J.; Rinza, J.; Heck, S.; Campos, H. Phenotyping of productivity and resilience in sweetpotato under water stress through UAV-based multispectral and thermal imagery in Mozambique. *J. Agron. Crop Sci.* **2023**, *209*, 41–55.

13. Lati, R.; Avneri, A.; Aharon, S.; Atsmon, G.; Smirnov, E.; Sadeh, R.; Abbo, S.; Peleg, Z.; Herrmann, I.; Bonfil, D.J. Uav-Based Imaging for Prediction of Chickpea Crop Biophysical Parameters and Yield. *Available at SSRN 4123863*.

14. Li, K.-Y.; Burnside, N.G.; Sampaio de Lima, R.; Villoslada Peciña, M.; Sepp, K.; Yang, M.-D.; Raet, J.; Vain, A.; Selge, A.; Sepp, K. The application of an unmanned aerial system and machine learning techniques for red clover-grass mixture yield estimation under variety performance trials. *Remote Sens.* **2021**, *13*, 1994.

15. Sobejano-Paz, V.; Mikkelsen, T.N.; Baum, A.; Mo, X.; Liu, S.; Köppl, C.J.; Johnson, M.S.; Gulyas, L.; García, M. Hyperspectral and thermal sensing of stomatal conductance, transpiration, and photosynthesis for soybean and maize under drought. *Remote Sens.* **2020**, *12*, 3182.

16. Sankaran, S.; Zhou, J.; Khot, L.R.; Trapp, J.J.; Mndolwa, E.; Miklas, P.N. High-throughput field phenotyping in dry bean using small unmanned aerial vehicle based multispectral imagery. *Comput. Electron. Agric.* **2018**, *151*, 84–92.

17. Pereira, F.d.S.; de Lima, J.; Freitas, R.; Dos Reis, A.A.; do Amaral, L.R.; Figueiredo, G.K.D.A.; Lamparelli, R.A.; Magalhães, P.S.G. Nitrogen variability assessment of pasture fields under an integrated crop-livestock system using UAV, PlanetScope, and Sentinel-2 data. *Comput. Electron. Agric.* **2022**, *193*, 106645.

18. Singhal, G.; Bansod, B.; Mathew, L.; Goswami, J.; Choudhury, B.; Raju, P. Estimation of leaf chlorophyll concentration in turmeric (Curcuma longa) using high-resolution unmanned aerial vehicle imagery based on kernel ridge regression. *J. Indian Soc. Remote Sens.* **2019**, *47*, 1111–1122.

19. Awais, M.; Li, W.; Cheema, M.; Hussain, S.; Shaheen, A.; Aslam, B.; Liu, C.; Ali, A. Assessment of optimal flying height and timing using high-resolution unmanned aerial vehicle images in precision agriculture. *Int. J. Environ. Sci. Technol.* **2022**, *19*, 2703–2720.

20. Kourouma, J.M.; Eze, E.; Negash, E.; Phiri, D.; Vinya, R.; Girma, A.; Zenebe, A. Assessing the spatio-temporal variability of NDVI and VCI as indices of crops productivity in Ethiopia: A remote sensing approach. *Geomat. Nat. Hazards Risk* **2021**, *12*, 2880–2903. https://doi.org/10.1080/19475705.2021.1976849.

21. Sharifi, A. Remotely sensed vegetation indices for crop nutrition mapping. *J. Sci. Food Agric.* **2020**, *100*, 5191–5196. https://doi.org/10.1002/jsfa.10568.

22. Lima, J.G.; Espínola, J.; Medeiros, J.F.d.; Viana, P.C.; Maniçoba, R.M. Water requirement and crop coefficients of sorghum in Apodi Plateau. *Rev. Bras. De Eng. Agrícola E Ambient.* **2021**, *25*, 684–688.

23. Zakarya, Y.M.; Metwaly, M.M.; AbdelRahman, M.A.; Metwalli, M.R.; Koubouris, G. Optimized land use through integrated land suitability and GIS approach in West El-Minia Governorate, Upper Egypt. *Sustainability* **2021**, *13*, 12236.

24. Guo, Q.; Wu, F.; Pang, S.; Zhao, X.; Chen, L.; Liu, J.; Xue, B.; Xu, G.; Li, L.; Jing, H. Crop 3D—A LiDAR based platform for 3D high-throughput crop phenotyping. *Sci. China Life Sci.* **2018**, *61*, 328–339.

25. Tedesco, D.; de Oliveira, M.F.; dos Santos, A.F.; Silva, E.H.C.; de Souza Rolim, G.; da Silva, R.P. Use of remote sensing to characterize the phenological development and to predict sweet potato yield in two growing seasons. *Eur. J. Agron.* **2021**, *129*, 126337.

26. Tedesco, D.; de Almeida Moreira, B.R.; Júnior, M.R.B.; Papa, J.P.; da Silva, R.P. Predicting on multi-target regression for the yield of sweet potato by the market class of its roots upon vegetation indices. *Comput. Electron. Agric.* **2021**, *191*, 106544.

27. Punalekar, S.M.; Verhoef, A.; Quaife, T.; Humphries, D.; Bermingham, L.; Reynolds, C. Application of Sentinel-2A data for pasture biomass monitoring using a physically based radiative transfer model. *Remote Sens. Environ.* **2018**, *218*, 207–220.
28. Thenkabail, P. Biophysical and yield information for precision farming from near-real-time and historical Landsat TM images. *Int. J. Remote Sens.* **2003**, *24*, 2879–2904.
29. Zhang, P.; Hu, S.; Li, W.; Zhang, C. Parcel-level mapping of crops in a smallholder agricultural area: A case of central China using single-temporal VHSR imagery. *Comput. Electron. Agric.* **2020**, *175*, 105581.
30. Mazarire, T.T.; Ratshiedana, P.E.; Nyamugama, A.; Adam, E.; Chirima, G. Exploring machine learning algorithms for mapping crop types in a heterogeneous agriculture landscape using Sentinel-2 data. A case study of Free State Province, South Africa. *S. Afr. J. Geomat.* **2020**, *9*, 333–347.
31. Karimi, N.; Sheshangosht, S.; Eftekhari, M. Crop type detection using an object-based classification method and multi-temporal Landsat satellite images. *Paddy Water Environ.* **2022**, *20*, 395–412.
32. Karlson, M.; Ostwald, M.; Bayala, J.; Bazié, H.R.; Ouedraogo, A.S.; Soro, B.; Sanou, J.; Reese, H. The potential of Sentinel-2 for crop production estimation in a smallholder agroforestry landscape, Burkina Faso. *Front. Environ. Sci.* **2020**, *8*, 85.
33. Guan, K.; Berry, J.A.; Zhang, Y.; Joiner, J.; Guanter, L.; Badgley, G.; Lobell, D.B. Improving the monitoring of crop productivity using spaceborne solar-induced fluorescence. *Glob. Change Biol.* **2016**, *22*, 716–726.
34. Shirzadifar, A.; Bajwa, S.; Nowatzki, J.; Bazrafkan, A. Field identification of weed species and glyphosate-resistant weeds using high resolution imagery in early growing season. *Biosyst. Eng.* **2020**, *200*, 200–214.
35. Shi, Y.; Murray, S.C.; Rooney, W.L.; Valasek, J.; Olsenholler, J.; Pugh, N.A.; Henrickson, J.; Bowden, E.; Zhang, D.; Thomasson, J.A. Corn and sorghum phenotyping using a fixed-wing UAV-based remote sensing system. In *Autonomous Air and Ground Sensing Systems for Agricultural Optimization and Phenotyping*; SPIE: Bellingham, WA, USA, 2016; pp. 46–53.
36. Wimalasiri, E.M.; Jahanshiri, E.; Suhairi, T.; Udayangani, H.; Mapa, R.B.; Karunaratne, A.S.; Vidhanarachchi, L.P.; Azam-Ali, S.N. Basic Soil Data Requirements for Process-Based Crop Models as a Basis for Crop Diversification. *Sustainability* **2020**, *12*, 7781. https://doi.org/10.3390/su12187781.
37. Everitt, J.; Yang, C.; Davis, M.; Everitt, J.; Davis, M. Mapping wild taro with color-infrared aerial photography and image processing. *J. Aquat. Plant Manag.* **2007**, *45*, 106–110.
38. Teng, P.; Ono, E.; Zhang, Y.; Aono, M.; Shimizu, Y.; Hosoi, F.; Omasa, K. Estimation of ground surface and accuracy assessments of growth parameters for a sweet potato community in ridge cultivation. *Remote Sens.* **2019**, *11*, 1487.
39. Waldner, F.; Chen, Y.; Lawes, R.; Hochman, Z. Needle in a haystack: Mapping rare and infrequent crops using satellite imagery and data balancing methods. *Remote Sens. Environ.* **2019**, *233*, 111375.
40. Adams, T.; Bruton, R.; Ruiz, H.; Barrios-Perez, I.; Selvaraj, M.G.; Hays, D.B. Prediction of Aboveground Biomass of Three Cassava (Manihot esculenta) Genotypes Using a Terrestrial Laser Scanner. *Remote Sens.* **2021**, *13*, 1272.
41. Hama, A.; Matsumoto, Y.; Matsuoka, N. Estimating Leaf Water Content through Low-Cost LiDAR. *Agronomy* **2022**, *12*, 1183.
42. Malinao, R.M.L.; Hernandez, A.A. Classifying Breadfruit Tree using Artificial Neural Networks. In Proceedings of Proceedings of the 6th ACM/ACIS International Conference on Applied Computing and Information Technology, Kunming, China, 13–15 June 2018; pp. 27–31.

Table S2-1: Band 4 JM distances

B4

	Taro	SP	NV	SU	BL	BU	M1	M2
Taro	0	0.963	0.699	0.783	0.836	0.849	0.694	0.770
SP	0.963	0	0.606	0.841	0.605	0.472	0.736	0.549
NV	0.699	0.606	0	0.698	0.574	0.531	0.401	0.470
SU	0.783	0.841	0.698	0	0.517	0.688	0.802	0.607
BL	0.836	0.605	0.574	0.517	0	0.361	0.749	0.318
BU	0.849	0.472	0.531	0.688	0.361	0	0.734	0.22
M1	0.69	0.736	0.401	0.802	0.745	0.734	0	0.676
M2	0.77	0.548	0.470	0.607	0.318	0.22	0.676	0

Table S2-2: Band 5 JM distances

B5

	Taro	SP	NV	SU	BL	BU	M1	M2
Taro	0	0.508	0.313	0.868	0.636	0.617	0.602	0.358
SP	0.508	0	0.365	1.034	0.687	0.653	0.813	0.538
NV	0.313	0.365	0	0.966	0.622	0.591	0.711	0.355
SU	0.868	1.034	0.966	1.490	1.050	1.053	0.806	0.859
BL	0.636	0.687	0.622	1.050	0	0.187	0.712	0.747
BU	0.617	0.653	0.591	1.053	0.187	0	0.717	0.736
M1	0.602	0.813	0.711	0.806	0.712	0.717	0	0.658
M2	0.358	0.538	0.355	0.859	0.747	0.736	0.658	0

Table S2-3: EXG index JM distances

EXG

	Taro	SP	NV	SU	BL	BU	M1	M2
Taro	0	0.686	0.334	0.523	0.706	0.705	0.613	0.254
SP	0.686	0	0.504	0.894	0.739	0.592	0.943	0.667
NV	0.334	0.504	1.490	0.681	0.629	0.553	0.755	0.332
SU	0.523	0.894	0.681	0	0.799	0.845	0.257	0.583
BL	0.706	0.739	0.629	0.799	1.490	0.425	0.836	0.734
BU	0.705	0.592	0.553	0.845	0.425	1.490	0.886	0.726
M1	0.613	0.943	0.755	0.257	0.836	0.886	0	0.663
M2	0.254	0.667	0.332	0.583	0.734	0.726	0.663	0
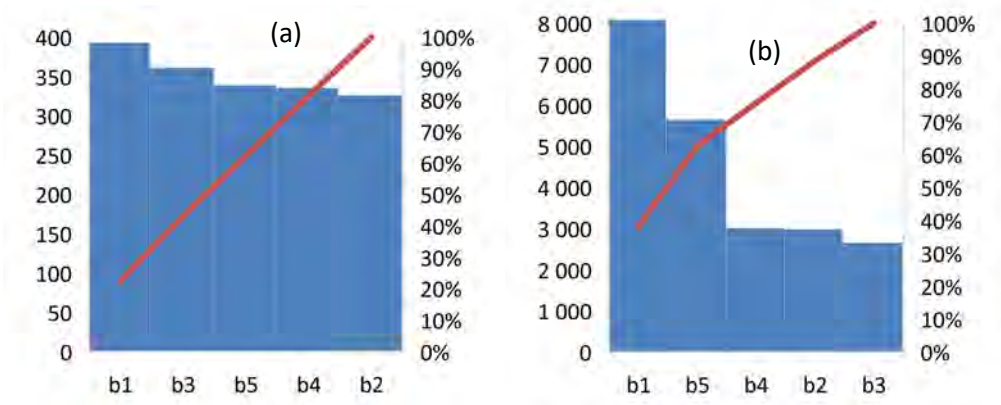
Figure S2-1: Variable importance scores of (a) RF and (b) GTB with dataset 1.
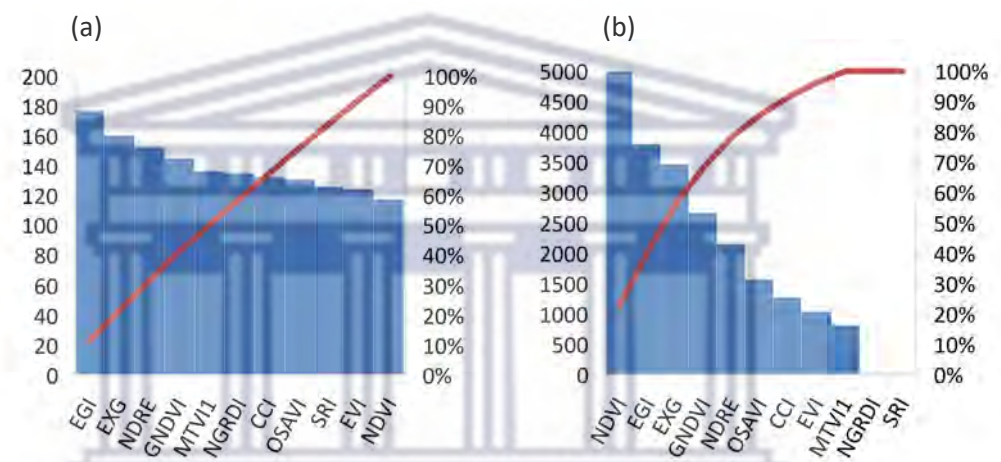
Figure S2-2: Variable importance scores of (a) RF and (b) GTB with dataset 2.
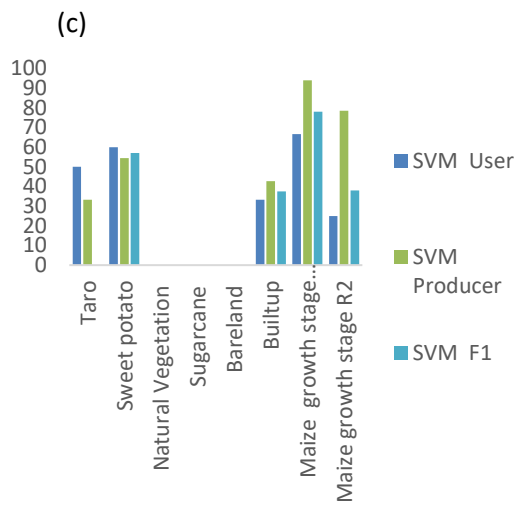
(c)
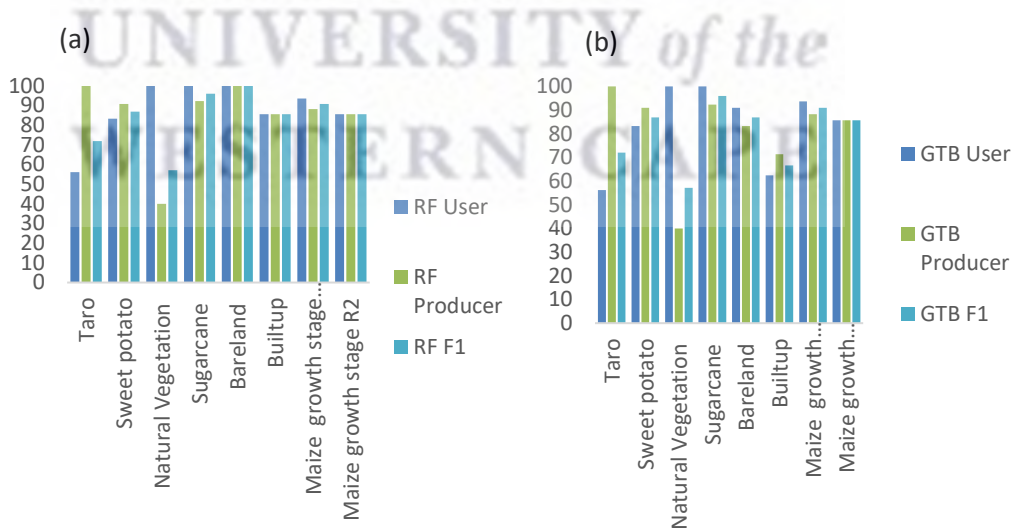
Figure S2-3: user and producer accuracies of (a) RF, (b) GTB & (c) SVM in conjunction with dataset 1
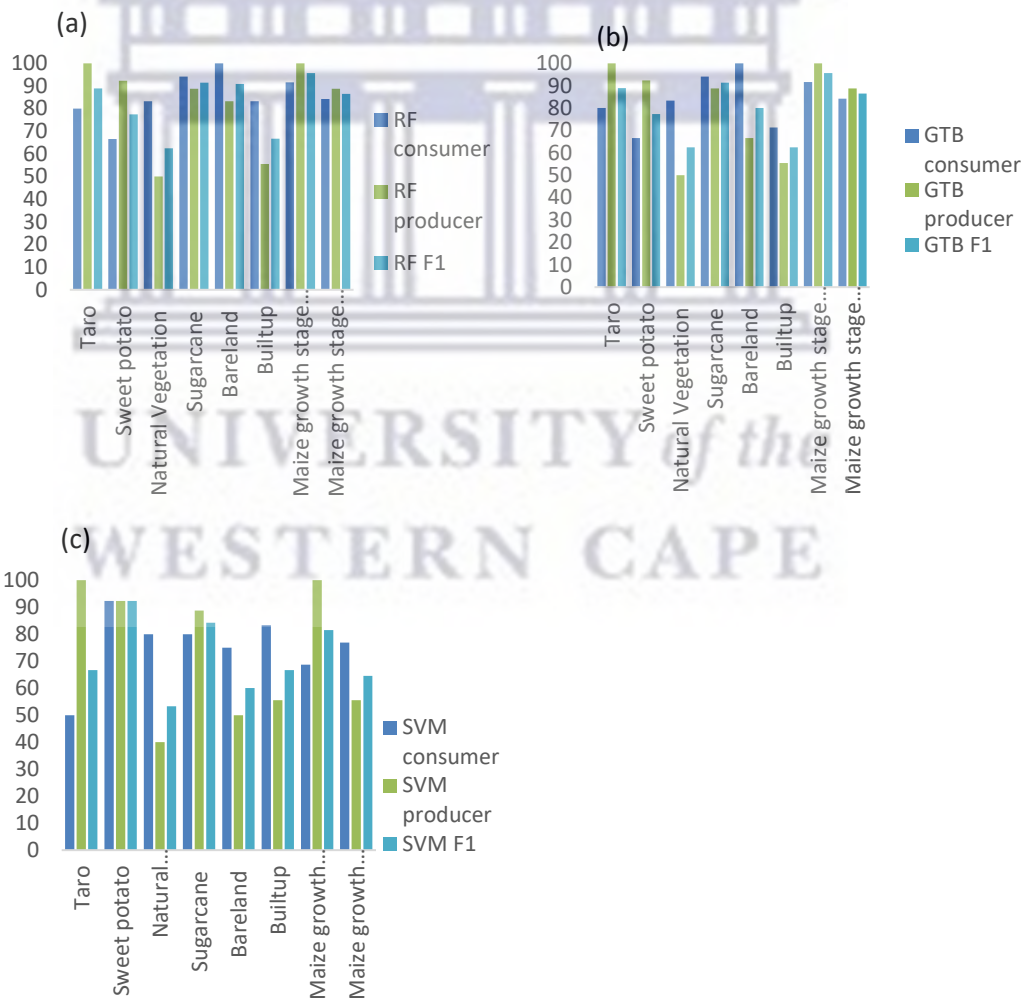

Figure S2-4: user and producer accuracies of (a) RF, (b) GTB & (c) SVM in conjunction with dataset 2.
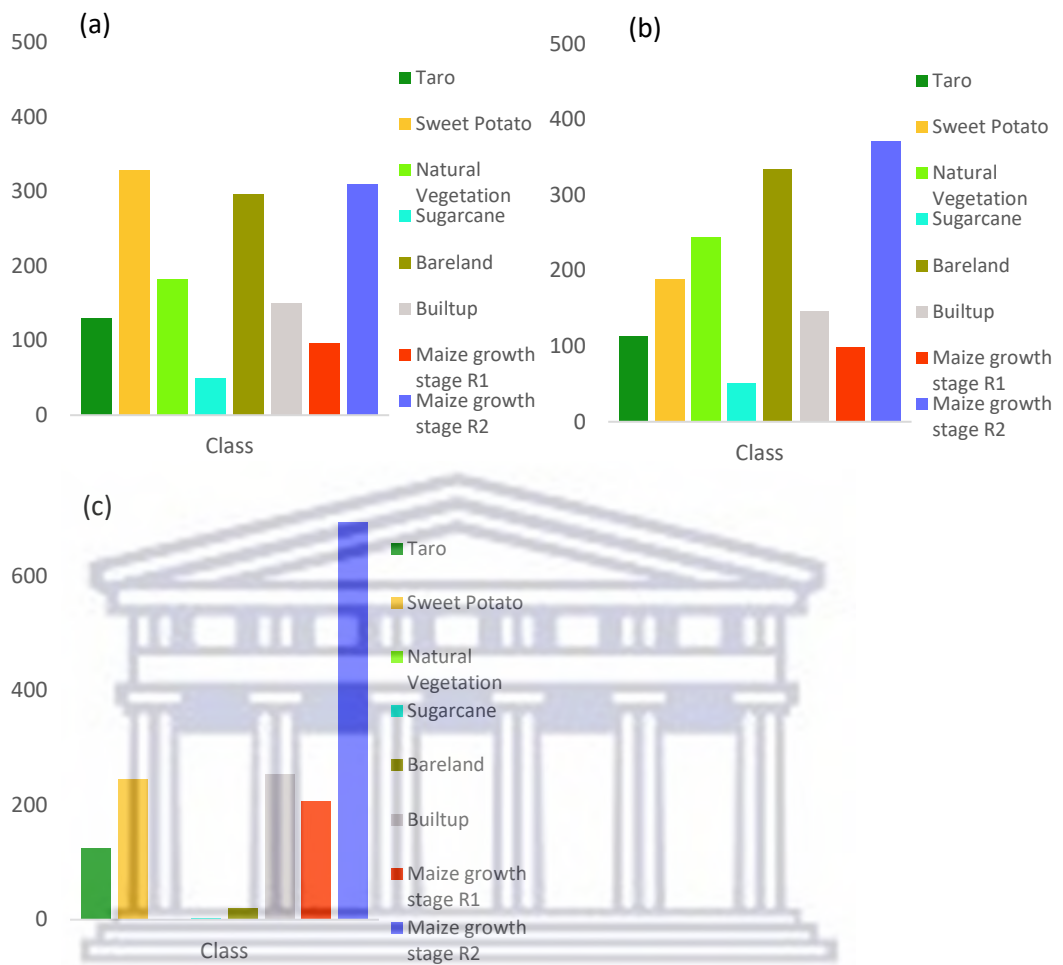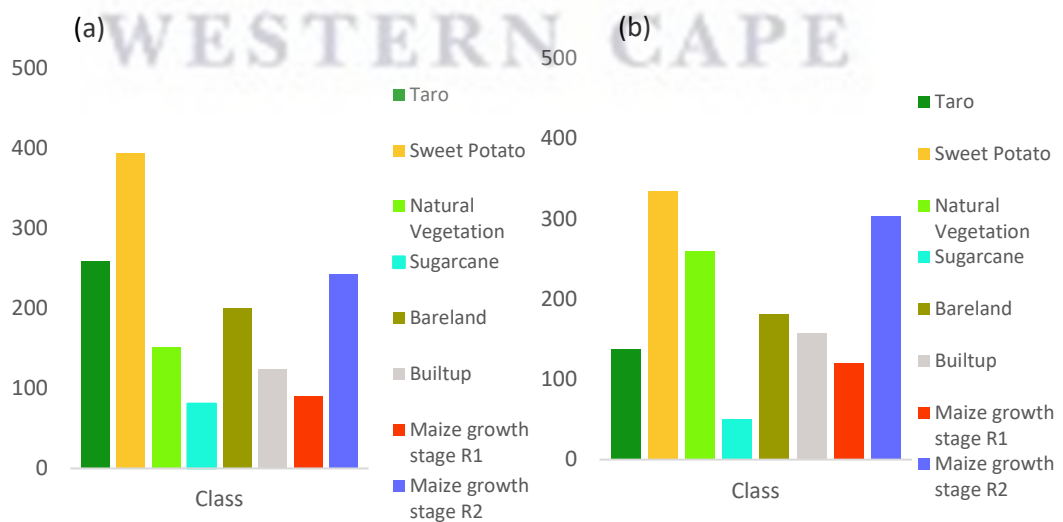
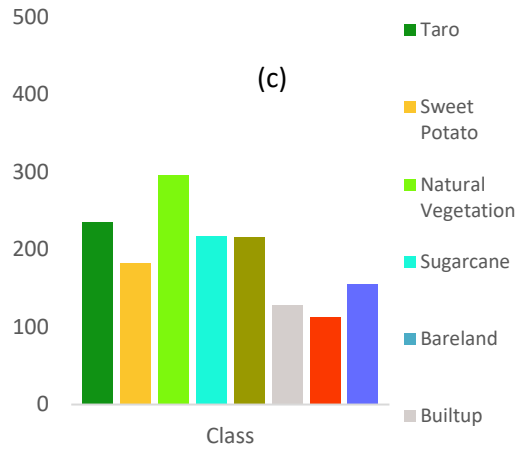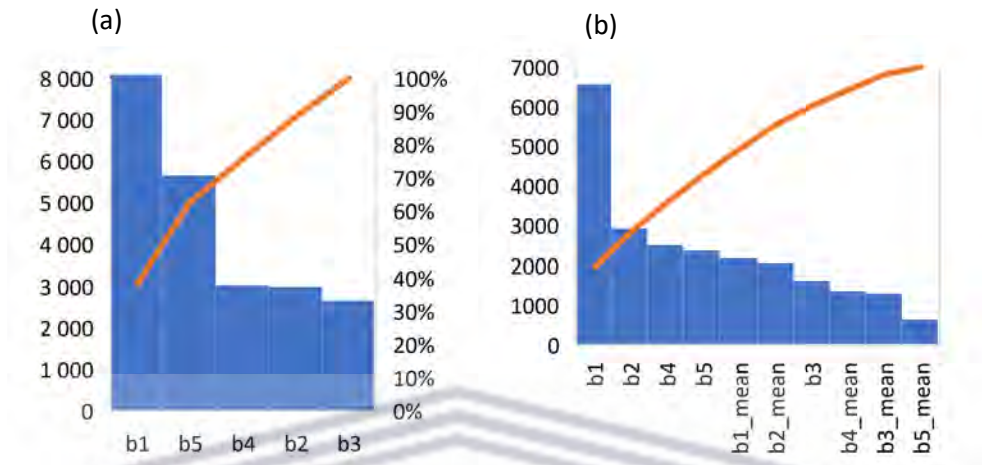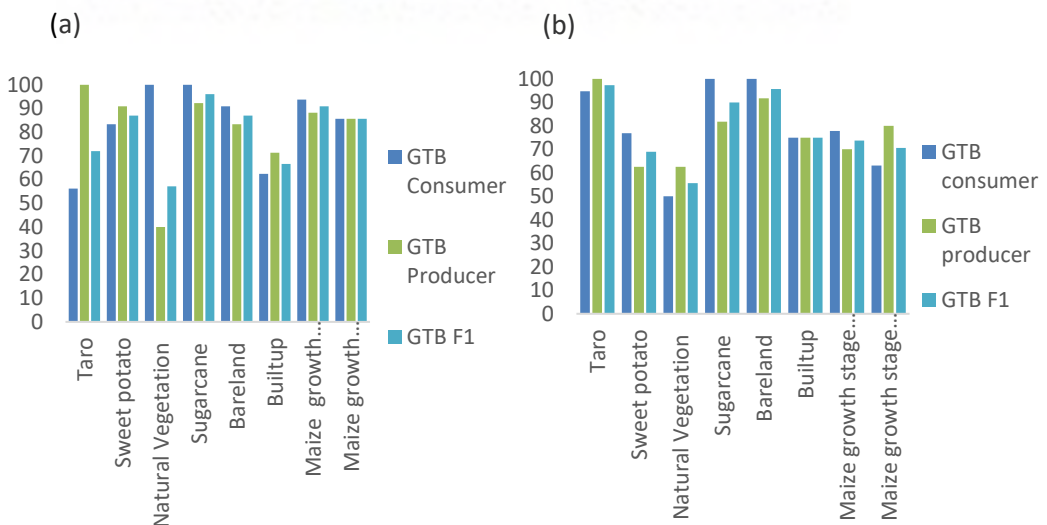Figure S2-5: areal extents per class of (a) RF, (b) GTB, (c) SVM with dataset 1

107

Figure S2-6: areal extents per class of (a) RF, (b) GTB, (c) SVM with dataset 2
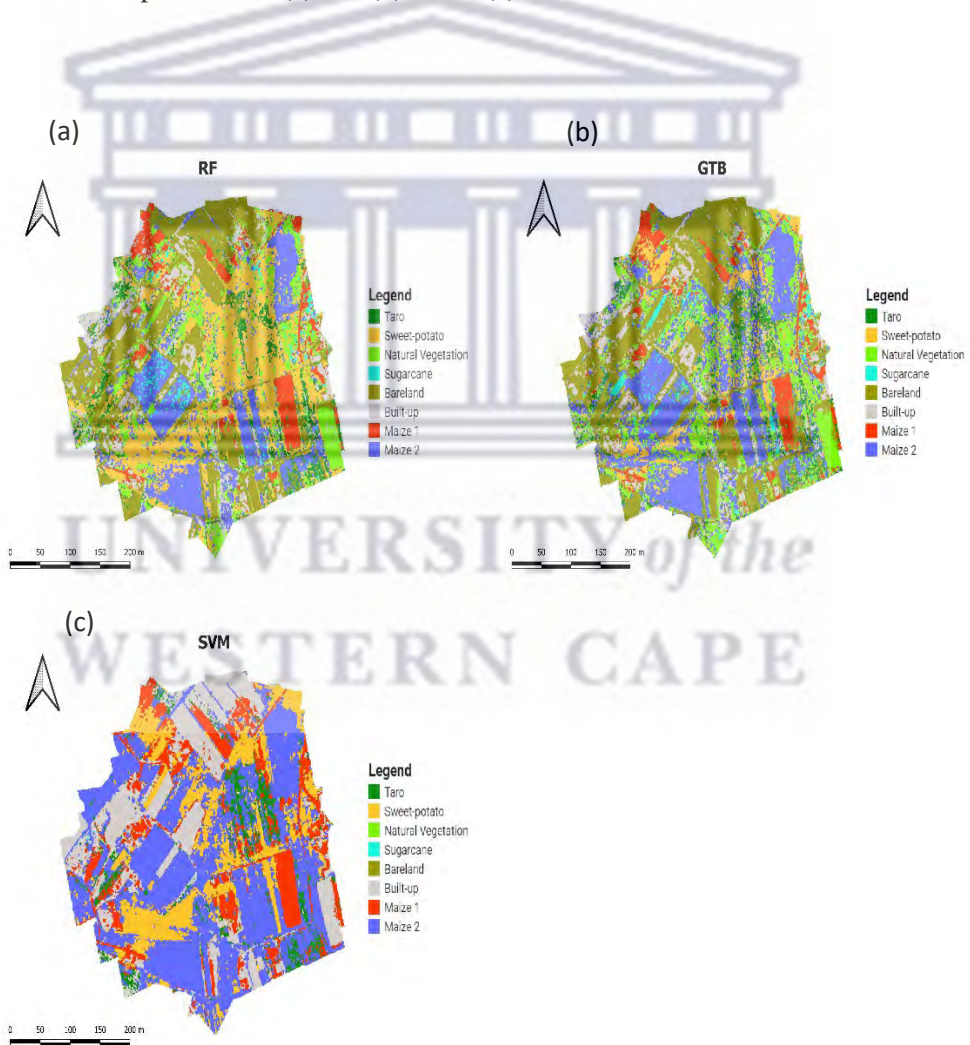
Figure S2-7: NUS crop distribution maps of (a) RF (b) GTB (c) SVM with dataset 1.
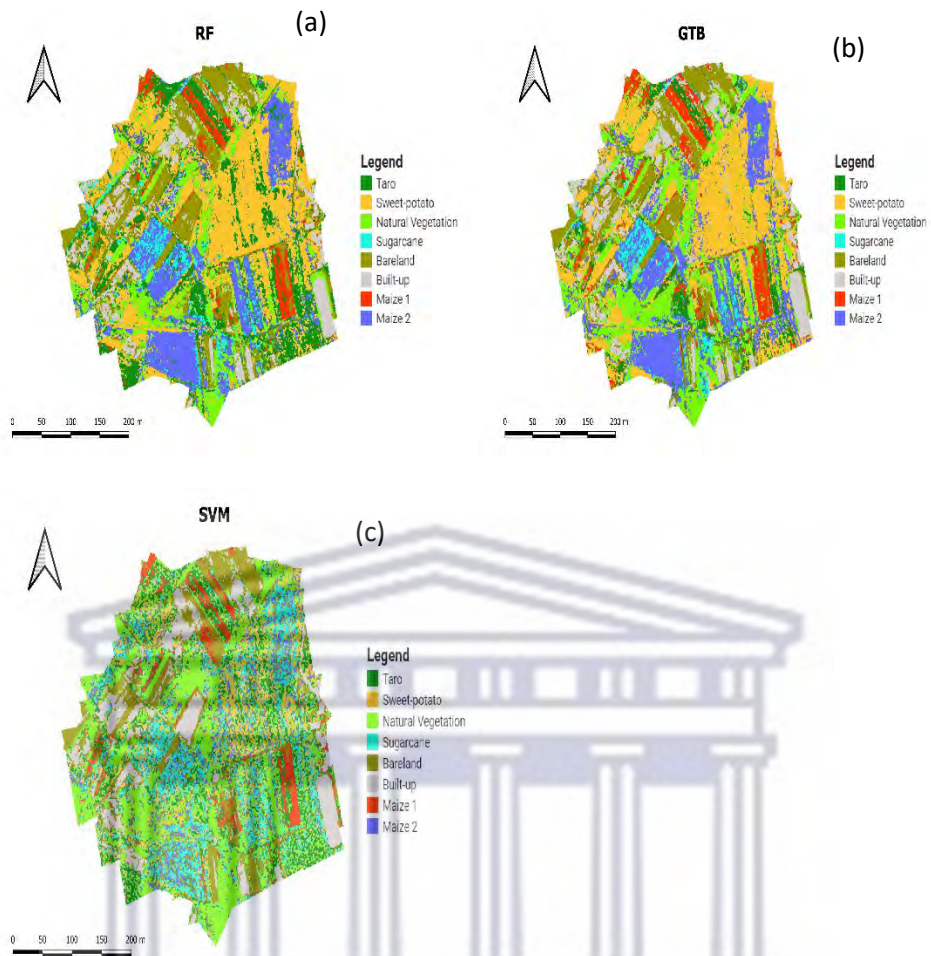
Figure S2-8: NUS crop distribution maps of (a) RF (b) GTB (c) SVM with dataset 2..

Chapter 4 Appendix

Figure S3-1: Variable importance scores of (a) PBIA-GTB, (b) OBIA-GTB with dataset 1.
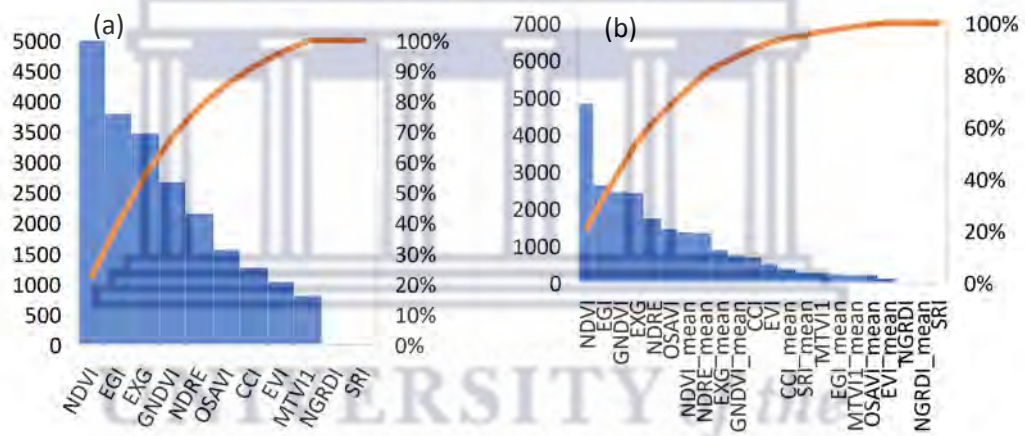
Figure S3-2: Variable importance scores of (a) PBIA-GTB, (b) OBIA-GTB with dataset 2.

Figure S3-3: user and producer accuracies of (a) PBIA-GTB, (b) OBIA-GTB with dataset 1.

110
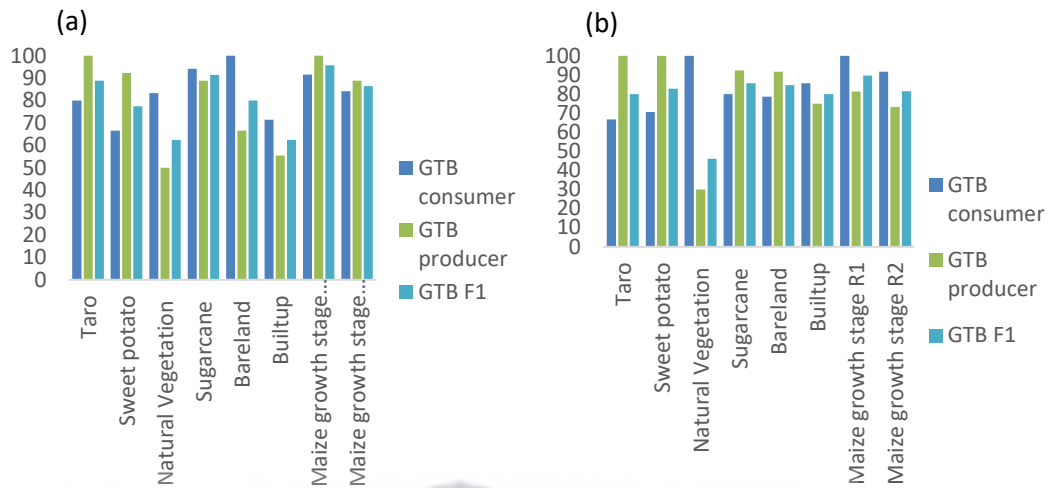
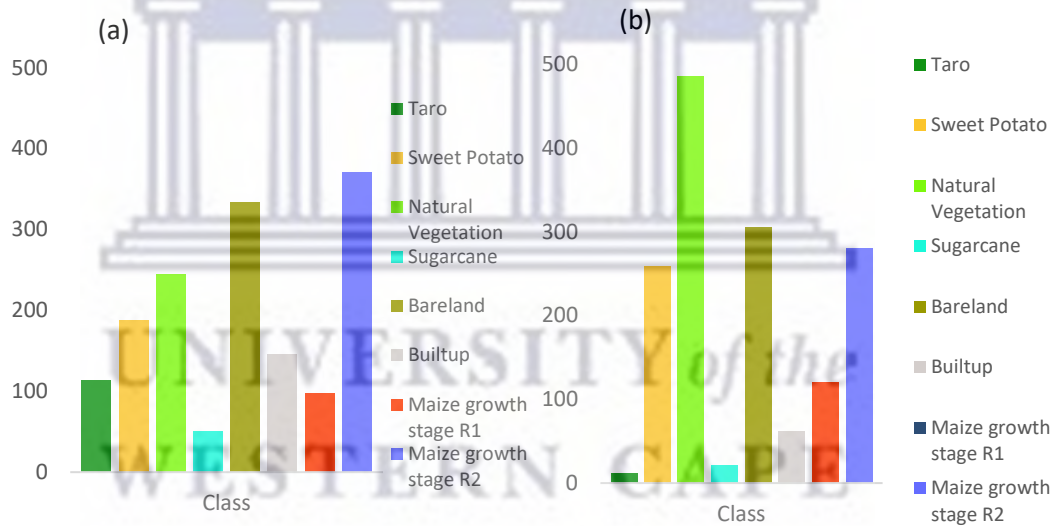Figure S3-4: user and producer accuracies of (a) PBIA-GTB, (b) OBIA-GTB with dataset 2.

Figure S3-5: Areal extents per class of (a) PBIA-GTB, (b) OBIA-GTB with dataset 1

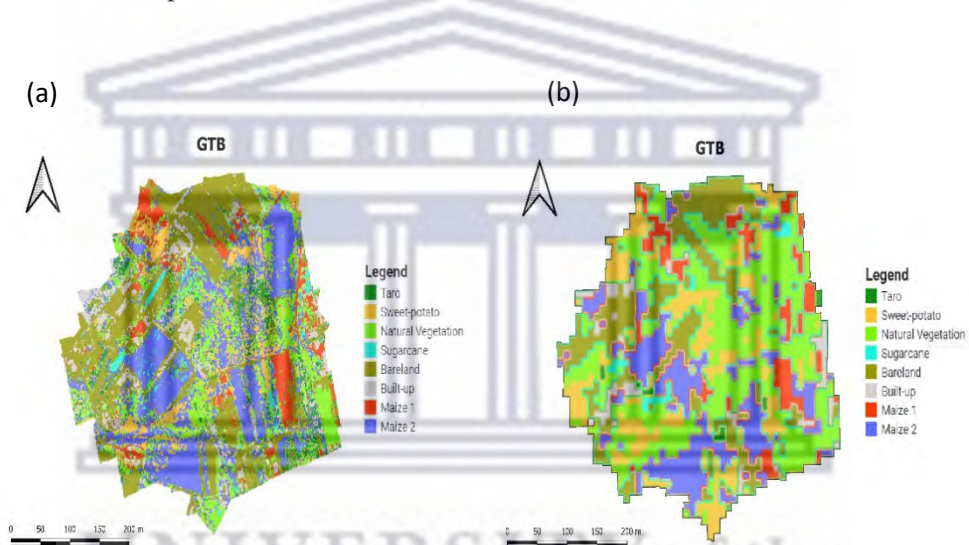Figure S3-6:Areal extents per class of (a) PBIA-GTB, (b) OBIA-GTB with dataset 2.

Figure S3-7: NUS crop distribution maps of (a) PBIA-GTB (b) and OBIA-GTB with dataset 1.
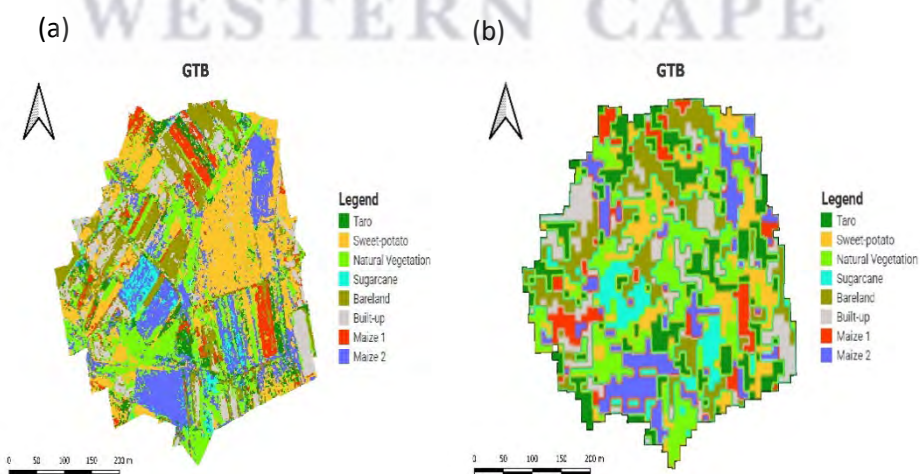

Figure S3-8:NUS crop distribution maps of (a) PBIA-GTB (b) and OBIA-GTB with dataset 2.

112